SYNTHESIS AND FUNCTIONALIZATION OF HYBRID MAGNETIC NANOPARTICLE COMPOSITES FOR ENERGY CONVERSION, LIGHT HARVESTING AND OPTICAL AND BIOMEDICAL APPLICATIONS

by

Marwan Abduljawad

A Dissertation Submitted to the Faculty of the

DEPARTMENT OF CHEMICAL AND ENVIRONMENTAL ENGINEERING

In Partial Fulfillment of the Requirements

For the Degree of

DOCTOR OF PHILOSOPHY

In the Graduate College

THE UNIVERSITY OF ARIZONA

2021

THE UNIVERSITY OF ARIZONA
GRADUATE COLLEGE

As members of the Dissertation Committee, we certify that we have read the dissertation prepared by: Marwan Abduljawad titled: SYNTHESIS AND FUNCTIONALIZATION OF HYBRID MAGNETIC NANOPARTICLE COMPOSITES FOR ENERGY CONVERSION, LIGHT HARVESTING AND OPTICAL AND BIOMEDICAL APPLICATIONS

and recommend that it be accepted as fulfilling the dissertation requirement for the Degree of Doctor of Philosophy.

Date: 5/17/2021
Dr. Roberto Guzman

Date: 5/17/2021
Dr. Erin Ratcliff

Date: 5/17/2021
Dr. Adam Printz

Date: 5/17/2021
Dr. Suchol Savagtrup

Final approval and acceptance of this dissertation is contingent upon the candidate's submission of the final copies of the dissertation to the Graduate College.

I hereby certify that I have read this dissertation prepared under my direction and recommend that it be accepted as fulfilling the dissertation requirement.

Date: 5/17/2021
Roberto Guzman
Dissertation Committee Chair
Chemical and Environmental Engineering

Acknowledgements

I would like to express my deepest appreciation to my Mom, my Dad, Ghada and Hala, my brothers and sisters, and Rio for their continues support all the way. You were always there for me. Honestly, I could not have finished my Ph.D. without the support of all of you.

I would also like to extend my deepest gratitude to my adviser, Dr. Guzman, whose expertise was invaluable in formulating this research. Your helpful advice pushed me to improve my thoughts and raise the quality of my work. I would also like to extend my sincere thanks to Dr. Ratcliff, Dr. Printz, and Dr. Savagatrup for serving on my committee.

I would like to thank my friends from the lab Daniel, David, Humberto, and everyone who worked with me for their support, collaboration, and making the work environment enjoyable and productive.

I would like to thank King Abdulaziz City for Science and Technology (KACST) for offering me the scholarship to get my Ph.D. degree.

Finally, I would like to acknowledge everyone who stood by me and supported me to make this journey possible and successful.

I love you Mom.

Table of Contents

List of Figures

Chapter 2

Chapter 3

Chapter 4

Chapter 5

Chapter 6

ABSTRACT

The primary objective of this dissertation was to develop and prepare hybrid multifunctional engineered composite contrast agent nanoparticles for applications in energy conversion, light harvesting in optical and biomedical systems. In this work, superparamagnetic iron oxide nanoparticles were the most common components in the preparation of synthesized nanocomposites. These nanoparticles were used as a core to add reactive moieties such as alkoxysilanes derivatives and polymers to introduce functional ligands including amino, epoxy and aldehyde groups. The most relevant working hypothesis in this dissertation is based on the concept that modified magnetic nanoparticles with semiconductor materials, specifically in this work, with titania thin films shells, provide a suitable surface for protein immobilization. Core-shell hybrid magnetic composites of an iron oxide core and a titania oxide shell were prepared by introducing a new method of synthesis that involves low temperature treatments, inexpensive precursors and with no special reaction conditions required. Magnetic derivatives modified with the linker, 3-Aminopropyltriethoxysilane (APTES) were used successfully to coat the nanoparticles with fluorescent dyes. The amino groups of the APTES moieties were further reacted with glutaraldehyde as a linker to attach amino group derivatives that included proteins (e.g., (enzymes, antibodies) and fluorescent dyes. Other nanostructures prepared in this work included hybrid materials with a core of iron oxide coated with intermediate layers of gold followed by an outer shell of titania oxide that can be used for further modifications. These systems provide properties of photo-corrosion resistance and protection from aggregation. Magnetic nanoparticles derivatives with specific applications in magnetic resonance imaging (MRI) were prepared with coatings of dextran that after further activation with reducing agents the surface was modified via amino moieties. The successful synthesis was demonstrated with

the attachment of the enzyme trypsin on different magnetic nanoparticle derivatives and the effective evaluation of the enzyme kinetic parameters. Based on these results it seems feasible to obtain similar effective attachment of any other protein, enzymes or antibodies. The nanoparticle magnetic derivatives coated with dextran provide a stable, water compatible without aggregation and thus suitable for diverse medical applications. Other nanoparticle derivatives produced in this work include quantum dots of different compositions, particularly simple methods to produce carbon dots for light harvesting applications. Silver and gold nanoparticles were produced as materials to promote synthesis of magnetic core and titania shell hybrids. Additionally, silver nanoparticles were used as seeds to deposit gold shells on the silver surface that after a galvanization process created hollow gold nanoparticles derivatives that are being used as photothermal agents to study their thermal ablation properties, technique with promising future in cancer therapy. The characterization of the nanoparticles was performed with SEM/TEM imaging for nanoparticle morphology and size. For optical properties, UV-vis spectroscopy has been used. EDS and XRD have been used to verify element composition. For functional groups analysis, we used FTIR. We used mathematical modeling, particularly, Mie theory to predict the behavior of light behavior and energy conversion of certain nanocomposites.

Thus, this work has particularly focused in the synthesis of hybrid magnetic engineered composite contrast agents (MECCA) nanoparticles with biomolecules, particularly with an enzyme as a system for applications at the interface between materials science, biotechnology, and medicine. Nanoparticle derivative of silver, gold and carbon dots were prepared that could be used to develop novel biomedical and technological systems, particularly as new materials for solar conversion, light harvesting, imaging and diagnostic biomedical applications.

CHAPTER 1 - INTRODUCTION

The research and development of materials from the atomic to the macromolecular levels translate into the fabrication and use of functionalized structures, devices, and systems that take advantage of specific properties that exist at the nanoscale. The combination of nanotechnology and molecular biology has developed into new emerging research areas in nanobiotechnology and the wide development of new nanoparticle derivatives. Examples of nanoparticles include those made from organic materials such as polymers and proteins, and those from inorganic materials such as dielectrics and metals, and those composed by both. Of this wide variety, gold nanostructures have drawn significant attention due to their optical properties related to their localized surface plasmon resonance (SPR) and their suitable conjugation with biomolecular probes [1]. Their use in biotechnology and medicine is increasing steadily with current applications in imaging, biosensing, immunoassays, photothermal heating, to mention some examples.

Magnetic nanoparticles are well-established nanomaterials that offer controlled size, ability to be manipulated externally, and enhancement of contrast in magnetic resonance imaging (MRI). As a result, these nanoparticles could have many applications in biology and medicine, including protein purification, drug delivery, and medical imaging. Because of the potential benefits of multimodal functionality in biomedical applications, researchers would like to design and fabricate multifunctional magnetic nanoparticles. In principle, there are two strategies to fabricate magnetic nanoparticle-based multifunctional nanostructures. The first one, molecular functionalization, involves attaching antibodies, proteins, and dyes to the magnetic nanoparticles. The second one integrates the magnetic nanoparticles with other functional nanocomponents,

such as quantum dots (QDs) or metallic nanoparticles. Because they can exhibit several features synergistically and deliver more than one function simultaneously, such multifunctional magnetic nanoparticles could have unique advantages in biomedical applications [2]. Superparamagnetic multifunctional nanocomposites have a unique combination of features that make them appealing for a range of different applications in light harvesting, energy conversion and biomedical applications, including superparamagnetism, biocompatibility, stability, imaging capabilities, and flexibility for surface functionalization.

Scope Of This Dissertation

The overall goal of this dissertation was to synthesize hybrid multifunctional magnetic nanocomposites with different properties so they can be used in different applications. The multifunctional nanocomposites refer to functionalizing the surfaces with different functional group linkers to incorporate fluorescent probes, proteins, such as enzymes, antibodies, peptides, etc. This work concentrated in the effectiveness of immobilization of enzymes in different magnetic derivatives and the determination and assessment of enzymatic activity.

Chapter 2 describes an overview of relevant literature background related to nanomaterials and current state of knowledge on functionalized nanoparticles for biomedical applications. It also includes references on gold nanomaterials and their use in photothermal applications and imaging. A description of the work performed on hybrid multishell nanocomposite platforms with respect to magnetic nanoparticles is also given. The relevance of magnetic nanoparticle studies, their synthesis and characterization and their surface functionalization with linker derivatives is emphasized.

Chapter 3 describes a simple method implemented in this work to prepare magnetic nanoparticles with a thin layer of titanium oxides. In this approach we avoided heat treatments

and the incorporation of surfactants and other mid layers adhesive components. This simple approach with simple titania precursors and control hydrolysis allowed the preparation of derivatives with different thickness of titania oxides. The resulting nanoalloys showed excellent hydrophilic behavior, ideal for further functionalization.

Chapter 4 describes the preparation of three component nanoalloys that includes a magnetic core and a gold, and a titania shell layers. In this work we used the approach described in Chapter 3 to incorporate a titania shell layer on a previously deposited gold thin film on the magnetic core. The size and the morphology of these derivatives were determined using scanning electron microscopy, transmitted electron microscopy. Energy dispersive spectroscopy (EDS) was performed to confirm the core-shell nanostructure. The experimental parameters obtained from these derivatives were applied to Mie theory and the comparison of the experimental plots and the ones produced with Mie theory was very good.

Chapter 5 describes the incorporation of fluorescent probes and immobilized proteins (particularly the enzyme trypsin) on the surface of the magnetic synthesized derivatives presented in previous chapter, namely, superparamagnetic nanoparticles, magnetic-titania and magnetic-gold-titania nanocomposites. The synthesis was carried using in general the same approach described previously, by incorporating first the amino alkane silane, APTES, followed by reactivation with glutaraldehyde and finally attach the enzyme trypsin. The enzyme kinetic activity for each of the preparations was evaluated using Michaelis-Menten kinetics. There results and kinetic parameters in all cases were determined successfully. The incorporation of the fluorescent dyes, fluorescein and rhodamine was performed by reacting directly to the nanoparticle-APTES derivatives.

Chapter 6 describes the modification of magnetic nanoparticles with the polysaccharide dextran, a branched glucan made of many glucose molecules, and thus a biocompatible material that can be used in biological systems and in biomedical applications. To test the effectiveness of the systematic modification and coating of the magnetic nanoparticles, trypsin was incorporated and immobilized covalently via periodate oxidation and similarly to the previous enzyme analysis describe in Chapter 5, the Michalis Menten kinetic parameters were experimentally evaluated consistently and accurately and compare well with values reported in the literature for similar trypsin immobilization.

Chapter 7 provides a general summary of the conclusions and outcomes of the work performed in this dissertation.

CHAPTER 2 - LITERATURE OVERVIEW

Nanomaterials and nanotechnology in general have significantly influenced modern science and have found their way into important applications such as information applications such as in information storage, catalysis, sensing, energy storage, coatings, food industry, water purification and biomedicine among others.

Biomedicine is a particularly promising direction for nanosciences as it can potentially transform the current therapeutic and diagnostic techniques. Among all types of nanomaterials, superparamagnetic iron oxide nanoparticles and derivatives are possibly the most studied type of nanoparticles for different applications. The high interest for using these materials in biomedical diagnosis and therapy is attributed to their superparamagnetic properties at room temperature (actuated by an external magnetic field but no magnetic remanence once the field has been removed), biocompatibility, and low cost. In particular, the use of nanoparticles in biological applications has been rapidly advancing towards practical applications in human cancer diagnosis and therapy. Upon modification biocompatible nanoparticles with specific ligands or antibodies, can be used to locate cancerous areas as well as for traceable drug delivery with high affinity and specificity [2]. Inorganic nanoparticles, such as the ones described and presented here can be synthesized in the nano-size range (5–30 nm) [3], which not only renders them suitable for unimpeded circulation in the bloodstream and extravasation into

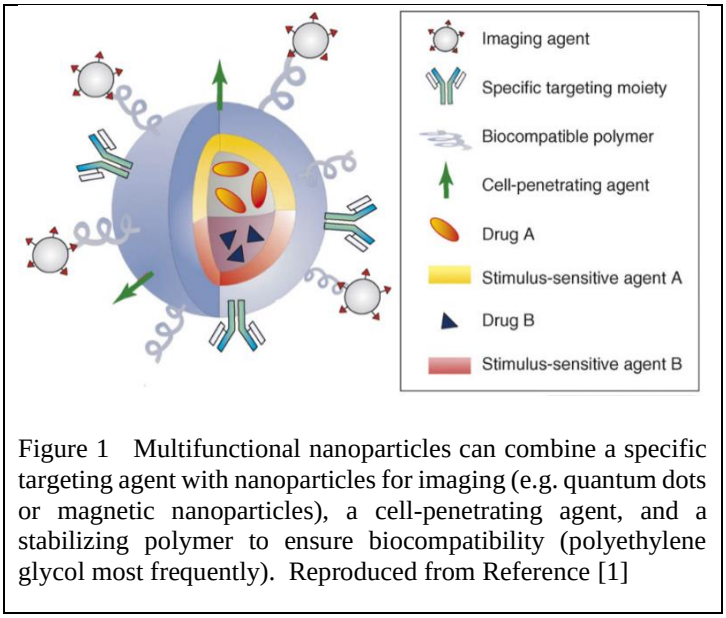

Figure 1 Multifunctional nanoparticles can combine a specific targeting agent with nanoparticles for imaging (e.g. quantum dots or magnetic nanoparticles), a cell-penetrating agent, and a stabilizing polymer to ensure biocompatibility (polyethylene glycol most frequently). Reproduced from Reference [1]

tumor tissues, but also permit excretion through renal filtration, without the need for their biodegradation [4]. Several such materials, including silica [5], gold nanoshell [6] and gold [7], nanoparticles are known for their non-antigenicity. Many such materials have unique characteristics, since they can also be used as image contrast agents, including quantum dots (QDs), quantum rods (QRs) [8] and iron oxide nanoparticles. However, their rigid matrix does not generally allow for the encapsulation and subsequent release of active molecules for conventional drug delivery purposes [9]. Nonetheless, drug molecules can be linked onto the nanoparticle surface for targeted delivery purposes [10]. Furthermore, certain nanoparticle systems could have a hybrid dual targeted therapeutic effect as for example thermal ablation and drug delivery features. In addition, nanoparticles with incorporated imaging agents offer opportunities to exploit optical imaging or MRI in cancer imaging, and guided hyperthermia therapy. Therefore, it has been suggested that the integrated systems that combine differing properties such as tumor targeting, therapy, and imaging in an all-in-one system can provide more useful multimodal approaches in the battle against cancer, for example. Figure 1 exemplifies a multifunctional nanoparticle complex similar to the ones proposed in our laboratory and in this research. By exploiting the varied chemistry, integrated systems could encapsulate multiple drugs and imaging agents, and label tumor-specific targeting moieties [1]. Such multifunctional nanoparticles can eventually detect cancer cells, pinpoint, and visualize their location in the body, kill the cancer cells, and monitor therapeutic responses. Ultimately, they will radically change the way we diagnose, treat, and prevent cancer in oncology, these systems show great promise in the emerging field of personalized medicine.

Functionalized nanoparticles for biomedical applications. Nanoparticles derivatives provide a novel class of biocompatible contrast agents with great potential in cancer imaging and therapy

[11]. The use of nanoparticles for bioimaging has several advantages [12]. First, the sensitivity of optical imaging can be significantly improved using functional nanoparticles [13]. For example, luminescent QDs and QRs have been used as contrast agent probes for cancer imaging [14]. QDs and QRs are usually composed of crystalline cadmium selenide (CdSe)-based semiconductor nanoparticles. They are ultra-small and bright, and have a narrow luminescence emission spectrum [15]. Optically-doped nanoparticles such as dye-doped ORMOSILs represent another important class of nanomaterials for cancer detection and therapy. In dye-doped nanoparticles, each silica particle typically contains hundreds to thousands of dye molecules, which enhance the fluorescence signal [12]. Dye-doped nanoparticles are generally smaller than cells, which makes them suitable for intra-cellular application. Similarly, gold NRs have been well studied for the last few years and have been successfully used for dark field imaging of cancer cells and for photothermal therapy. Nanoparticles can be much more photostable and biocompatible (if properly functionalized) than traditional chromophores (e.g. organic dye molecules) [16]. This forms the basis for their use for ultrasensitive and real-time monitoring of cancer progression. Photostable nanoparticles will allow non-invasive imaging of cancer tissue multiple times for monitoring tumor growth and the effect of cancer drugs during therapy [17]. For example, QDs and QRs are extremely photostable and exhibit low toxicity if their surface is carefully passivated [18]. The effective surface passivation of QDs or QRs with a wide-band gap semiconductor material such as zinc sulfide (ZnS) will make them photostable and lower their toxicity. In the case of optically-doped nanoparticles, chromophores remain embedded in the particle matrix, which protects the dyes from photobleaching and prevents the dyes from interacting with the biological environment [19]. This allows the safe use of dyes that are known to be toxic. Improved photostability of the embedded dyes is achieved because the silica particle matrix protects the dye from interaction with

oxygen molecules that otherwise causes the chromophores to degrade irreversibly. Finally, multiple functionalities can be combined in a single or multi-component nanoparticle, allowing simultaneous monitoring via multiple modalities [20], as can be seen schematically in Figure 1. If a nanoparticle incorporates two or more contrast agents, it can be used for precise location and non-invasive imaging using positron emission tomography (PET), CT, and magnetic resonance imaging (MRI) simultaneously for pre-surgical assessment [21]. During the surgical process, tumor tissue could be directly visualized in real-time, using fluorescent or luminescent nanoparticles. This mode of tumor visualization would provide direct guidance to surgeons for effective and complete tumor resection, enabling them to clearly differentiate the boundary between the tumor and normal tissues [12]. Already, some of these nanostructures have been successfully used in vitro and in vivo for diagnostic imaging purposes, examples of applications of these nanoparticles include dye-doped silica nanoparticles, dextran coated iron oxide nanoparticles and targeted QDs. According to the National Cancer Institute (NCI), nanotechnology has great potential to make an important contribution in cancer prevention, diagnosis, imaging, and treatment [22]. In a broad scheme, nanoparticles as colloidal systems can be fabricated from a multitude of materials in a variety of compositions [23], including quantum dots (QDs) [24] polymeric nanoparticles [25], gold nanoparticles [26], paramagnetic nanoparticles [27], and so on.

Gold Nanomaterials for Photothermal Therapy. Metallic gold nanomaterials have been extensively studied for potential applications in the emerging and highly interdisciplinary field of nanotechnology [28]. Gold nanomaterials have several attractive characteristics for diagnostic applications, including 1) biocompatibility and stability, 2) unique tunable optical properties, and 3) easy conjugation of biomolecules (i.e., antibodies) to the surface for tumor specific targeting. Thus, many biodiagnostic applications of gold nanomaterials have been developed for bioassays

or colorimetric assays to quantify proteins [29] polynucleotides [30], and bacteria [31]. However, the application of gold nanomaterials for therapeutic purposes is a largely undeveloped field. Two characteristics of gold nanomaterials make them particularly suitable for therapeutic applications: antibodies and other bioactive molecules can be easily conjugated to the surface of gold nanomaterials, and gold nanoparticles have absorption efficiencies with 4 to 5 orders of magnitude greater than conventional photothermal dyes and are not affected by photobleaching [6]. More complex shapes with excitation wavelengths of 800–1200nm could absorb NIR light, and then be converted to heat. Once gold nanomaterials are highly accumulated at the target site, they are activated via the absorption of irradiation of an appropriate wavelength, and thereby cause the irreversible thermal cellular destruction [32]. Hypothetically, this property could provide an opportunity for therapeutic treatment in deep tissues.

Hybrid Multishell Nanocomposite Platforms. Nanoalloys are particles in a nanosize range structures composed of two or more metallic elements that combined possess unique optical, magnetic, and thermal properties [33]. These particles show strength with higher conductivity and reactivity [34]. The large surface area of these particles makes them more reactive for their use in different applications. In the last few years, bimetallic/trimetallic (alloy) nanoparticles have gained much interest due to their unique optical and chemical properties [35]. Combining metallic materials together, enhances specific properties due to synergetic effects, and rich diversity of compositions, structures and properties of metallic nanostructures which let to use them in different applications. Chemical and physical properties of nanoalloys can be controlled by

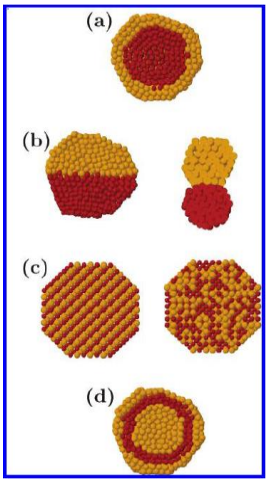

Figure 2 Schematic representation of some possible mixing patterns: core-shell (a), subcluster segregated (b), mixed (c), three shell (d). The pictures show cross sections of the clusters [36].

changing the compositions and atomic ordering as well as the size of the nanostructures. They also show different structures that could be quite different than the ones of a pure element. In addition to display different properties than bulky alloys due to finite size effects according to Ferrando et al. [36]. Ferrando et al. describes how nanoalloys structures can be classified into four general patterns as shown schematically in Figure 2, where (a) describes core-shell segregate nanoalloys, (b) subcluster segregate nanoalloys, (c) mixed A-B nanoalloys, and (d) Multishell nanoalloys. These structures can also be considered as: free/bare or passivated/coated composites.

While bare/free nanoalloys are created in the gas phase or molecular beams, coated/passivated ones are created in both gas and solution phase. In addition, they can be also supported on the surface or inside porous materials. One problem with studying bare metals is that it is difficult to study them individually due to aggregation and agglomeration. To overcome this issue, these nanoalloys can be coated or embedded onto substrates, such as metal oxides [37] or metallic shells [38]. Some of the work presented in this dissertation involves the use of this approach with coatings of titanium oxide.

The core-shell nanostructures with silica either core or shell have been found in many applications including enhanced spectroscopy or cancer therapy [39]–[41]. Titania was also found to be suitable material for environmental applications because of its biological and chemical inertness, strong oxidizing powder, cost effectiveness and long term stability against chemical corrosion and photo corrosion [42]–[44]. In fact, TiO_2 nanomaterials have been studied for their applications in so many applications such as photovoltaics and sensors [45], [46]. It is also known that titania has been used because of its ability to absorb light in the UV region, and this is because of its wide band gap of 3.2 eV [47]. However, using titania alone makes the ability of light harvesting really poor due to its low absorbance factor [48]. To increase light harvesting efficiency, titanium dioxide

have been coupled with other semiconductors that have smaller band gaps [49] or plasmonic nanoparticles [50]. The main reason of lacking of coating materials with titania is that TiO_2 precursor has a very fast hydrolysis rate, which makes the coating process really hard to control [51]. To overcome this limitation, more complex and expensive titania precursors can be used, in addition to adding more additives such as surfactants or salts, and special reaction conditions in order to slow down the reaction rates during the preparation [51]–[54]. These coating methods were used in the synthesis of gold core-titania shell nanostructures ($Au@TiO_2$ core-shell nanostructures) [55], as well as $Fe_3O_4@TiO_2$ [56]–[58], and more general method [51]. The core-shell nanostructure with the noble metal such as Au as a core or shell gained great interest in medical and environmental applications [59], [60]. The surface plasmon resonance properties of gold nanoparticles in core-shell structures with titania for example, have been found to increase the optical absorption of titania and that it also helps in extending its absorption band to the visible light region [37]. Gold as a shell has also been shown that in Au-coated Fe_3O_4 nanoparticles it helps in reducing surface oxidation of iron oxide nanoparticles [61]. It also has been proved that gold is an excellent nanoalloy candidate component because of its easy reductive preparation and high chemical stability. In fact, it has been used in coating magnetic nanoparticles due to their multifunctional properties and these have been used in different biomedical applications, such as magnetic resonance imaging contrast agent [62], [63], drug delivery [64], hyperthermia [65], and in optical sensors applications [66].

Magnetic Gold Nanoshells for Photothermal Therapy and Imaging. In biomedical applications, various types of nanomaterials have been studied, including QDs as fluorescence imaging agents, MNPs as contrast agents in MRI, and gold nanomaterials for hyperthermia. The combination of these different nanomaterials can lead to the development of multifunctional

nanoparticle platforms for simultaneous targeted delivery, fast diagnosis, and efficient therapy. Recently, the fusion system of gold nanoshells, magnetic nanoparticles, and cancer-cell-specific antibodies has been explored as a multifunctional platform for simultaneous diagnosis via MRI and NIR photothermal therapy [67]. Results of these types of work are illustrated in Figure 3.

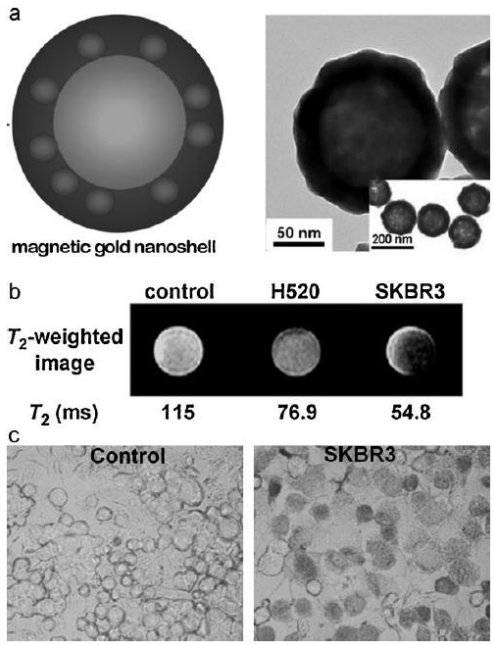

Figure 3 a) Scheme and TEM images of the magnetic gold nanoshells (Mag-GNS). b) T2-weighted MR images of control SKBR3 cells, HER2/neunegative H520 cells incubated with Mag-GNS-AbHER2/neu, and HER2/neu-positive SKBR3 cells incubated with Mag-GNS-AbHER2/neu after irradiation and subsequent staining. Reproduced from [31]

For targeted MRI and NIR photothermal therapy magnetic gold nanoparticles that are composed of a 15 nm-thick gold shell with embedded Fe_3O_4 nanoparticles (7 nm) around the silica sphere core (100 nm) have been prepared as illustrated in Figure 3a. The surfaces of these two magnetic gold nanoshell particles were further modified with anti-HER2 to specifically target epidermal growth factor receptors (EGFR). These anti-HER2 conjugated magnetic gold nanoshell particles, which display an optical resonance peak, decreased the MR signal intensity (darkening), this is

illustrated in Figure 3b, while exhibiting strong surface plasmon-enhanced scattering properties in SKBR3 cells. Furthermore, SKBR3 cells treated with NIR light, after incubation with anti-HER2 conjugated magnetic gold nanoshell particles, were selectively destroyed only in the NIR laser treated region, this is shown in Figure 3c. These results demonstrated that targeted multifunctional magnetic gold nanoshell particles can be used as molecular imaging agents, optical imaging contrast agents, and targeted photo-based therapeutic agents for diagnosis and therapy of breast cancer. Thus, these inorganic nanostructures, of semiconductor quantum dots and plasmonic structures of gold and other metals, have emerged as highly useful materials for new classes of photonic components that can control and operate light absorption and emission at the nanoscale. Quantum dots and gold nanoshells, for example, have demonstrated properties of great interest for optical imaging [68]. Their exceptional stabilities, tunability of optical properties, and high yield of optical signals they generate are superior to the more traditional probes based on organic molecules.

Magnetic Nanoparticles (Fe_3O_4)

Magnetite Fe_3O_4 nanoparticles are common materials that have been studied over decades now over so many applications, as contrast agents for cancer diagnosis for example [69]–[71]. They have attracted much more interest due to their potential applications in medical and electronic areas. The application of iron oxide nanoparticles always requires the size to be controlled in order to get specific tunable magnetic properties [72]. Magnetic nanoparticles are found to be good candidates in core-shell structures as a core for applications in photocatalysis, due to many reasons, such as (1) low toxicity and biocompatibility, (2) high magnetization, (3) it has low curie temperature [73]–[75] , and (4) strong band between small molecules due to dipole-dipole interactions [76]. Magnetic nanoparticles are in general not ideal to be used alone because of low

electrical conductivity and limited optical properties [77]. Another reason that they can't be used without surface modification is that since they have large surface area to volume ratio and low surface charge at neutral pH, using them without coating leads to aggregation when they are dispersed in working solvents [78]. This challenge can be overcome using surface coatings and modifications [79]. Modifying the surface allows these nanoparticles to be used for enzyme immobilization, for example, consequently enhancing their solubility properties. Immobilization of enzymes on magnetic nanoparticles have several advantages, such as ease of separation of enzymes from reaction mixtures and their reuse in principle, many times [80]. Enzyme immobilization can be divided into : (1) bindings to a support, (2) entrapment, and (3) crosslinking [81]. In this dissertation, our working enzymes were directly bound to the surface of magnetic derivatives.

Synthesis of magnetic nanoparticles

Magnetic nanoparticles can be synthesized following different physical methods, such as gas phase deposition [82] and electron beam lithography [83]. However, these methods are difficult to follow in order to control the size and the shape of nanoparticles. Magnetic nanoparticles can also be synthesized following different chemical methods, such as microemulsions [84], polyol method [85], sol-gel [86], hydrothermal [87] and electrospray syntheses [88]. The most common method to synthesize magnetic nanoparticles is coprecipitation [89]. Which involves coprecipitation of Fe^{2+} and Fe^{3+} aqueous salt solutions in alkaline solution.

Oxidation of magnetic nanoparticles can easily affect the physical and chemical properties of the particles. This is the reason for using an oxygen free environment during the synthesis of these iron oxide nanoparticles. This approach helps in reduction of the magnetic nanoparticles size compared to the method that doesn't follow an oxygen free environment reaction [90]. Magnetic

nanoparticles have also been coated with organic and inorganic materials in order to protect them from agglomeration and oxidation, these include dextran, gold and gadolinium [91]–[93]. These coatings are also known to reduce the cytotoxicity of these particles as well. Coating magnetic nanoparticles makes them more stable in solution and more dispersible especially for biomedical applications. Controlling the size and the shape of the magnetic nanoparticles depends on the type of salt used in their preparation, such as chlorides, sulphates and nitrates, Fe^{2+} to Fe^{3+} ratio, pH of the solution, temperature of the reaction and the ionic strength of the media [94]–[96].

Nanoparticle Characterization

The physicochemical properties of nanoparticles are determined by the size, morphology and similar structural characteristics. Three typical methods for determining the size of nanoparticles are transmission electron microscopy (TEM), X-ray diffraction (XRD), and dynamic light scattering (DLS).

TEM works resembles a digital camera that captures the association between an electron and the substance being studied. Since electrons have a short wavelength of 0.1nm, TEM can resolve minor information in a substance down to the atomic level [97]. As a result, this technique will reveal the size of nanoparticles in a sample as well as their mono- or polydispersity. It may also provide details on the nanoparticles' morphology and aspect ratio. Furthermore, since polymeric shells and organic ligands are weak scatterers of electrons and appear translucent in an electron beam, this technique allows adequate electron densities to achieve high-quality TEM imaging. To achieve enhanced contrast, heavy-metal special staining or cryogenic methods are required and also, in order to obtain a proper representation of the sample, an image treatment study on a statistically relevant number of particles is often needed. Since sample preparation may often

cause nanoparticle aggregation, TEM measurements cannot be indicative of the size and distribution of nanoparticles in a solution.

Powder X-ray diffraction (XRD) can be used to figure out effectively the size of the iron oxide cores. This is a bulk approach, which ensures it can include data that is descriptive of the whole sample. It may be used to measure phase structure and possible impurities in addition to probing the size of nanoparticles. The only disadvantage of this approach is that it can only be used for crystalline materials and suggests that the nanoparticles have a spherical structure. This approach does not include detail about the nanoparticles' morphology. It is, however, an excellent supplement to TEM for confirming the size of nanoparticles, such as Fe_3O_4 cores.

DLS is a technique for determining the hydrodynamic size of nanoparticles in solution as well as their size distribution. A laser beam travels through a sample (nanoparticle dispersion) during DLS tests, and the light is dispersed by the nanoparticles in solution. Rapid testing times, as well as ease of operation and suitability for qualitative agglomeration control [98], are all advantages of DLS. As a result, DLS dimensions are often used in combination with TEM and XRD.

Surface functionalization

To improve the stability of magnetic nanoparticles, functionalizing the surface with organic or inorganic materials is desired. Functionalizing the surface with organic materials is an effective method that has been used widely. Since magnetic nanoparticles are hydrophobic, they tend to interact with each other and form larger-sized particles. In order to overcome this issue, functionalizing the surfaces with certain compounds will enhance the stability of the particles and inhibit the aggregation. Magnetic nanoparticles should be coated to have colloidal stability, allowing them to avoid agglomeration and precipitation. Electrostatic or steric repulsion can be used to achieve colloidal stability, these features are all illustrated schematically in Figure 4. By

creating an electrical double layer around the nanoparticles, which increases the repulsion between charged nanoparticles, electrostatic stabilization may be achieved. By grafting polymers to the surface of nanoparticles, steric stability can be achieved.

Ameneh Heidari *et al*. [116] coated magnetic nanoparticle with cetyltrimethylammonium bromide (CTAB) and benzyl-secondary ammonium chloride (BKC) and were able to obtain efficient results in reducing the size of the particles and enhanced the stabilization as well [99].

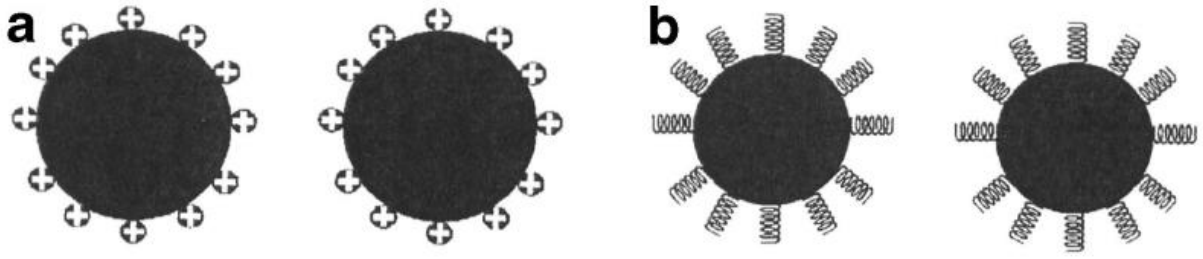

Figure 4 Types of colloidal stabilization : a) electrostatic repulsion and b) steric repulsion [100]

The structure of magnetic nanoparticles functionalized with an organic molecule consists of magnetic nanoparticles and an incorporation of an organic compound, where iron oxide is used as a core. Jiang *et al.* illustrated the structure of the magnetic nanocomposite into structures of, core-shell, matrix, and $shell_a$-core-$shell_b$ as shown descriptively in Figure 5 [101].

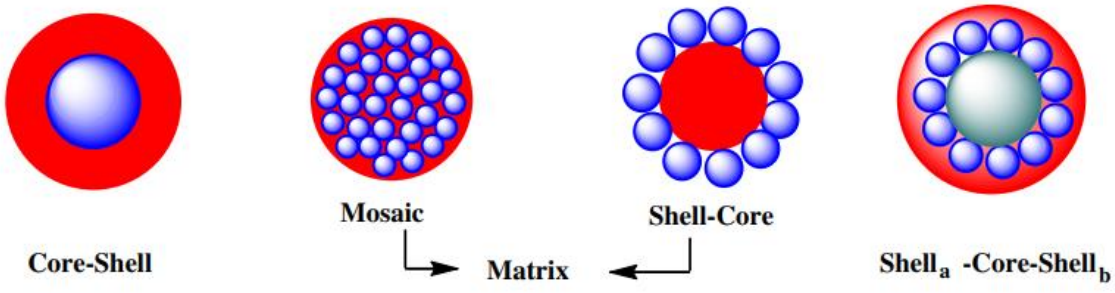

Figure 5 The main structure of magnetic nanoparticles modified by inorganic materials [101]

In essence, functionalizing these surface with the organic materials add features of biocompatibility and biodegradability to these structures. Also, organic molecules on the surface can provide other functional groups that can favor the attachment of specific ligands, such as aldehyde, hydroxyl, carboxyl, and amino groups relevant in different applications [102]. For example, Jin Soon Han *et al.* functionalized iron oxide nanoparticles with polyethylene imines (PEI) and polyacrylic acid (PAA) to stabilize the particles and to add different functional groups [103].

The polysaccharide dextran and polyethylene glycol (PEG) are the most commonly used functionalizing coatings used especially for biomedical applications, such as in magnetic resonance imaging (MRI) [104]–[106], drug targeting [107], [108], and magnetic fluid hyperthermia [109], [110]. Coating magnetic nanoparticles with these materials helps to avoid aggregation and improve cellular uptake of the particles. In fact, magnetic nanoparticles coated with dextran have been already approved to be used in biomedical applications by the Food and Drug Administration (FDA) especially for MRI applications [111]. In addition, functionalizing magnetic nanoparticles with thermo-responsive polymers has been investigated for drug delivery which resulting in release of the drug due to changes in the matrix structure at specific temperatures [92], [112], [113].

Functionalizing the surface of magnetic nanoparticles with inorganic materials is also common to stabilize and protect the particles from aggregation and oxidation. Coating the particles with silicon oxide (SiO_2) for example become quite common due to its biocompatibility and this feature allows further activation with other functional groups for different applications, such as in catalysis, adsorption and magnetic separations [114]. For instance, Thi Kieu Hanh Ta *et al*. coated magnetic nanoparticles with SiO_2 to increase the biocompatibility to be used in bio-

conjugation studies [115]. Cong Hailin *et al*. also coated magnetic nanoparticles with SiO_2 to be used in catalysis, gas separation and biomedicine [116].

Another method to protect the magnetic nanoparticles from aggregation and oxidation is to coat them with a layer of a shell of metal. Coating magnetic particles with another metal not only protects them but also expand the application of these magnetic nanoparticles. Luiz Fernando Oliveira Maia *et al*. [134] synthesized magnetic nanoparticles following a coprecipitation method, then coated them with gold shell to adsorb Hg from sewage [117].

Aminopropyltriethoxysilane (APTES) functionalization

One of the most common linkers used with nanoparticles is aminopropyl triethoxysilane (APTES), its general chemical formula of this silane derivative is $Y\text{-}(CH_2)_n\text{-}Si\text{-}R_3$, where Y represents the head group, $(CH_2)_n$ an alkane chain, and $Si\text{-}R_3$ is the anchor group where the silane is attached to the metal oxide surface. Functionalizing the surfaces of metal oxides, such as silica, titania or magnetic nanoparticles with APTES makes these particles reactive and ready for modifications with a variety of functional groups can be used in different applications [118]–[120].

Glutaraldehyde functionalization

Glutaraldehyde is the most popular bis-aldehyde homobifunctional crosslinker in use nowadays [121]. It has been used extensively as homobifunctional crosslinking reagent especially for antibody-enzyme conjugations [122], [123]. The reaction of the glutaraldehyde with proteins and other amine-containing molecules occur through the formation of Schiff base reactions. Schiff base formation usually occur sat alkaline pH. The higher the pH, the more efficient the Schiff base is. Glutaraldehyde may react with other amine modified particles either through the Schiff

base or through addition at other point of unsaturation [121] as illustrated schematically in Figure 6.

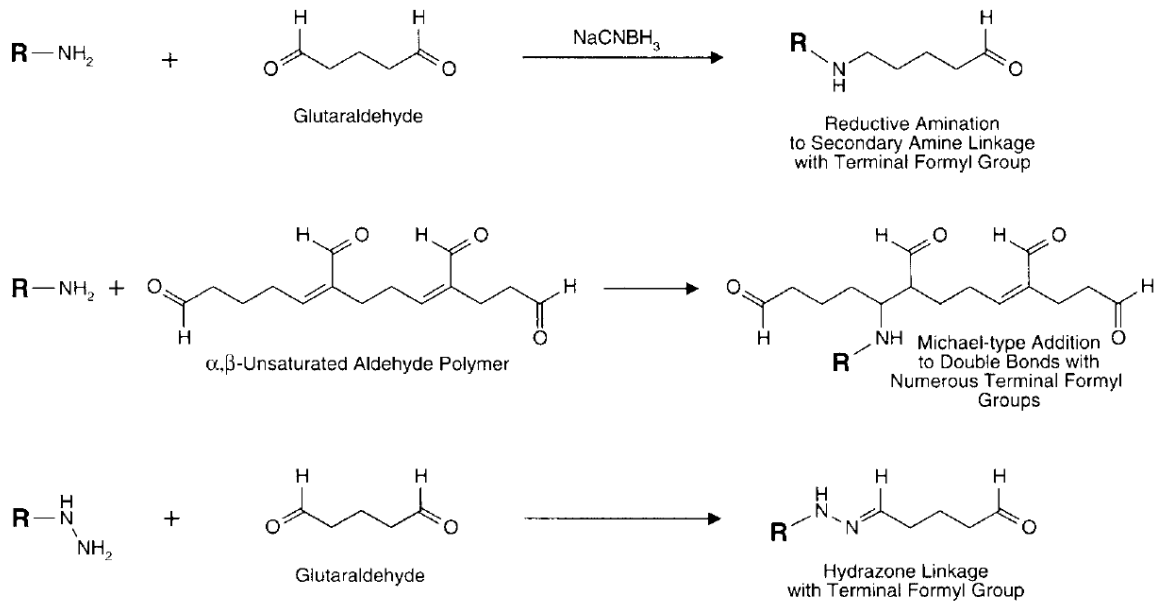

Figure 6 Glutaraldehyde may react by several routes to form covalent crosslinks with amine-containing molecules [121]

Quantum dots (QD)

Quantum dots (QDs) have attracted increasing interest due to their electrical and florescence properties [124]–[126]. These features allow these nanoparticles to be used in different applications and different fields, such as light-emitting devices [127], photonic crystals [128], and antibiotics detection [129]. Unlike organic fluorophores, QDs luminescence emission spectra can be controlled rather precisely [130], [131]. At different emission spectra, QDs can be excited by a wide range of wavelengths [125], [132]. Besides, the quantum yield for these nanoparticles is really high and is resistant to photoleaching, thus represents a huge advantage when compared to organic fluorophores [133]–[135].

The synthesis of multifunctional magnetic nanoparticles (MNPs) is a highly active area of current research that finds applications at the interface between materials science, biotechnology, and medicine. These can be used to develop novel biomedical and technological systems with unique characteristics. By virtue of their unique physical properties, functional hybrid nanoparticles are emerging as a new class of materials that have proven to increase solar conversion efficiency and provide new sources of light harvesting and imaging and diagnostic biomedical applications. At present, nanomaterials' development has moved beyond the discovery of totally new materials and compositions to a broader impact that includes the investigation of more complex, composite systems, in which the recombination of known materials into structures of higher complexity opens new possibilities of functionality and applications.

The work performed in this dissertation in terms of syntheses of multifunctional derivatives made use of the techniques presented in this literature review. We carried out several variations of the procedures to complement the synthesis of specific nanoparticle derivatives, particularly in the modification of magnetic nanoparticles and attachment of active enzyme molecules.

CHAPTER 3 - SYNTHESIS AND CHARACTERIZATION OF MAGNETIC-TITANIA CORE-SHELL NANOPARTICLES

Abstract

In this chapter an experimental protocol that facilitates the preparation of magnetic titania nanoalloys, specifically magnetic core-titania shell derivatives is presented. In this approach, the traditional method of preparing this alloys involve a cumbersome heating treatment [136], or the incorporation of an adhesive m mid layer between the magnetic nanoparticles and the titania shell, steps usually required for most titania coating methods [58]. This approach here was adapted from two reported methodologies, first iron oxide nanoparticles were synthesized using the method of s Song *et al.* [137], followed by the hydrolysis and polycondensation reaction of titanium (IV) butoxide (TBT) described by Bartosewicz *et al.* [37], [138] on the surface of the magnetic nanoparticles. The preparation of the magnetic-titania core-shell nanoparticles in this work offered a simple direct method of synthesis that did not require the use of high temperature, an oxygen free atmosphere or the use of a surfactant layer between the magnetic nanoparticle and the titania shell. This coating process of magnetic nanoparticles with different uniform shell thickness of titanium dioxide is shown schematically in Figure 7. These nanoparticles combine the magnetic field properties of the iron oxide (core), and the photoactivity of the TiO_2 shell. The size and the morphology were determined using Transmitted Electron Microscopy, and Energy Dispersive Spectroscopy (EDS) was performed to confirm the core-shell nanostructure.

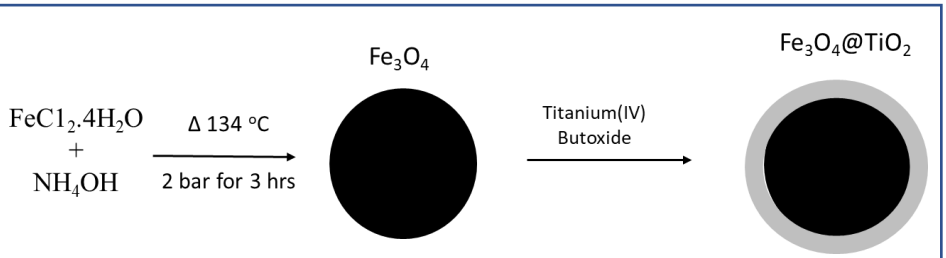

Figure 7 Fe_3O_4@TiO_2 core-shell NPs

Introduction

The potential for biomedical and environmental applications has sparked interest in magnetic nanoparticles recently. While the in vivo application of other types of nanoparticles is still limited by concerns over their toxicity, superparamagnetic nanoparticles have received the approval of the Food and Drug Administration (FDA) for clinical use in humans, for example, as magnetic resonance imaging (MRI) signal enhancers and hyperthermia therapeutical agents. They could be used as external field regulated carriers of drugs and biomolecules, negative contrast agents in magnetic resonance imaging (MRI), supplementing Gd complexes, and heating agents in AC magnetic field induced hyperthermia for cancer tissue therapy [100], [104]. All of these different applications require particles that are less than 100 nm in size, and narrow particle size distribution. They also require surface coating of the particles, that would protect the particles from aggregation, oxidation and corrosion. At the same time they have to be non-toxic, soluble, biocompatible [139], stable, and serve as anchors for attaching specific functional moieties [140]. This coating would allow to target these particles to use in different application areas [100]. The nanoalloy particles after coating and functionalization would be able to bind to drugs, proteins (enzymes, antibodies) or nucleotides, so they can be directed to interact with specific organs, tissues, or tumors using an external magnetic field [141].

These magnetic nanoparticles after proper modification can also be used in the treatment of wastewater, for example remediation of heavy metals and different pollutants from water [142]. They have been used, for example when modified with specific chelating agents for the removal of different radioactive metals [143], [144].

Titania (TiO_2) is a semiconducting material that is n-type material and has a wide direct band difference (3.2 eV) [145]. Because of its very high refractive index in the visible light region, TiO_2 absorbs UV radiation (wavelength 390 nm) while allowing visible light to pass through very slowly (2.6). Nontoxicity, high free hydroxyl production, and thermal stability, environmentally friendly, biological and chemical inertness, and cost effectiveness are among other advantages of titania oxides materials[146], [147].

Salmat *et al.* synthesized magnetic nanoparticles coated with titania using the dust of an electric-arc furnace at 180^{o}C and calcinated at 400 ^{o}C, and evaluated its photocatalytic activity for organic removal from wastewater [58]. Kumara *et al.* also synthesized porous titanium silicate-Fe_3O_4 using a hydrothermal method [57]. In addition, Chanhom *et al.* synthesized nanocomposites of $Fe_3O_4@SiO_2@TiO_2$ to investigate the effect of thickness of silica interlayers between titania (outer shell) and magnetic (core) nanoparticles [136].

Coating magnetic nanoparticle with titania has been used widely, where heat treatment at high temperature was considered essential [148], or was necessary to add a layer between the titania and the magnetic nanoparticles [136]. The magnetic properties show a deterioration with the magnetic nanoparticles when exposed to a high temperature. The process also can involve diffusion of impurities between the two layers (the magnetic-core and the titania-shell), that could result in a decrease of the photodegradation activity [145]. In other words, these reported

methods affect the size, shape, structure and the performance of photocatalytic activity of these magnetic nanocomposites.

In this work, we synthesized iron oxide nanoparticles and coated them with a layer of titania with different shell thicknesses, by following Song *et al* [137], for the synthesis of Fe_3O_4 nanoparticles, followed by hydrolysis and polycondensation reaction of titanium(IV) butoxide (TBT) as reposrted by Bartosewicz *et al.* [37], [138] on the surface of the magnetic nanoparticles. The combination of these two methods allowed the preparation of magnetic core-titania shell nanoparticles in easier steps, that according to experimental analysis with substantial stability, and effective nanostructure surface properties (oxide group saturation). These nanoparticles combine the magnetic field properties of the iron oxide (core), and the photoactivity of the TiO_2 shell. The size and the morphology were determined using Transmitted Electron Microscopy, and Energy Dispersive Spectroscopy (EDS) was performed to confirm the core-shell nanostructure.

Materials and methods

Experimental. First, the synthesis of Fe_3O_4 nanoparticles was performed following the hydrothermal approach reported by Song *et al.* [137]. The coating of the Fe_3O_4 nanoparticles with titania was performed followed hydrolysis and polycondensation reaction of titanium (IV) butoxide (TBT) described by Bartosewicz *et al.* [37], [138].

Chemicals. Ammonium hydroxide (NH_4OH, 28%), iron chloride $FeCl_2 \cdot 4H_2O$ (99%), titanium (IV) butoxide (>97%) and methylamine (40% w/w aq. soln.) were purchased from Sigma-Aldrich. Ethanol 100% was purchased from the University of Arizona. Acetonitrile was purchased from Fisher-Chemicals.

Methods

Synthesis of Fe_3O_4 NPs. Magnetic nanoparticles were synthesized following the aforementioned hydrothermal approach. Briefly, (0.25 g) of $FeCl_2 \cdot 4H_2O$ was dissolved in 12.75 mL of DI water. Under continued stirring, (1.25 mL) of ammonium hydroxide 28% was added and the solution turned suddenly into a dark greenish blue solution. To allow the iron (II) to be oxidized, the solution was continuously stirred in air for 10 min. The dark mixture was then transferred into a 40 ml Teflon-lined stainless-steel autoclave at 134 °C for 3 h with a gauge pressure of 2 bar, then cooled down to room temperature. The black precipitate was collected and purified with water and ethanol via a centrifugation process. The final Fe_3O_4 NP suspension was lyophilized to finally obtain a black dry powder that was stored at room temperature until further use.

Synthesis of Fe_3O_4@TiO_2 core-shell NPs. The magnetic-titania nanocomposites were synthesized following the hydrolysis and polycondensation reaction of titanium (IV) butoxide described previously. Briefly, 20 ml of ethanol was mixed with 20 ml of acetonitrile before adding 300 μL of Fe_3O_4 nanoparticles and stir it for 5 minutes. Next, 45 μL of methylamine water solution was added and let it stir for another 5 minutes. Afterwards, 8 mL of the TBT solution (4mM) in ethanol were added dropwise using a syringe pump. In about 15 min of reaction the stirred solution turned milky. The stirring continued for 12 h and afterwards (presumably after the reaction reached completion), the synthesized magnetic-titania nanoparticles were collected with a magnet, centrifuged and washed several times with ethanol. The final precipitate was stored at room temperature and kept until further use.

Nanoparticle Characterization:

TEM analysis was carried out using a Hitachi HF-5000 High resolution analytical, 200 kV transmission electron microscope (TEM) at the University of Arizona at the spectroscopy core facility. TEM samples are prepared by placing a drop of diluted suspensions onto a 200 mesh

carbon coated cupper grids and allowed to dry in air at room temperature, before the measurements. Energy dispersive spectroscopy (EDS) will be performed on the Magnetic properties will be measured using vibrating sampling magnetometer (VSM).

Results and discussion

The synthesis of magnetic nanoparticles was obtained without any experimental difficulty. The size of the average magnetic nanoparticles was 31 nanometers of diameter as determined by TEM. problems. The titanium oxide (TiO_2) shell deposited on the magnetic core was carried out straight forward without particular precipitation or aggregation problems. It appears that the interaction of the titanium precursor reacted quite effectively with the hydroxyl groups of the magnetic surface and that after hydrolysis of the titania derivative a more saturated hydroxyl layer on the titania surface emerged. A hypothetical two step route of the possible modification on the magnetic surface is shown schematically in Figure 8 (observation based on similar reactions reported in the literature [149] . Because metal alkoxides are known to hydrolyze quickly, controlling hydrolysis processes is one of the most important aspects of sol-gel processing with transition metal alkoxides [150]. It appears that the use of titanium (IV) butoxide allowed better control the fast hydrolysis usually observed in similar functionalizations. [37].

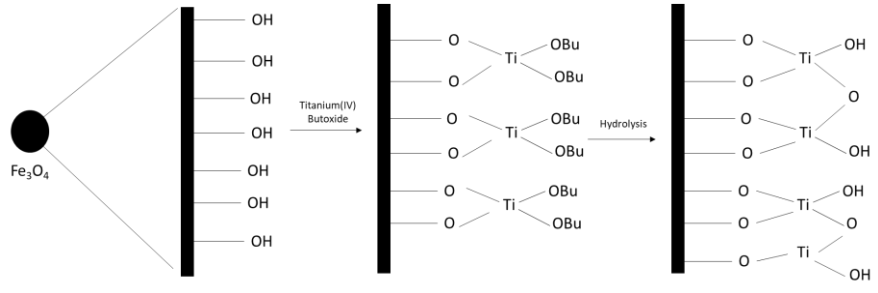

Figure 8 The reaction on the formation of TiO2 layer on the surface of magnetic nanoparticles

The synthesized iron superparamagnetic nanoparticles was performed effectively following the referenced typical hydrothermal approach, that allowed the implementation of an effective method to control the size of magnetic nanoparticles at the end of the reaction. The iron oxide nanoparticles were synthesized by oxidation of $FeCl_2 \cdot 4H_2O$ in ammonium hydroxide under high temperature and pressure. The average diameter of the prepared nanoparticles was 31 nm. The incorporation of the titania oxide on the bare magnetic nanoparticles was evident by observing their stability in terms of aggregation and further modification of the hydroxyl moieties on the titania surface. TEM and EDS images of the synthesized $Fe_3O_4@TiO_2$ core-shell nanostructure are presented in Figure 9 and Figure 10, respectively. Figure 9 and Figure *10* describe the morphology and elemental analyses of the Fe_3O_4 covered with titanium oxides, a clear core-shell nanostructure. The superparamagnetic cores coated with a layer of titania was observed to be in all samples spherical in shape, as shown in Figure 9. The magnetic-titania nanoparticles are clearly larger than bare magnetic nanoparticles, with an average size of 60 nm, thus indicating a layer of 15 nanometers of thickness. Magnetic particles with a diameter of less than 30 nm are reported to show superparamagnetism [151]. Based on the literature and the results in this work, the magnetic nanoparticels obtained here are superparamagnetic and in principle could be used effectively in biomedical applications.

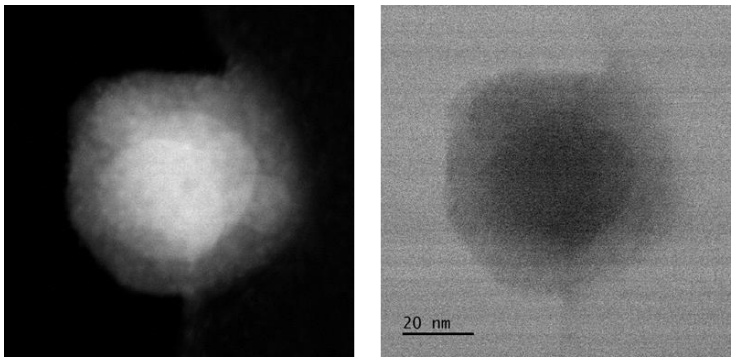

Figure 9 TEM images of Fe3O4@TiO2

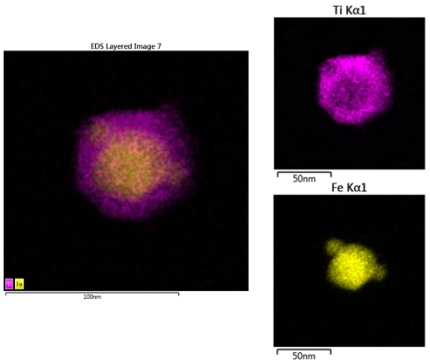

Figure 10 Energy Dispersive spectroscopy EDS images of Fe3O4@TiO2 magnetic-titania core-shell nanostructure

Conclusions

In conclusion, following and combining two reported methods for preparation of magnetic nanoparticles and surface modification, a simple approach to synthesize core-shell magnetic titania nanoparticles was obtained. These nanocomposites exhibit excellent hydrophilic behavior, and the implementation of the method allows a simple preparation of these nanocomposites with different titania shell thickness. The method in general requires simple titania precursors and a step of control hydrolysis. The method does not require the addition of any additives, with the ability to control the thickness of the shell by changing only the concentration of the titania precursor. These nanoparticles combine the magnetic field properties of the iron oxide (core), and the photoactivity of the TiO_2 shell. To confirm the effectiveness of this coating method, TEM and EDS imaging were performed and show very clearly a well-defined structure of a magnetic core and a titania shell. These nanocomposites offers a surface rich in hydroxyl moieties that can be functionalized effectively with other functional groups for further applications.

CHAPTER 4 - SYNTHESIS AND CHARACTERIZATION OF MAGNETIC-GOLD TITANIA CORE-SHELL NANOSTRUCTURES

Abstract

This chapter describes a new approach to prepare nanocomposites with a magnetic core (Fe_3O_4), a middle noble metal (Au) thin film layer and a titania oxide (TiO_2) outer shell. These structures hypothetically combine the magnetic properties of the iron oxides, the surface plasmon resonance properties of the gold layer and the intrinsic photoactivity of the TiO_2 shell. The magnetic core nanoparticles were synthesized as described previously. The gold layer was incorporated on the magnetic core quite effectively following an electroless deposition step. The titania shell coating was incorporated following a reported method that intrinsically produces stable nobel metal coatings and allows better control of shell formation kinetics and does not require additives or special reaction conditions. The size and morphology of the nanocomposites were determined using scanning electron microscopy, transmitted electron microscopy. Energy dispersive spectroscopy (EDS) was performed to confirm the core-shell-shell nanostructure. The optical characteristics of the structures were obtained using UV-vis spectroscopy. The experimental nanocomposite absorbance spectrum compared quite well with the theoretical spectrum expected with Mie theory using the experimental parameters from this work.

Introduction

Core-shell nanostructures like the ones presented here have been studied widely in the literature [152], [153] due to their unique features of combining two or more materials and therefore

properties together. Controlling the size and the morphology of core and shells could lead to materials with new optical, resonance and photonic features and properties that cannot be observed in one material alone. These properties can be modified either by the structure of the material or the ratio of the core to shell or ration of shells [154], for instance in their abilities to control the surface function to meet specific application requirements [28], [155]. Core-shell nanostructures for example, with silica either core or shell have been used in many applications including enhanced spectroscopy or cancer therapy [39]–[41]. Titania has been also used as a suitable material in environmental applications because of its biological and chemical inertness, strong oxidizing properties, cost effectiveness and long term stability against chemical corrosion and photo corrosion [42], [44], [156]. TiO_2 nanomaterials have also been extensively studied for their applications as photovoltaics and sensor platforms [43], [46]. It is also known that titania has been used because of its ability to absorb light in the UV region, and this is because of its wide band gap 3.2 eV [45]. This wide bandgap allows titania to only absorb light from the UV range.

Magnetite (Fe_3O_4) nanoparticles are common materials that have been studied over decades now over so many applications, as contrast agents for cancer diagnosis for example [47], [69], [71]. They have attracted much interest due to their potential applications in medical and electronic areas. The application of iron oxide nanoparticles always required the size to be controlled to get specific tunable magnetic properties, which is a great challenge. Magnetite nanoparticles are commonly synthesized using coprecipitation of Fe(II) to Fe(III) ions in solution [70], [157], [158].

The core-shell nanostructures with noble metals such as Au or Ag as a core or shell have gained great interest in medical and environmental applications [38], [60]. The surface plasmon

resonance properties of gold nanoparticles in core-shell structures with titania for example, have been found to increase the optical absorption of titania. Also, it has been found that it helps in extending its absorption band to visible light region. Gold as a shell has also been shown that the Au-coated Fe_3O_4 nanoparticles helps in reducing surface oxidation of iron oxide nanoparticles [61]. It also has been proved that gold is an excellent candidate because of its easy reductive preparation and high chemical stability [72].

The main reason of lacking of coating materials with titania is that TiO_2 precursors have a very fast hydrolysis rate kinetics which makes the coating process really hard to control [51]. To overcome this limitation, more expensive titania precursor can be used, in addition to adding more additives such as surfactants or salts, and special reaction conditions in order to slow down the reaction rate [51]–[54]. These coating methods have been reported in the synthesis of $Au@TiO_2$ core-shell nanostructures [55].

Mie theory is used to calculate the scattering of light as a function of wavelength. By solving the Maxwell equations for absorbed light by metallic nanoparticles in spherical polar coordinates, the Mie theory can be implemented [159]. The constant coefficients can be obtained using suitable boundary conditions at the surface of the spherical nanocomposites, while the solution is expressed in term of infinite series. In this chapter we implemented Mie theory to compare the experimental results obtained with the core-shell-shell nanostructures.

In the present work, the schematic shown in Figure 11 summarizes the typical process used to synthesize the magnetic-gold-titania core-shell-shell nanostructures. In general, three steps were followed. First, the preparation of iron oxide nanoparticles with an average size of 30 nm following a hydrothermal approach [137]. Second, the coating of Fe_3O_4 nanoparticles with a Au shell to form core shell nanoparticles were prepared first by the simple citrate reduction of

Au(III) [38]. Finally, the TiO_2 shell was created on the core-shell nanostructure following the method reported by Bartosewicz *et al.* [37], [138]. The size and the morphology were determined using scanning electron microscopy, transmitted electron microscopy, and Energy dispersive spectroscopy (EDS) was performed to confirm the core-shell nanostructure. The optical properties of the synthesized core-shell structure were characterized using UV-vis spectroscopy and compared with theoretical analysis of Mie theory.

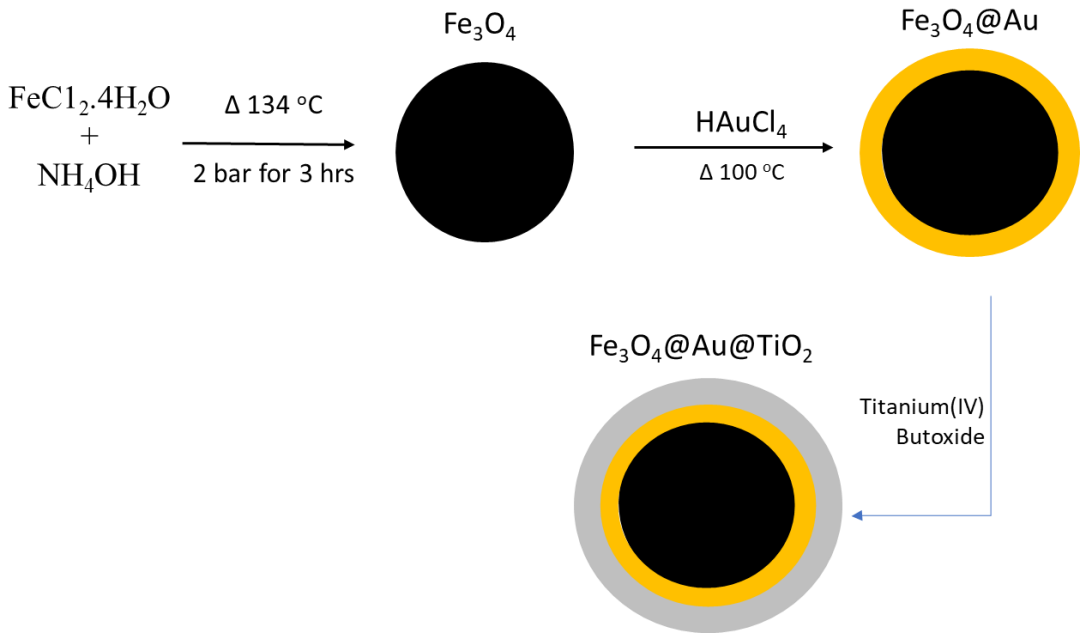

Figure 11 Schematic of synthesis of magnetic-gold-titania core-shell nanostructure. Iron oxide nanoparticles are first produced then gold and titania shell were coated, respectively.

Materials and methods

Experimental

We followed the hydrothermal approach described by Song *et al.* [137], for synthesis of Fe_3O_4 nanoparticles. For coating Fe_3O_4 nanoparticles with Au, we followed Choi *et al.* [38]. To coat the core-shell nanoparticles, we followed the hydrolysis and polycondensation reactions of titanium(IV) butoxide (TBT) by Bartosewicz *et al.* [37], [138].

Chemicals:

Ammonium hydroxide (NH_4OH, 28%), gold(III) chloride trihydrate ($HAuCl_4 \cdot 3H2O$, ≥ 99.9 %), $FeCl_2 \cdot 4H_2O$ (99%), sodium citrate, titanium(IV) butoxide (>97%) and Methylamine (40% w/w aq. soln.) were purchased from Sigma-Aldrich. Ethanol 100% was purchased from the University of Arizona. Acetonitrile was purchased from Fisher-Chemicals.

Methods

Synthesis of Fe_3O_4 NPs

Briefly, (0.25 g) $FeCl_2 \cdot 4H_2O$ was dissolved in 12.75 mL of DI water. Under continues stirring, (1.25 mL) of ammonium hydroxide 28% was added and the solution turned suddenly into a dark greenish blue solution. To allow the iron (Fe(II)) to be oxidized, the solution was continuously stirred in air for 10 min. The dark mixture was then transferred into a 40 ml Teflon-lined stainless-steel autoclave at 134 °C for 3 h with a gauge pressure of 2 bar, then cooled down to room temperature. The black precipitate was collected and purified with water and ethanol via a centrifugation process. The final Fe_3O_4 NP suspension was lyophilized, a black dry powder was obtained and kept at room temperature until further use.

Synthesis of Fe_3O_4@Au core-shell NPs.

In order to create core-shell nanoparticles of Fe_3O_4@Au, 15 ml of $HAuCl_4 \cdot 3H_2O$ with a concentration of (2mg/ml) solution was dissolved into 100 ml of DI water and heated until boiling. When the temperature reached 90 ^oC, 5 mg of pre-synthesized iron oxide nanoparticles were added into the flask. At this point the solution turned into a dark brown solution. Then, 5 ml of sodium citrate solution with a concentration of (80 mM) was added to the reaction mixture. The color of the mixture turned from dark brown to a red wine color and kept under continues stirring for another 5 minutes. After cooling down to room temperature the reaction mixture was

centrifuged, and 3 mL of concentrated colloidal gold solution were collected from the bottom of the tube.

Synthesis of Fe_3O_4@Au@TiO_2 core-shell NPs.

Briefly, 20 ml of ethanol was mixed with 20 ml of acetonitrile before adding 300 μL of the Fe_3O_4@Au core-shell nanoparticles and stir it for 5 minutes. Next, 45 μL of methylamine water solution was added and let it stir for another 5 minutes. Next, 8 mL of the TBT solution (4mM) in ethanol were added dropwise using a syringe pump. In about 15 min the stirred solution turned milky. The stirring was allowed to continue for 12 h. After this time, the synthesized CSNs were collected with a magnate, centrifuged and washed several times with ethanol.

Characterization:

UV-vis measurements

Spectra were measured with a Shimadzu UV-1800 spectrometer in a range of 190 to 1100 nm. Samples with absorbance of more than 1.5 units were diluted with water. Suspensions of the synthesized nanoparticles were measured in a quartz cuvette.

Scanning Electron Microscopy (SEM)

The morphology of Fe_3O_4@Au@TiO_2 structures were characterized using a FEI Helios SEM/FIB at the University of Arizona. The samples prepared by dropping suspensions of core-shell nanoparticles on a silicon wafer and let it dry in air at room temperature.

Transmission Electron Microscopy (TEM)

TEM analysis was done using a Hitachi HF-5000 High resolution analytical, 200 kV transmission electron microscope (TEM) at the University of Arizona. TEM samples were prepared by placing a drop of diluted suspensions onto a 200 mesh carbon coated cupper grids and allow it to dry in air at room temperature before measurements. Energy dispersive

spectroscopy (EDS) was performed on the same sample to obtain their elemental composition and to confirm the core-shell nanostructure.

Results and discussion

Synthesis of Fe_3O_4 NPs

The iron oxide nanoparticles in this section were produced by the same approach described in the previous chapter and thus the results were similar. The average diameter of these nanoparticles was 31 nm. However, the magnetic nanoparticles will aggregate if left untreated with a surface modifier to make them hydrophilic.

Synthesis of Fe_3O_4@Au core-shell NPs.

The gold thin film was effectively formed in the presence of the reducing environment provided by the citrate derivative. These nanocomposites magnetite gold as a core-shell structure were rather stable and reproducible in their preparation. No specific problems were observed and the processed run very smoothly with no signs of aggregation under the working conditions at room temperature. UV-visble spectra analysis show a characteristic light absorbance behavior of gold nanoparticles.

Synthesis of Fe_3O_4@Au@TiO_2 core-shell NPs

The formation of the titania shell on the magnetic-gold nanocomposite worked well by following the Bartosewicz *et al.* the method, that appears to work better when the size of the nanostructure to cover is larger than 50 nm in diameter. The addition of the titania layer was characterized by UV-Visible spectra analysis that upon modification was switched to the near infrared absorbance region as will be described further in discussion of results.

One of the main objectives of developing this type of 3 material nanocomposites was to obtain reactive oxides that can allow the attachment of sensing probes and biomolecules. This approach

helped incorporate back hydroxyl groups on the magnetite-gold nanocomposites. In addition, the titania shell provided an enhance stability of the nanoparticles. The titania coating method used did not require any special condition and was performed at room temperature. It was shown that the titanium (IV) butoxide (TBT) used as a TiO_2 precursor, was less sensitive to water compared to other titania precursors such as titanium (IV) isopropoxide and titanium(IV) ethoxide. According to findings in the literature TBT is more stable and reacts really slow with smaller alkyl groups [160], [161]. In addition, TBT as titania precursor is relatively less expensive than other TiO_2 precursors and it is more stable. Most of the synthesis was performed using anhydrous solvents in order to prevent the hydrolysis of TBT in the ethanol solution. However, since water is necessary for TBT hydrolysis, water was introduced to the reaction from two sources, (1) from the aqueous core-shell nanostructure solution and (2) from the aqueous methylamine solution, which was used as a catalyst for the reaction. These two aqueous suspensions were added to the reaction before the addition of the titania precursor [37]. The overall process worked quite well as seen from the morphology analysis and UV-Visible spectra and later described in the next chapters when enzymes were attached to the surface of these platforms.

Morphology and size of Fe_3O_4@Au@TiO_2 core-shell-shell NPs

The morphology of the synthesized nanoparticles was performed with SEM, TEM and EDS. The resulting images of the synthesized Fe_3O_4@Au@TiO_2 core-shell nanostructures are presented in Figure 12. The figure (a-c) shows a very clear picture of the synthesized nanoparticles with uniformly sized particles and spherical in shape. The image clearly shows titania particles on the outer shell and equally dispersed on the surfaces of the magnetic-gold nanoparticles with no agglomeration and with an average particle size of 1 from the TEM-EDS analyses clearly reveal

that the nanoparticles have a multilayer structure of the 3 components, a magnetic (core), an intermediate layer of gold and an outer titania layer shell.

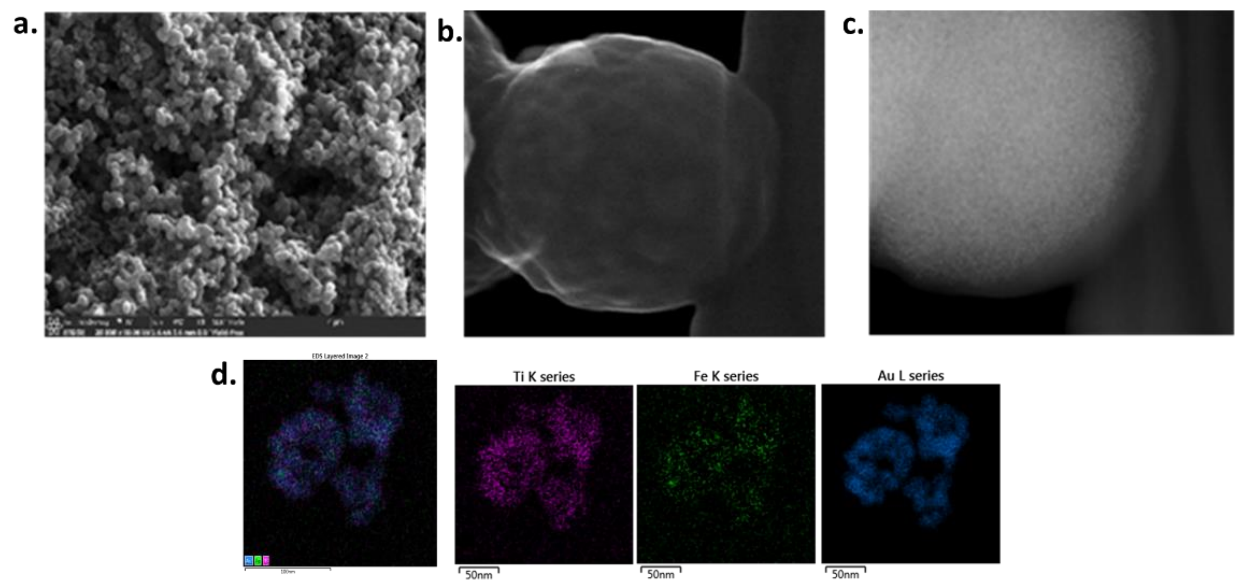

Figure 12 Scanning Electron Microscopy (SEM), Transmission Electron Microscopy (TEM), Energy Dispersive spectroscopy images of Fe3O4@Au@TiO2 core-shell nanostructure: (a) SEM of surface morphology, (b) and (c) TEM images for the core-shell structure, and (d) EDS images

Optical properties of Fe_3O_4@Au@TiO_2 core-shell-shell NPs

The UV-vis spectra of the core-shell-shell nanostructures are presented in Figure 13. Here it can be observed how the shift in absorbance of the gold plasmon changes to the red when modified by the magnetic core and when modified by the outer layer of titania.

It can be seen clearly in the absorbance of gold nanoparticles and the Fe_3O_4@Au core-shell nanoparticles a the redshift of the maxima of absorption where the core-shell nanostructure shows a λ_{max}= 528 nm vs λ_{max}= 520 nm for the gold nanoparticles. Similarly, a second redshift was observed for the Fe_3O_4@Au@TiO_2 core-shell-shell NPs with a λ_{max}= 542 nm. This result is due to the fact that the refractive index (n) of the surrounding medium affects the spectral position of plasmon resonance of single noble metal nanoparticles [162], [163]. These results are

in agreement with report in the literature where it has been reported that coating metal NPs with TiO_2 causes an average rise in the refractive index of their local dielectric environment, resulting in plasmon resonance red shift.

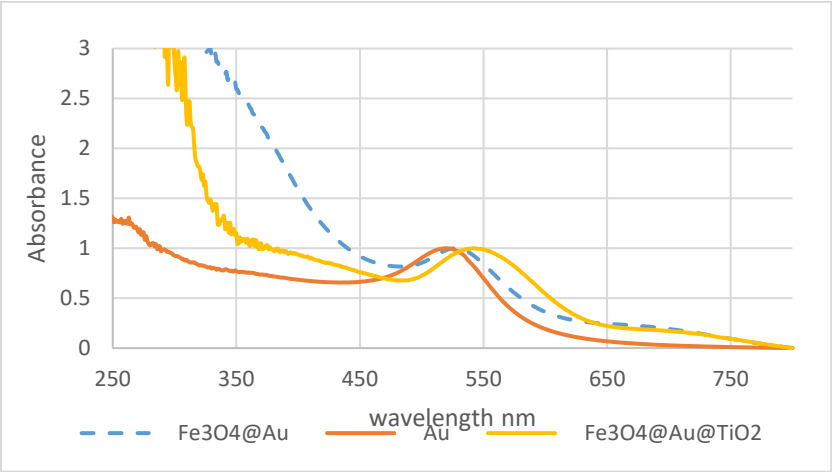

Figure 13 Normalized UV-vis spectra of Au, Fe3O4 and Fe3O4@Au@TiO2 core-shell nanostructure. All peaks were normalized upon presenting

The optical properties of the nanostructures were also quantified in term of their calculated absorption and their optical resonance wavelength using nano the software Composix tool [164] to theoretically determine the absorbance behavior of nanoparticles. Figure 14 describes the application Mie theory with the parameters provided for the materials used in the preparation of the core-shell-shell in this chapter. The parameters fed to the program were the refractive index of the materials, and the size of the magnetic core, gold shell and the titania shell obtained experimentally. The refractive index of the titania is required because it plays an important role in controlling the absorbance of the gold shell, since it depends in the refractive index of the surrounding media. The red shifts observed in the theoretical analysis and shown in Figure 4 agree fundamentally with the experimental absorbance results obtained for the magnetic core-gold shell-titania shell nanocomposites.

The results on Figure 14 agrees with the fact of coating metals with titania leads to a significant increase in the refractive index of the dielectric environment, in addition to the red shift of the plasmon resonance of Au nanoparticles, which matches well the experimental results. Titania-based hybrid nanostructures have improved optical properties, making them promising materials for dye-sensitized solar cells (DSSCs) and photocatalysis. In reality, plasmonic nanostructures have been shown to improve the efficiency of DSSCs across different mechanisms [165].

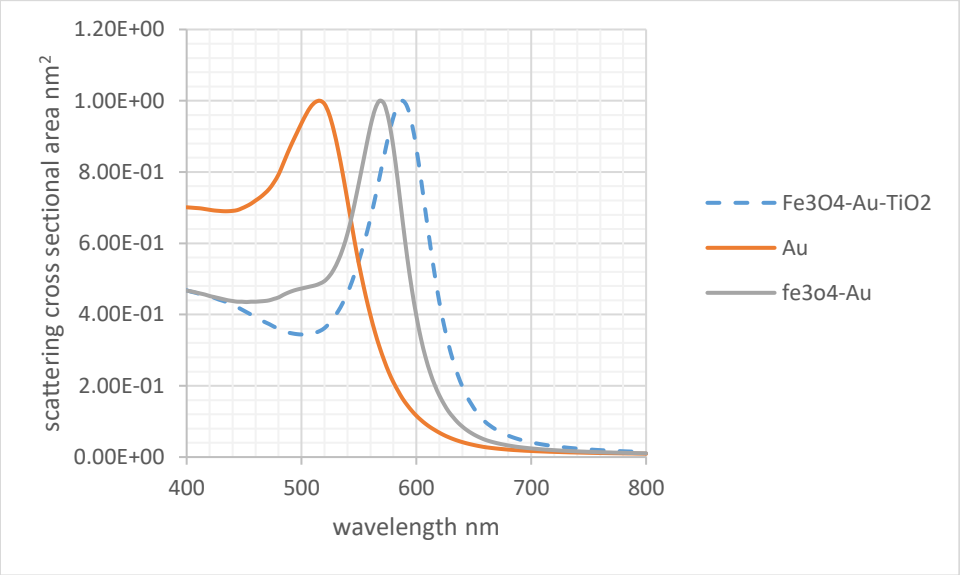

Figure 14 Normalized calculated scattering cross sectional area of Au, Fe_3O_4@Au and $Fe3O_4$@Au@TiO_2 core-shell nanostructure. All peaks were normalized upon presenting

Conclusions

The iron oxide nanoparticles in this section were produced by the same approach described in the previous chapter and thus the results were similar. The average diameter of these nanoparticles was 31 nm. The Choi *et al*. method was used to coat the iron oxide nanoparticles with the layer of gold that was formed initially by the interaction of the hydroxyl groups of the magnetite with

positive gold ions followed by a systematic incorporation of more gold molecules by a method that resembles an electroless deposition where the gold shell kept forming a stable gold layer as long as more gold ion solution was available.

In this work, it was shown that it is possible to produce core-shell magnetic nanoparticles coated with noble metals, such as gold with different shell thicknesses. It was established the effectiveness of the approach of depositing layers of titania using titanium (IV) butoxide as a reliable and affordable organic titanium alkoxides. The deposition can be performed at moderate reaction conditions with no inert environment or special glassware. Fabricated core–shell nanostructures have significant UV and visible extinction, and hence could be of major interest for solar-light-driven photocatalysis, photovoltaics, and biomedical applications. It is anticipated that future research in our laboratory will involve development of reaction conditions to adapt the approach presented here to coat various other nanocomposites such as hollow golds and gold nanorods. The optical properties of these nanocomposites indicated that that refractive index of the noble metal depends on the refractive index of the surrounding medium. These finding were confirmed also using Mie theory. Coating these nanocomposites with a layer of titania, offers a surface rich of accessible hydroxyl moieties for further modification and attachment of molecular dyes, organic or inorganic and biomolecules in general, as it will be exemplified in this work in later chapter of this work (Chapters 5 and 6).

CHAPTER 5 - SURFACE FUNCTIONALIZATION OF HYBRID MAGNETIC NANOCOMPOSITES WITH LIGANDS AND BIOMOLECULES

Abstract

This chapter describes the systematic covalent attachment of the enzyme trypsin on the surface of activated magnetic nanocomposite derivatives. The previously synthesized magnetic platforms described in chapters 3 and 4 were surface modified with the amino alkane silane linker 3-Amino propyl triethoxysilane (APTES). The enzyme immobilization was carried out using in general a classical approach reported in the literature to modify metal oxide surfaces. First, the oxide surfaces of the nanoparticles were functionalized with APTES, followed by reactivation with glutaraldehyde and finally by the attachment of the enzyme. The enzyme kinetics of trypsin free in solution and of the immobilized enzyme nanocomposite derivatives were measured, and the results were compared in order to find out the effectiveness of the enzyme attachment on the magnetic derivatives. The evaluation and comparison of enzyme activity was determined by comparing the values of enzyme kinetic parameters, which was carried out using the synthetic substrate DL-BAPNA, a classical substrate for trypsin. Trypsin follows Michaelis-Menten kinetics, and the parameters K_M (Michaelis constant) and V_{max} (maximum enzyme rate) are evaluated by linearization of the Michaelis Menten equation. This approach was applied to all the enzyme nanocomposite systems and in all cases the determination and evaluation of these parameters were successfully performed. As expected, the values of the parameters K_M and V_{max} were in all cases different since the enzyme on the surfaces usually would react and attach differently. However, based on the observed enzyme activity and the determination of parameters,

it was verified in all cases the successful immobilization of the enzyme on the magnetic nanocomposites. The incorporation of the fluorescent dyes, fluorescein and rhodamine was performed by reacting directly to the nanoparticle-APTES derivatives. These results provide evidence that by following the functionalization steps described here, many other biomolecules (proteins, such as enzymes and antibodies, peptides or nucleotides) can be similarly and successfully incorporated in these magnetic nanocomposites.

Introduction

Superparamagnetic iron oxide nanoparticles have a low toxicity profile and magnetic properties that makes them ideal platforms for a wide variety of applications for example in magnetic resonance imaging (MRI), drug delivery, magnetic hyperthermia, and magnetic separation of biomolecules [110], [166]–[173]. Surface coating and functionalization of these nanoparticles are relevant because this allows design of new biomolecular platforms for biosensing and diagnostics, allow for solubility and dispersibility in various conditions, as well as protection of the magnetic core from the oxidation and aggregation. Simultaneously, the functionalization allows for further chemical development, such as conjugation of active biomolecules and complementary imaging labels, like fluorescent tags. Functional coatings on magnetic nanoparticles have been introduced using a variety of methods and the use of coordinative, electrostatic, hydrophobic, and covalent interactions has been studied for many of these systems [169]–[172], [174]. Covalently attached coatings can provide a strong bond with the nanoparticle's surface while also providing a wide range of surface functionalities, making them an ideal platforms for their use in different applications. Organosilane ligands, especially alkoxysilanes, can form stable covalent bonds with metal oxide surfaces [110], [170], [175]–[180]. As a classical example, first, the oxide surfaces of the nanoparticles are functionalized

with the amino alkane silane derivative APTES, followed by reactivation with glutaraldehyde as seen schematically in Figure 15. What follows is the systematic incorporation of fluorescent dyes that react directly with the amino derivative APTES or enzyme attachment via the glutaraldehyde derivative as shown schematically in Figure 16.

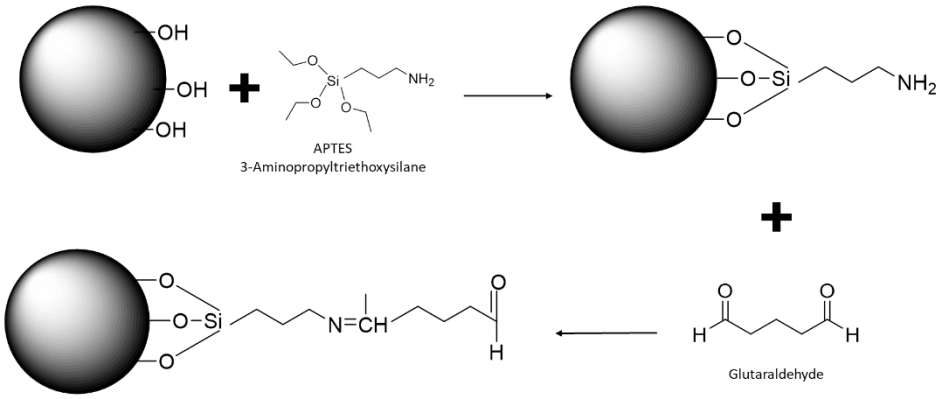

Figure 15. Surface modification of magnetic nanoparticles with APTES (3-Aminopropyltriethoxysilane) followed by activation with glutaraldehyde.

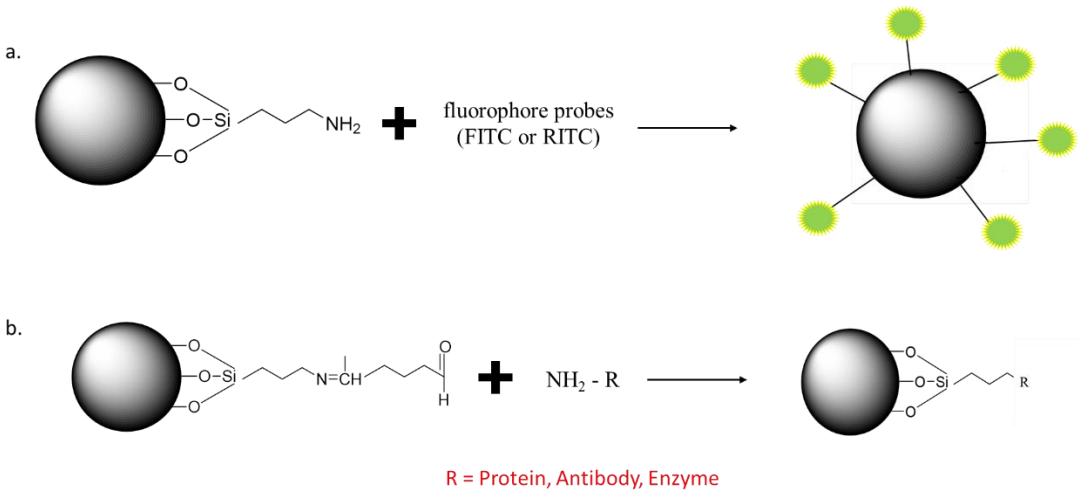

Figure 16 Reaction scheme for attachment of (a) fluorophore probes; (b) biomolecules proteins, peptides

Several phases are involved in the reaction of alkoxysilanes with the magnetic oxide surfaces as seen schematically in Figure 17. Initially, during the final dehydration reaction, hydrolysis of the

alkoxy groups of the silane to reactive silanol groups, condensation of the silanol groups, adsorption of silanols on the nanoparticle surface, and formation of covalent bonds with the surface [175], [181]. Silanes can be used to incorporate a number of organic functionalities on the magnetic surface as mentioned and exemplified above, in addition to strong covalent bonding, which are essential for further effective biofunctionalization.

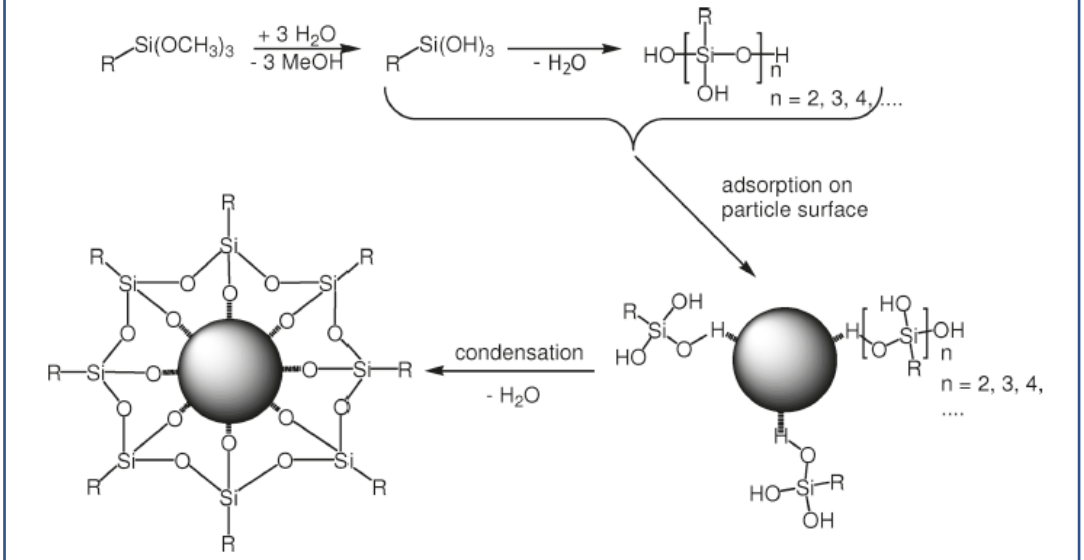

Figure 17 Surface Modification of Fe_3O_4 Nanoparticles with Alkoxysilanes [176]

3-aminopropyltriethoxy silane (APTES), one of the most commonly used silane ligands for biological applications, was used to graft amino functional groups ($-NH_2$) on the surface of magnetic nanocomposites [175], [182]–[185]. Organic functional groups like amines are interesting for biological applications since it enables biomolecules to be coupled under benign conditions of room temperature and in physiological buffers. In addition, chemical multifunctionality is essential, especially when using different conjugation chemistries to bind bioactive molecules.

Model Enzyme-Trypsin

Trypsin is a peptidase enzyme that cleaves peptide bonds of proteins by hydrolysis to form smaller peptides and amino acids. Trypsin is produced in the pancreas of mammals and secreted into the duodenum, where it is essential for digestion. It is a specific enzyme that binds the peptide in positions carboxyl residue arginine (Arg) or lysine (Lys) in the chain, both of positively charged amino acids, fragmenting the initial peptide R groups [186].

Chemistry and function:

The enzymatic mechanism of trypsin (crystalline structure shown in Figure 4) is the same as other serine proteases: a catalytic triad makes the nucleophilic serine in the active site. Trypsin has an optimum operating pH for its enzymatic activity at 8 and the optimum operating temperature at 37 ° C. The aspartate residue (Asp 189) located in the catalytic region (S1) of trypsins serves to attract and stabilize lysines and arginines (both positively charged) and therefore is responsible for the specificity of the enzyme. Trypsins are endopeptidases, i.e., the enzymatic cut is performed in the middle of the peptide chain rather than in the terminal residues of the same. The trypsin activated in turn promotes more trypsinogen (autocatalysis) and the other enzyme, so that only a small amount of enteropeptidase (enterokinase) is needed to start the reaction [187]. This mechanism of activation is very common among serine proteases, and serves to prevent self-digestion in the pancreas.

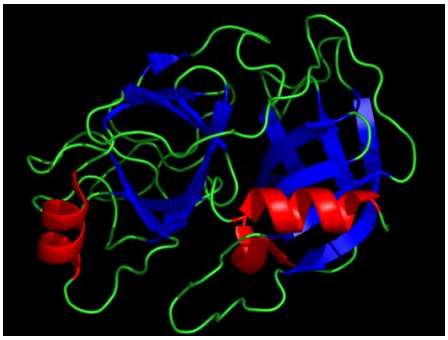

Figure 18 X-ray crystallographic structure of Trypsin

In this chapter, trypsin was attached on magnetic nanocomposites via APTES and glutaraldehyde intermediates. APTES was used to graft amine groups on the surface of the magnetic metal oxide nanocomposites, followed by the introduction of the linker (glutaraldehyde) forming now a surface susceptible to nucleophilic attack by primary amino derivatives, like the ones found in proteins and other biomolecules. The reaction of the glutaraldehyde with proteins and other amine-containing molecules occurs through the formation of Schiff base reactions. Schiff base formation likely occurs at alkaline pH. The higher the pH, the more efficient the Schiff base is [121].

Materials and methods

Magnetic-Nanoparticles Functionalization. We followed the hydrothermal approach by Song *et al.* [137] for synthesis of Fe_3O_4 nanoparticles exactly as described previously. The outer layer of the magnetic composite is functionalized with APTES in order to provide compatibility with biological or chemical species. This was carried out by simply immersing the magnetic composite into an ethanol solution of APTES (3-aminopropyltriethoxysilane), while stirring. The new APTES-functionalized composite is easily washed with ethanol and water while retaining all the magnetic particles with a magnet, this is a classical method and here described by Liu *et al.* [188]. The activation of APTES-magnetic nanoparticles with glutaraldehyde was performed following the approach described by Aquinas [189]. These functionalized nanoparticles were used for the immobilization of fluorophore probes and enzyme biomolecules.

Magnetic-Titania and Magnetic-Gold-Titania Nanocomposite Functionalization. Similarly, the systems, Magnetic-Titania and Magnetic-Gold-Titania nanocomposites were also modified with trypsin and similarly, immobilized enzyme kinetic analysis was performed.

Chemicals. Tris-hydroxymethyl-aminomethane (tris) buffer (pH 8.15). The enzyme substrate, Nα-Benzoyl-DL-arginine-pnitroanilide (DL-BAPNA), Trypsin, and DMSO (Dimethyl Sulfoxide) were purchased from Sigma. APTES 99% (3-aminopropyltriethoxysilane), and glutaraldehyde 50% aqueous solution, Fluorescein isothiocynate FITC, and Rhodamine isothiocynate RITC were also from Sigma Aldrich. Methanol was purchased from the University of Arizona. Acetonitrile was purchased from Fisher-Chemicals.

Methods

Synthesis of Fe_3O_4 NPs. Magnetic nanoparticles were synthesized following a hydrothermal approach as described previously. Briefly, (0.25 g) $FeCl_2 \cdot 4H_2O$ was dissolved in 12.75 mL of DI water. Under continues stirring, (1.25 mL) of ammonium hydroxide 28% was added and the solution turned suddenly into dark greenish blue solution. To allow the iron (II) to be oxidized, the solution was continuously stirred in air for 10 min. The dark mixture was then transferred into a 40 ml Teflon-lined stainless-steel autoclave at 134 °C for 3 h with a gauge pressure of 2 bar, then cooled down to room temperature. The black precipitate was collected and purified with water and ethanol via a centrifugation process. The final Fe_3O_4 NP suspension was lyophilized and a black dry powder was obtained and kept in storage until further use.

Synthesis of Fe_3O_4@TiO_2 nanostructures. These magnetic nanocomposites were synthesized following hydrolysis and polycondensation reaction of titanium(IV) butoxide (TBT) by Bartosewicz *et al*. as described previously [37]. Briefly, 20 ml of ethanol was mixed with 20 ml of acetonitrile before adding 300 μL of Fe_3O_4 nanoparticles and stir it for 5 minutes. Next, 45 μL of methylamine water solution was added and let it stir for another 5 minutes. Next, 8 mL of the TBT solution (4mM) in ethanol were added dropwise using a syringe pump. In about 15 min the stirred solution turned milky. The stirring was allowed to stir for 12 h. After this time, the

synthesized CSNs were collected with a magnate, centrifuged and washed several times with ethanol.

Fe_3O_4 magnetic NPs surface activation. Briefly, (0.01 g) of pre-synthesized Fe_3O_4 NPs was dissolved in 10 ml of APTES/Methanol solution and sonicated for 10-15 seconds. Then the solution was placed on the shaker at 500 rpm for 24 hrs. Afterwards, unbounded APTES was removed by decanting the solution while holding the magnetic particles with a strong magnet. The particles were washed with methanol (3 times) and DI water (one time). The same methods of surface and reaction preparation were used for magnetic-titania nanoparticles

Fe_3O_4@APTES and fluorophore probes. Fe_3O_4@APTES derivatives were dissolved in a FITC or RITC ethanol solution [0.01 M] and left to shake in the dark for 24 hrs. The same methods were used for magnetic-titania nanoparticles.

Fe_3O_4@APTES and enzyme immobilization. Fe_3O_4@APTES derivatives were dissolved in 8 ml of glutaraldehyde solution, sonicated and then placed on the shaker for 1 more hour to carry out the reaction. To remove glutaraldehyde residues, a strong magnet was used to hold the particles, and these ones were washed 3 times with a PBS solution. Fe_3O_4@APTES@GLU NPs were dissolved in 5 ml of PBS buffer solution and sonicated for 10-15 seconds. The same method was used for magnetic-titania nanoparticles. The enzyme (trypsin) attachment was carried out by reaction of the primary amino groups of the protein (Lysine residues) with the aldehyde moieties of the glutaraldehyde. Briefly 5 ml of a protein solution was prepared (the enzyme trypsin) to obtain a concentration of 2 mg/ml and added to the magnetic-glutaraldehyde activated nanoparticle suspension. The suspension was placed on a shaker for one hour at 300 rpm, then, decanted and saved until further use. The modified Fe_3O_4@APTES@glu@Trypsin nanoparticles were washed 3 times with PBS and one time with HCl-Tris buffer solution at pH 8.0. The particles afterwards

were then suspended in HCl-Tris buffer solution and were ready to conduct the UV/VIS analysis and enzyme kinetic studies.

Enzym+e kinetics. Enzyme kinetics was performed following established methods described in the literature and readjusted to be used for this work. For this purpose, pipette to the reference cell of the spectrophotometer 2.5 ml of HCl-Tris buffer, pH 8.0. To the sample cell add an aliquot of the (previously dissolved in DMSO) substrate (DL-BAPNA) solution (250 μl) of a 10^{-4}M solution and dilute with buffer to 2.4 ml. Then, zeroth the spectrophotometer at 410 nm, and at 25 ^{o}C. At this point, add an aliquot of 100 μl of the enzyme solution (trypsin) with concentration of 10^{-5} M, to the sample cell and at time equal zero start measuring the increase in absorbance that results from the conversion of DL-BAPNA to tri-nitro-phenol, the chromophore product. This step is repeated several times for several substrate concentrations and at a constant enzyme concentration. The same procedure is followed for other enzyme concentrations.

Results and discussion

3-aminopropyltriethoxysilane (APTES) adds highly reactive silanol groups on the nanoparticles' surface. APTES acts as a barrier between magnetic nanosized particles, reducing interparticle attraction. As a result, the propensity for nanosized particles to aggregate together can be reduced considerably. In addition, the free amine group in APTES helps in the further functionalization of other reactive materials. The reaction between the hydroxyl groups on the nanoparticle surface and the ethoxy silane groups of APTES forms a covalent Fe-O-Si bond during the functionalization of the magnetic and hybrid magnetic nanocomposites with APTES. This step is schematically illustrated in Figure 19.

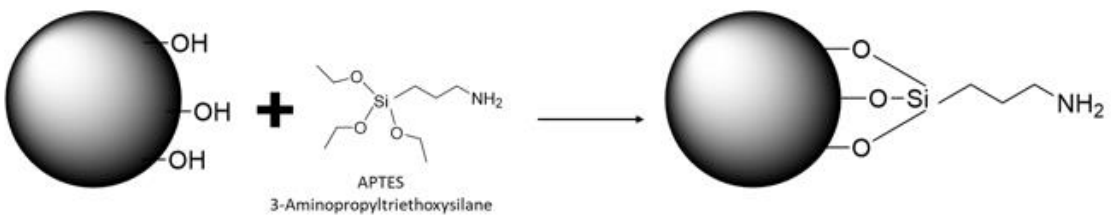

Figure 19 Aminopropyltriethoxsilane (APTES) functionalization

In order to introduce other functional groups on the surface of the magnetic nanoparticles to test the reactivity of the amine groups, a followed reaction with glutaraldehyde was carried out. With glutaraldehyde one carbonyl group reacts with APTES and the other one can react with many other amine group derivatives, in this case for instance, with the amino acid lysine of trypsin.

Standard enzyme kinetics analysis was performed with a free enzyme solution at different substrate concentrations. These results when compared with the immobilized enzyme on nanoparticles will help elucidate the effectiveness of the activity of the immobilized enzyme on the surface of magnetic nanoparticles.

Free enzyme kinetics. DL-BAPNA was used as a substrate at concentrations ranging from 0.01 to 0.0025 M, with different trypsin concentrations measured at 25°C and pH 8.15 in the form of free or immobilized trypsin. The results of substrate conversion from the free enzyme kinetics in solutions are presented graphically in Figure 20 (with 400 μl of the stock enzyme concentrations) and Figure 21 (with twice the enzyme concentration). Values of absorbance at 410 nm of the products of the enzymatic reaction for different values of substrate (DL-BAPNA) and at fixed enzyme concentration (and different for each graph) show results that can be analyzed effectively with Michaelis-Menten kinetics.

Magnetic bound enzyme kinetics. Figure 22 shows the activity of the immobilized enzyme on the surface of bare-magnetic nanoparticles at the same experimental conditions of pH and

temperature as with the free enzyme. A variety of kinetic experiments were carried out at different substrate concentrations and with different amounts of enzyme immobilized nanoparticles. Figure 23 shows the kinetic results of the immobilized enzyme on the magnetic nanoparticles with two substrate concentrations. It looks evident that the product formation behavior follows Michaelis Menten kinetics. This demonstrates that the enzyme was effectively immobilized with substantial remaining enzymatic activity. A kinetic control experiment was performed using all the components in the reaction but without the enzyme in the preparations, the result for the control is observed in Figure 23 where no absorbance increase is observed, and it can be deduced that no substrate transformation and product formation were present. It also shows that the enzyme activity of the nanoparticles is quantitative, and the enzyme immobilized on the nanoparticles quite stable Thus, the change in absorbance was clearly due to the immobilized enzyme on the nanoparticles. . This same control was used to compare other enzyme-nanoparticle immobilized systems. Results in Figure 24 show the enzyme activity when immobilized on magnetic-titania nanoparticles with clear evidence that the immobilized enzyme maintains substantial enzymatic active, reaching total conversion of substrate (In this experiment, the concentration of the substrate was 0.01 mM) in less than 600 minutes. Similar to the previous cases, the enzyme was also effectively attached to the surface of magnetic-gold-titania nanocomposites. Figure 25 shows the kinetics results of enzyme attached on the magnetic-gold-titania nanocomposites. The results shown in this figure were conducted with a concentration of substrate of 0.0025 mM.

From the experimental results, it can be observed that the enzyme trypsin was attached successfully on the 3 magnetic derivatives, on the magnetite alone, on the magnetic-titania composite and on the magnetic-gold titania nanoparticles. In each case, the degree of activity was different, and, in most cases, it was necessary to use different substrate concentrations to consider that the amount

of enzyme on some of the surfaces was very relatively small. The relevance however is that the enzyme was attached effectively in all the 3 magnetic nanoparticles considered here, on the magnetic nanoparticles, on the magnetic-titania and on the magnetic-gold-titania nanocomposites. In addition, the results were good enough to allow the evaluation in all cases of the Michaelis-Menten parameters, as described separately in the next section.

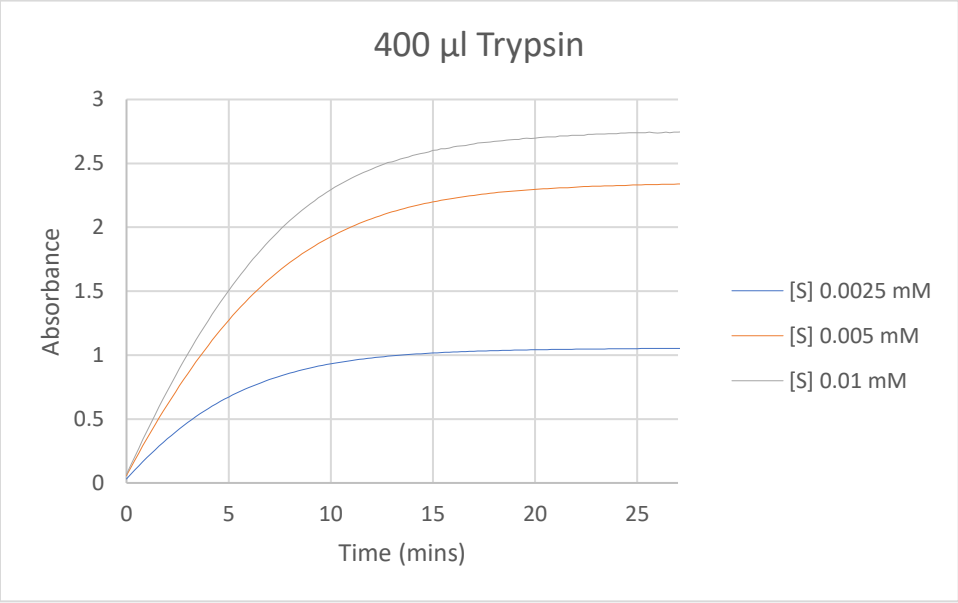

Figure 20 Enzyme activity at different substrate concentrations and constant enzyme concentrations

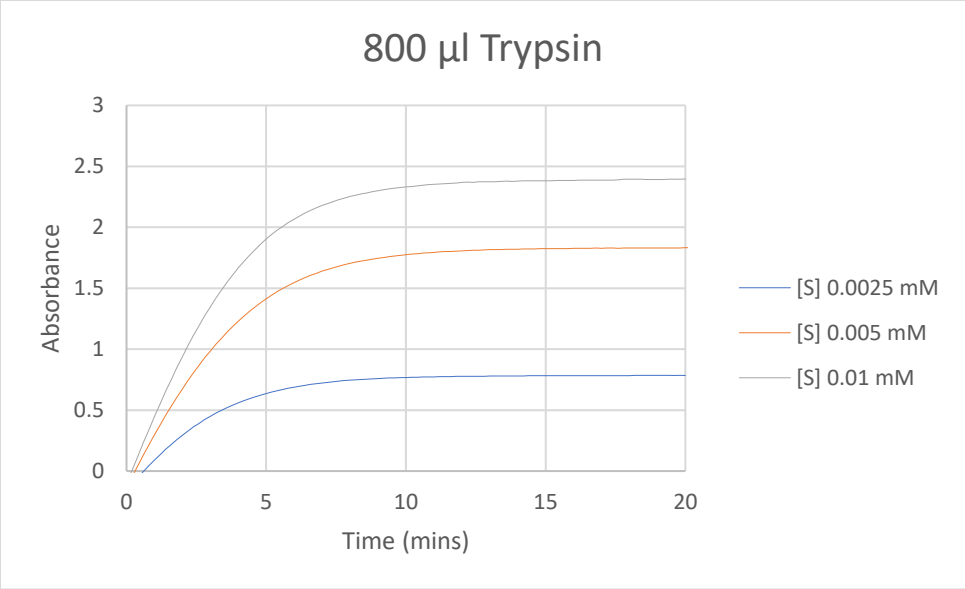

Figure 21 Enzyme activity at different substrate concentrations and constant enzyme concentration

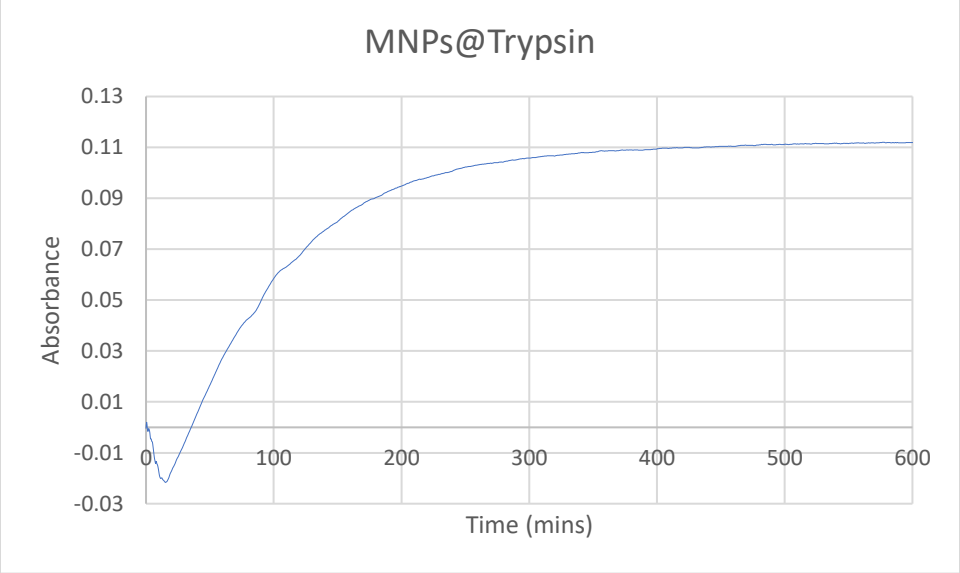

Figure 22 Enzyme activity on the surface of the magnetic nanoparticles

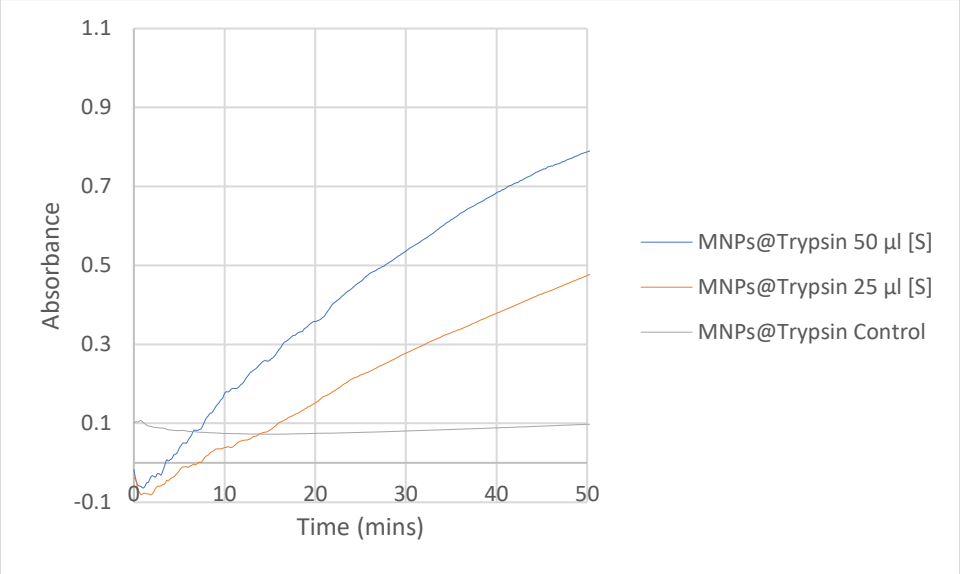

Figure 23 Enzyme activity at two substrate concentrations and constant enzyme on the surface of magnetic nanoparticles

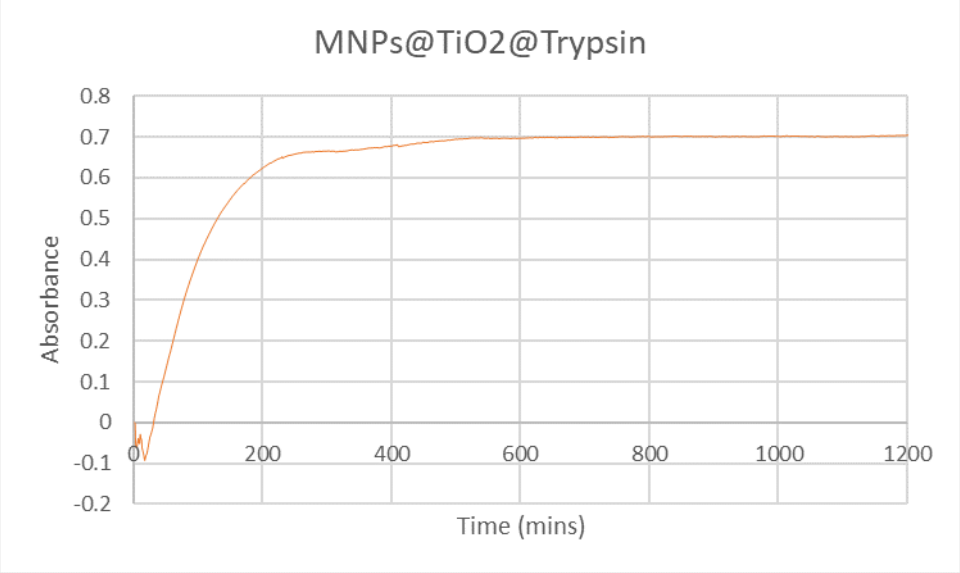

Figure 24 Enzyme activity on the surface of the magnetic-titania nanoparticles

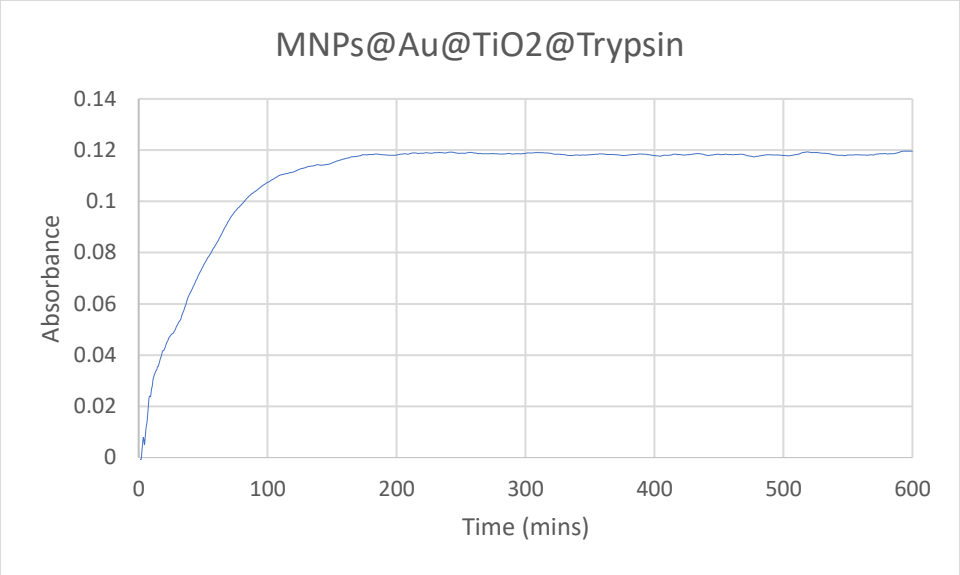

Figure 25 Enzyme activity on the surface of the magnetic-gold-titania nanoparticles

Michaelis-Menten Kinetics Analysis

Parameter analysis of enzyme kinetics in solution and on the surface of the magnetic nanoparticles and nanocomposites was performed using Michaelis-Menten kinetics Models. The analysis of enzymes in solution follows the classical equation,

$$v_0 = \frac{V_{max}\,[S]}{K_M + [S]} \qquad (1)$$

This equation describes the rate of reaction product formation [P] or d[P]/dt which is equal to -d[S]/dt, or -Vo. Where the variation of the parameters V_{max} and K_M help determine the effective enzyme activity of enzymes as a function of substrate concentration at constant temperature. This form oft he equation provides a tool to determine quantitatively (1) evidence of the effectiveness of enzyme binding and (2) remaining biological activity of biomolecules (enzymes or proteins). These results will help determine indirectly the expected biological activity of enzyme upon binding on the surface of any nanoparticle nanoplatform. The kinetic results from all the derivatives were used to evaluate the V_{max} and K_M parameters.

The kinetic parameters for the free enzyme is solution were evalauted in general by the linearization of the Michaelis Menten equation in the form of the Lineweaver-Burk double reciprocal plot [190], given in equation 2. Figure 26 shows the typical data plotted using the linearized equation and the slope and intercept used to estimate the parameters of the equation. A double-reciprocal plot of enzyme kinetics is generated by plotting $1/V_0$ as a function 1/[S]. The slope is the K_M/V_{max}, the intercept on the vertical axis is $1/V_{max}$, and the intercept on the horizontal axis is $-1/K_M$.

$$\frac{1}{V} = \frac{1}{V_{max}} + \left(\frac{K_m}{V_{max}}\right)\frac{1}{[S]} \qquad (2)$$

.

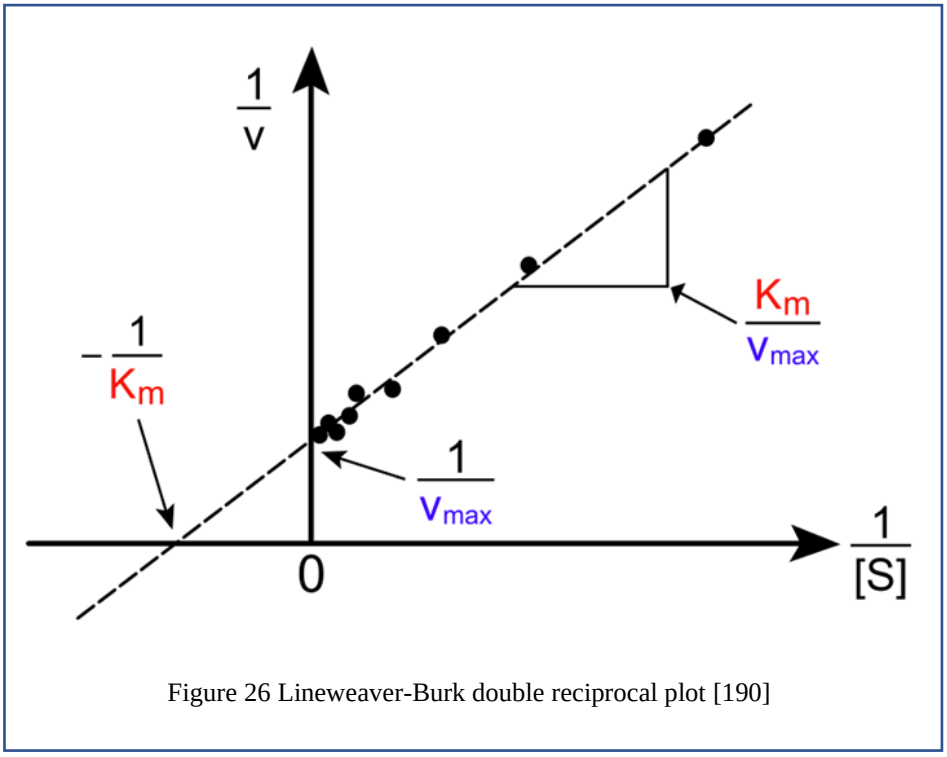

Figure 26 Lineweaver-Burk double reciprocal plot [190]

As seen in

Figure *27*, shows a strong linear relationship and could thus be used to determine K_m and V_{max} for free enzyme at different enzyme concentration (400 µl and 800 µl) using the data from Figure 20

and Figure 21. The estimated values of Km were 0.0117 and 0.0267 10^{-6}M respectively and as seen proportional to the amount of substrate used in the analysis. The values determined for V_{max} were 0.681234 and 2.250154 mM/min, respectively. Since V_{max} represents the product of the initial enzyme concentration and the kinetic rate constant (or catalytic constant), these values are therefore in accordance to the increase of enzyme concentration.

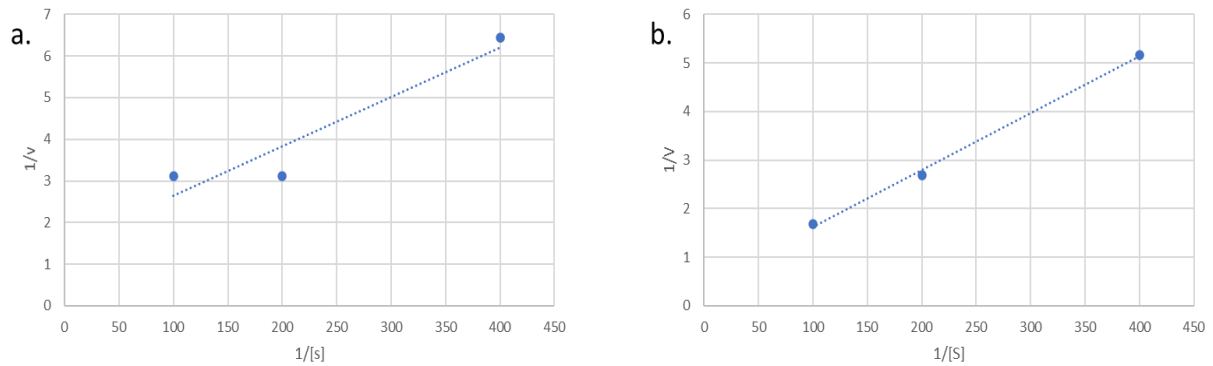

Figure 27 Lineweaver-Burk plots for the hydrolysis the substrate in the presence of the free trypsin at constant enzyme concentration and different substrate concentrations, a) 400 µl and b) 800 µl

The determination of the kinetic parameters for the enzyme attached to nanoparticles was also obtained using the Michaelis Menten equation however in the integrated form. In this manner the linearization of the equation is done after integration of the equation.

$$-\frac{dS}{dt} = \frac{V_{Max}\, S}{K_M + S} \tag{3}$$

Equation that can be written as

$$\int_{So}^{S} \frac{dS}{\frac{V_{Max}\, S}{K_M + S}} = \int_0^t -dt \tag{4}$$

Or

$$\int_{So}^{S} \frac{K_M}{V_{Max}\, S} dS \int_{So}^{S} \frac{dS}{V_{Max}} = \int_0^t -dt \tag{5}$$

Where So is the initial substrate concentration. Upon integration and linearization, the resulting equation can be written as,

$$\frac{ln\left({\left(\frac{S}{So}\right)}\Big/{(So - S)} \right)}{(So - S)} = Vmax \frac{t}{(So - S)} - \frac{1}{K_M} \tag{6}$$

Since the values given by the kinetic studies are for the transformation of S (substrate) to P (product), using a mass balance the values needed for the plot and evaluation of KM and Vmax, where S = So – P.

Using these equations and the enzyme kinetic values from Figure 22 (for magnetic nanoparticles), Figure 24 (magnetic-titania nanoparticles) and Figure 25 (Magnetic-gold-titania nanoparticles), Figure 28 describes the calculated values for the parameters KM and Vmax for all trypsin-nanoparticle derivatives.

The estimated values of K_M were 0.077, 0.595, and 0.692 10^{-6}M, for magnetic, magnetic-titania, magnetic-gold-titania nanoparticles respectively. Similarly, the values for Vmax were 0.001, 0.019, and 0.016 mM/min, respectively. These results suggest that the immobilized enzyme on the coated magnetic nanoparticles had a less enzymatic activity as expected because of more unwanted interactions of the enzyme with the iron oxide nanoparticles. The relevance of these results is that the enzyme kinetics can be evaluated and proved the effective attachment of enzymes on the surface of nanocomposites. Optimization of enzyme immobilization is still a challenge to overcome on all enzyme surface attachments. However, results like the ones obtained here is an indication that it is possible to attach enzymes, and in general it can be hypothesized that by following similar methods other biomolecules can be attached as well.

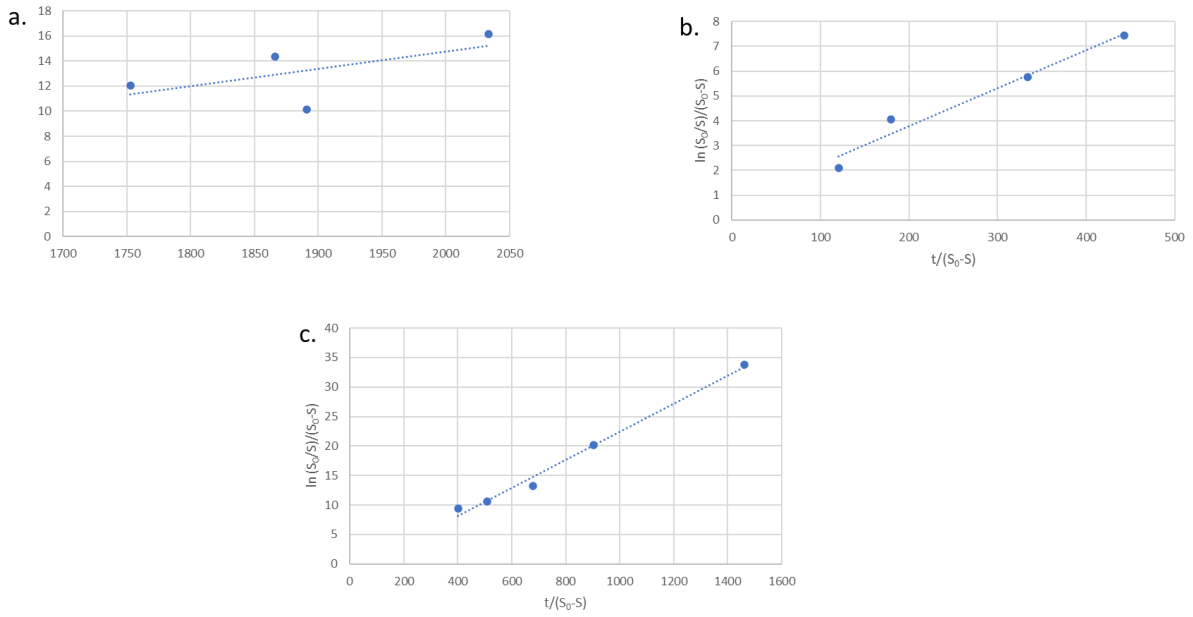

Figure 28 the calculated values for the parameters K_M and V_{max} for all trypsin-nanoparticle derivatives using the integrated form of Michalis Menten.

Conclusions

The effective enzyme (trypsin) immobilization was carried out on magnetic, magnetic-titania and magnetic-gold-titania nanocomposites using classical methods of surface functionalization with APTES and glutaraldehyde reported in the literature to modify metal oxide surfaces. This functionalization also was demonstrated with the incorporation of fluorescent probes with rhodamine and fluoresceine attachment. All the enzyme-nanoparticle composites were enzymatically active at different degrees. The evaluation and comparison of enzyme activity was determined by comparing the values of enzyme kinetic parameters using the synthetic substrate DL-BAPNA, a classical substrate for trypsin. The enzyme activity in all cases followed Michaelis-Menten kinetics and the parameters K_M (Michaelis constant) and V_{max} (maximum enzyme rate) were all evaluated by linearization of the Michaelis Menten equation. For the free enzyme the

linearization of the Michaelis Menten equation was done using the differential method that involves using directly the reciprocal form of the Michaelis-Menten equation. For the analysis and parameter evaluation of the enzyme-nanocomposite systems the integration of the Michaelis Menten equation was performed before linearization. Both methods allow the determination of the enzyme parameters, K_M and V_{max}. These results provide evidence that by following the functionalization steps described here, many other biomolecules (proteins, such as enzymes and antibodies, peptides or nucleotides) can be similarly and successfully incorporated in these or other magnetic nanocomposites.

CHAPTER 6 - SYNTHESIS AND SURFACE FUNCTIONALIZATION OF MAGNETIC-DEXTRAN NANOCOMPOSITES WITH LIGANDS AND BIOMOLECULES

Abstract

This work describes the attachment of the enzyme trypsin on the surfaces of iron oxide nanoparticles coated with the polysaccharide, dextran, followed by reactivation by oxidation of the dextran for incorporation of reactive amino groups. Modifying these surfaces allows us to attach different biomolecules such enzymes, antigens and antibodies, so these nanocomposites can be used in different biomedical applications. In the attachment of enzymes, the kinetics of attached enzyme activity were assessed using UV-VIS spectroscopy and Michaelis-Menten analysis to evaluate experimental enzyme kinetics parameters for both free enzymes and immobilized enzymes. The reaction scheme is schematically shown in Figure 29.

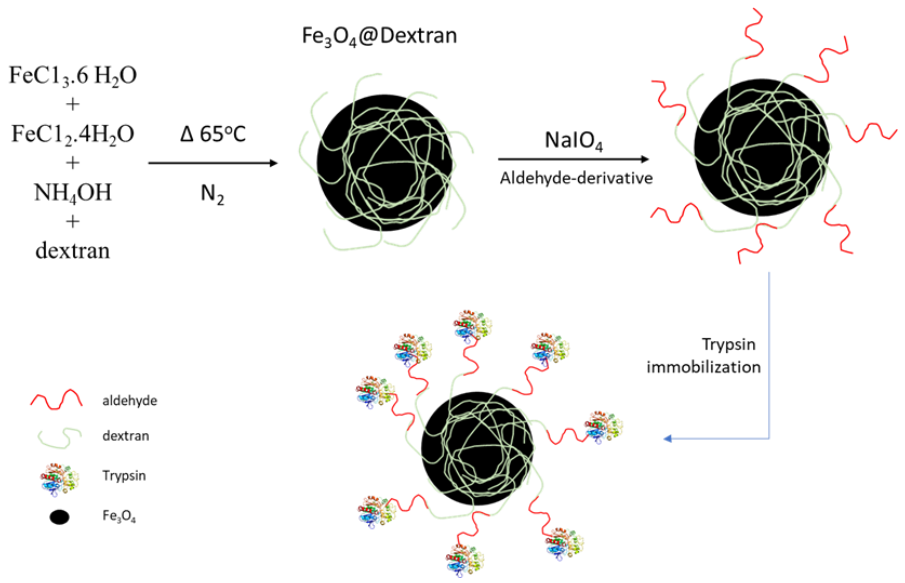

Figure 29 Reaction scheme of synthesis and functionalizing the surface of Magnetic-Dextran nanoparticles

Introduction

In the food industry, trypsin is sometimes used as a protein digestion reagent because it selectively hydrolyzes the arginine and lysine residues of proteins [191], [192]. Free trypsin, on the other hand, has a range of drawbacks in practical implementations, including high cost, inconsistency, and difficulty recovering from the reaction system. Furthermore, due to the trypsin's self-digestion, protein digestion in solution is normally slow and inefficient [193]. Immobilization of the enzyme, which leads to improved efficiency, has been studied extensively to solve these issues. An immobilized enzyme is one that has been physically or chemically bound to a solid support, such as membranes [193], nanoparticles [194], [195], or porous materials [196], [197]. Immobilization has many benefits, including increased enzyme stability, ease of separation from protein digestion solutions, and the ability to reuse [198], [199]. Similarly, magnetic nanoparticles have been used widely recently for enzyme immobilization [200]–[202]. The amount of enzyme available in a reaction mixture can be reduced by immobilizing it, enhancing its stability [203], and provide way for separation of enzyme from reaction mixtures [204], [205]. Because of the reduce diffusion and increase surface area for high enzyme loading, the performance of immobilized enzyme may be increased by modifying the structure and reducing the size of the carrier materials [204], [206], [207]. Magnetic nanoparticles (MNPs) are a type of nanostructure that can be used to immobilize proteins and enzymes, as well as in bioseparation systems, immunoassays, drug delivery [208], and biosensors [200], [205], [209]. In a fluidized bed reactor, MNPs can be quickly stabilized for continuous enzyme activity [205]. They had many appealing characteristics in biotechnology [210] and unusual properties, such as super paramagnetism, low toxicity, and biocompatibility [211]. New biomedical applications such as MRI [212], [213], cell sorting/targeting [214], and

sensing necessitate a thorough understanding of MNP toxicity. The toxicity of MNPs is determined by their size, surface area, structure, composition, and coating. Surface modification of MNPs is an essential method for reducing their toxicity [215]. However, since the enzyme and the Fe_3O_4 magnetic nanoparticles have poor interactions, using naked Fe_3O_4 nanoparticles for trypsin immobilization results in low loading and instability of the enzyme, this observation was also reported previously in chapter 5 of this work. The stability of Fe_3O_4 nanoparticles, as well as the performance of enzyme immobilization, can be increased by modifying them. To ensure excellent dispersion, most superparamagnetic iron oxide (SPIO) and ultrasmall superparamagnetic iron oxide (USPIO) agents have been modified with dextran and/or other forms of polymer coatings [216]–[218]. The coating of polymer onto the Fe_3O_4 MNPs surface is needed to minimize aggregation and improve biocompatibility between the Fe_3O_4 MNPs and water or tissue fluid [219].

In this work, magnetic nanoparticles with a controlled size were coated with dextran, and the immobilization of trypsin was obtained using sodium periodate to obtain the aldehyde group on the dextran magnetic modified surface, which was found to prevent enzyme degradation and helps to improve trypsin stabilization. Kinetics of trypsin in free and immobilized form was analyzed and parameter determination of enzyme kinetics in solution and in on the surface of nanoparticles was performed using Michaelis-Menten kinetics. The kinetics follows the equation

$$v_0 = \frac{V_{max}\,[S]}{K_M + [S]} \tag{7}$$

Where the variation of the parameters V_{max} and K_M help detemine the effective enzyme activity. These results provide a tool to determine quantitatively (1) evidence of the effectiveness of binding the enzyme and (2) remaining biological activity of biomolecules (enzymes or proteins). These results will help determine indirectly the expected biological activity of enzyme upon

binding on the surface of the nanoparticle. V_{max} and K_M can be obtained by linearization, for example with the Lineweaver-Burk double reciprocal plot [190], Figure 30 shows here the parameter estimation values. A double-reciprocal plot of enzyme kinetics is generated by plotting $1/V_0$ as a function of 1/[S]. The slope of the plotted values is K_M/V_{max}, the intercept on the vertical axis is $1/V_{max}$, and the intercept on the horizontal axis is $-1/K_M$.

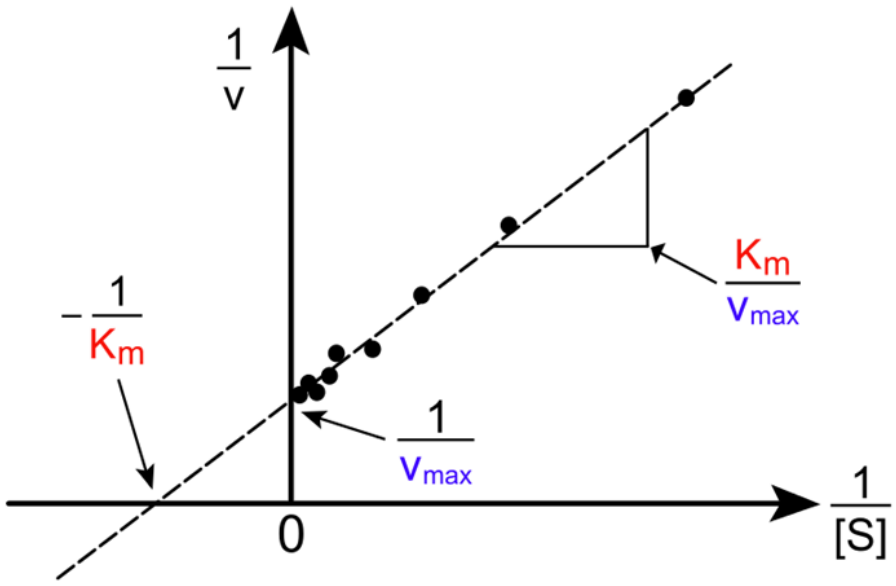

Figure 30 Lineweaver-Burk double reciprocal plot [190]

Materials and methods

Experimental

We followed the reaction mixture of ferric and ferrous ions with dextran polymers under alkaline conditions [220], [221] and reported previously in this work. Once the coating of dextran on the surface of the magnetic nanoparticles was obtained, in order to couple the enzyme with on the magnetic composites, oxidation of the dextran was performed under mild conditions using sodium periodate ($NaIO_4$) as oxidant at specific concentrations [222]. Enzyme attachment was

carried out by the reaction of the primary amino groups of the protein (lysine residues) to the aldehyde resulting derivative on the dextran moieties. The reaction scheme is schematically shown in Figure 31.

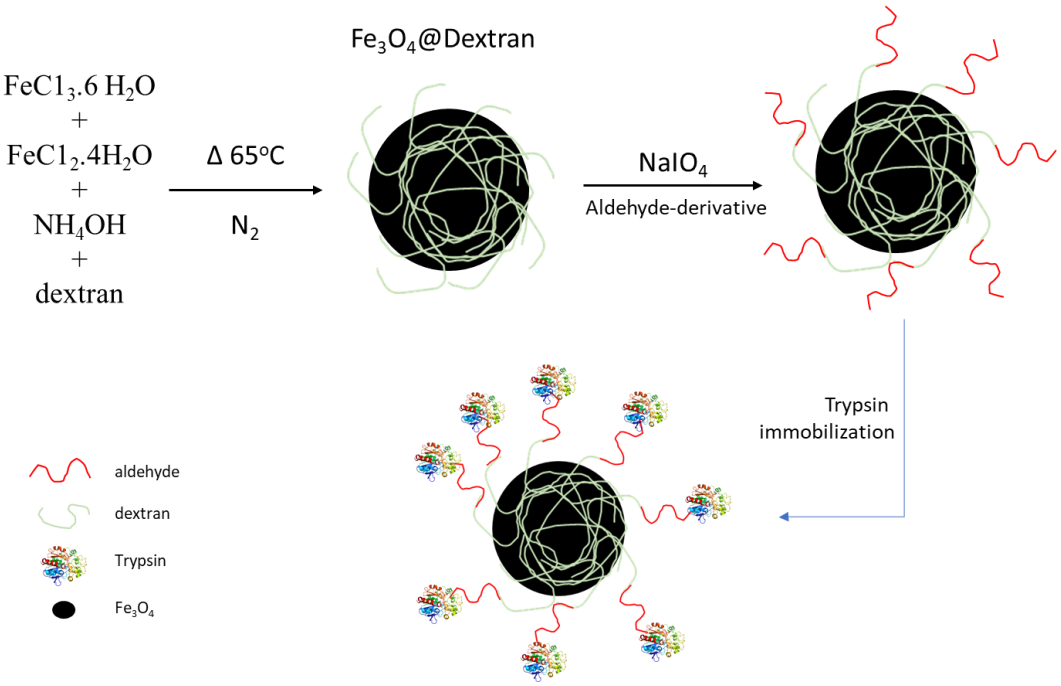

Figure 31 Chemical reaction scheme for functionalization of magnetic nanoparticles with biomolecules (antibodies or enzymes).

Materials

The polymer sample used in this study was commercial dextran with a molecular weight of 40 kD (T-40) obtained from Pharmacia, Uppsala, Sweden. Sephacryl S-300 gel was available from Sigma Corporation. Ferric chloride hexahydrate ($FeCl_3 \cdot 6H_2O$), ferrous chloride tetrahydrate ($FeCl_2 \cdot 4H_2O$), and ammonium hydroxide 28% were purchased from sigma Aldrich. For enzyme kinetic studies , Tris-hydroxymethyl-aminomethane (tris) buffer (pH 8.15). The enzyme substrate, Nα-Benzoyl-DL-arginine-pnitroanilide (DL-BAPNA), Trypsin, and DMSO (Dimethyl Sulfoxide) is purchased from Sigma.

Methods

Synthesis of magnetic iron-dextran nanoparticles. Magnetic iron-dextran particles were prepared by mixing 10 ml of 50% (w/w) dextran with an equal volume of an aqueous solution containing 1.51 g $FeC1_3$.6 H_2O and 0.64 g $FeC1_2$.4H_2O. While stirring, the mixture was titrated to pH 10--11 by the dropwise addition of 7.5% (v/v) NH_4OH and heated to 60--65°C in a water bath for 15 min. Aggregates will then be removed by 3 cycles of centrifugation in a low-speed clinical centrifuge at 600 × g for 5 min. The ferromagnetic iron-dextran particles are separated from unbound dextran by gel filtration chromatography on Sephacryl S-300. Five milliliters of the reaction mixture will be applied to a 2.5 cm × 33 cm column and eluted with buffer containing 0.1 M Na acetate and 0.15 M NaC1 at pH 6.5. The purified ferromagnetic iron-dextran particles will be collected in the void volume and the concentration will be determined by dry weight analysis.

Periodate oxidation of ferromagnetic iron-dextran. Periodate oxidation is carried out by a modification of the procedure used by Barbara Wilson *et al.* 5 ml of iron-dextran particles at a concentration of 5 mg/ml are oxidized with 5 mM $NaIO_4$. After stirring for 6 hrs at 25°C [220], the iron-dextran solution is dialyzed overnight against 1 liter of 20 mM sodium borate buffer pH 8.5 at 4°C and protected from light by covering the reaction flask with aluminum foil. Now these aldehydes activated iron-dextran particles can be used to attach the desired enzyme to the nanoparticles via amino group interaction.

Enzyme Immobilization. Enzyme attachment was carried out by reaction of the primary amino groups of the protein (Lysine residues). Briefly, add 5 ml of a protein solution (the enzyme trypsin) to get the concentration 2 mg/ml to the magnetic-dextran activated nanoparticle suspension. The suspension is placed on a shaker for one hour at 300 rpm. Then, decant and save

the magnetic-dextran-trypsin nanoparticles (Fe_3O_4@dextran@Trypsin NPs), and wash it 3 times with PBS and one time with HCl-Tris buffer solution at pH 8.0. The particles are then suspended in HCl-Tris buffer solution to conduct UV/VIS analysis and enzyme kinetic studies.

Enzyme kinetics. Enzyme kinetics were performed following established methods developed in our laboratory and described previously in chapter 5. Pipette to the reference cell of the spectrophotometer 2.5 ml of HCl-Tris buffer, pH 8.0. To the sample cell add an aliquot of the substrate (DL-BAPNA) solution (250 µl) and dilute with buffer to 2.4 ml. Then, zero the spectrophotometer at 410 nm, and at 25 ^{o}C. At this point, add aliquots of 100 µl of the enzyme solution (magnetic@dextran@Trypsin) to the sample cell and at time equal zero start measuring the increase in absorbance that results from the conversion of DL-BAPNA to tri-nitro-phenol, a chromophore product. This step is repeated several times for several substrate concentrations (0.01, 0.005, and 0.0025) M and at a constant enzyme concentration.

Results and discussion

Properties of magnetic-dextran nanoparticles

Magnetic-dextran nanoparticles were brownish-black suspension as can be observed in Figure 32. After purification, the resulting particle suspension was obtained and resuspended in DI water. They were stable in DI water. The particles were readily water soluble and only aggregated in the presence of an external magnetic field. In the absence of a magnetic field, the particles have no magnetic moment, indicating that they were superparamagnetic.

Figure 32 magnetic-dextran suspension in DI water

Trypsin immobilization results

While trypsin is one of the most widely used enzymes for protein hydrolysis, it is unstable in its natural state. As a result of covalent bonding, trypsin was irreversibly immobilized onto the aldehyde-functionalized Fe_3O_4@dextran nanoparticles in this study. The aldehyde acted as a linker arm, interacting with the amine groups in trypsin and covalently bonding the trypsin to the surface of the Fe_3O_4@Dextran nanoparticles.

Activity evaluation of immobilized Trypsin

Examining the Michaelis constant (K_m) and the maximal hydrolysis reaction rate (V_{max}) of trypsin before and after immobilization on the surface of Fe_3O_4@Dextran nanoparticles provided a more precise measurement of the activity changes of trypsin after immobilization. The K_m of trypsin was determined using the Lineweaver-Burk equation, which is shown below:

$$\frac{1}{V} = \frac{1}{V_{max}} + \left(\frac{K_m}{V_{max}}\right)\frac{1}{[S]} \quad (8)$$

Where [S], is the substrate concentration, V, the hydrolysis reaction rate, the Michaelis constant is K_m, and the maximum hydrolysis reaction rate is V_{max}. The values of $1/[S]$ were plotted versus values of $1/V$ according to the Lineweaver-Burk equation. The substrate DL-BAPNA was used

at concentrations ranging from 0.01 to 0.0025 M, with trypsin activity measured at 25°C and pH 8.15 in the presence of free or immobilized magnetic-dextran-trypsin.

The results from the free and immobilized enzyme kinetics in solutions are presented graphically in Figure 33 and Figure 34, respectively. Values of absorbance at 410 nm of the products of the enzymatic reaction for different values of substrate (DL-BAPNA) and at fixed enzyme concentration show values that can be analyzed effectively with Michaelis-Menten kinetics equation.

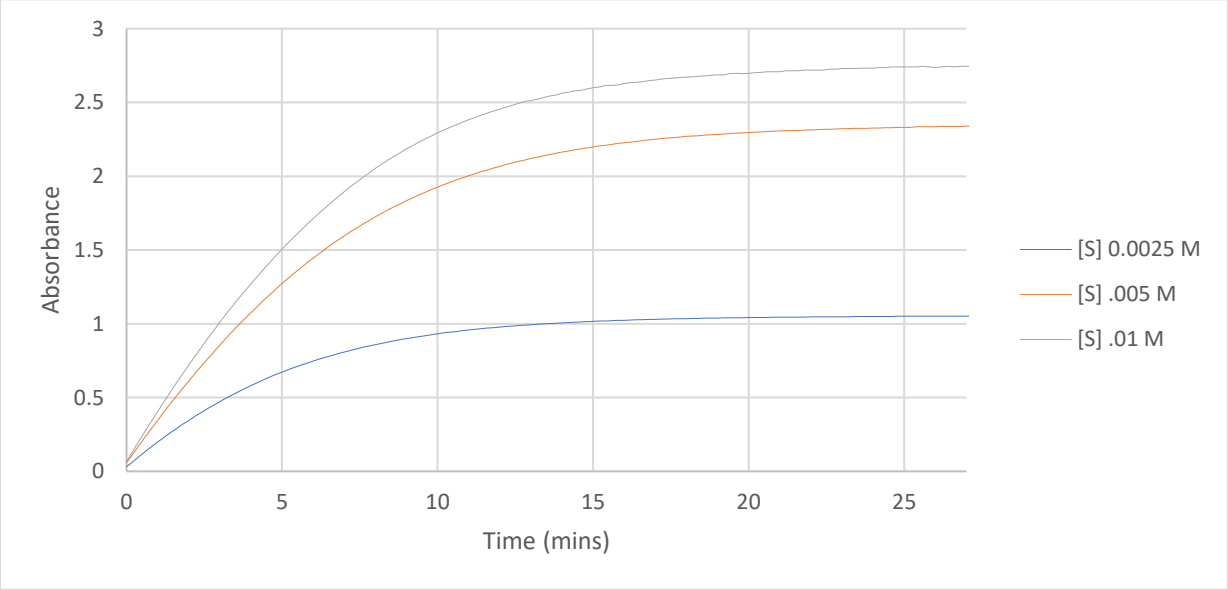

Figure 33 free enzyme activity at different substrate concentrations and constant enzyme concentration

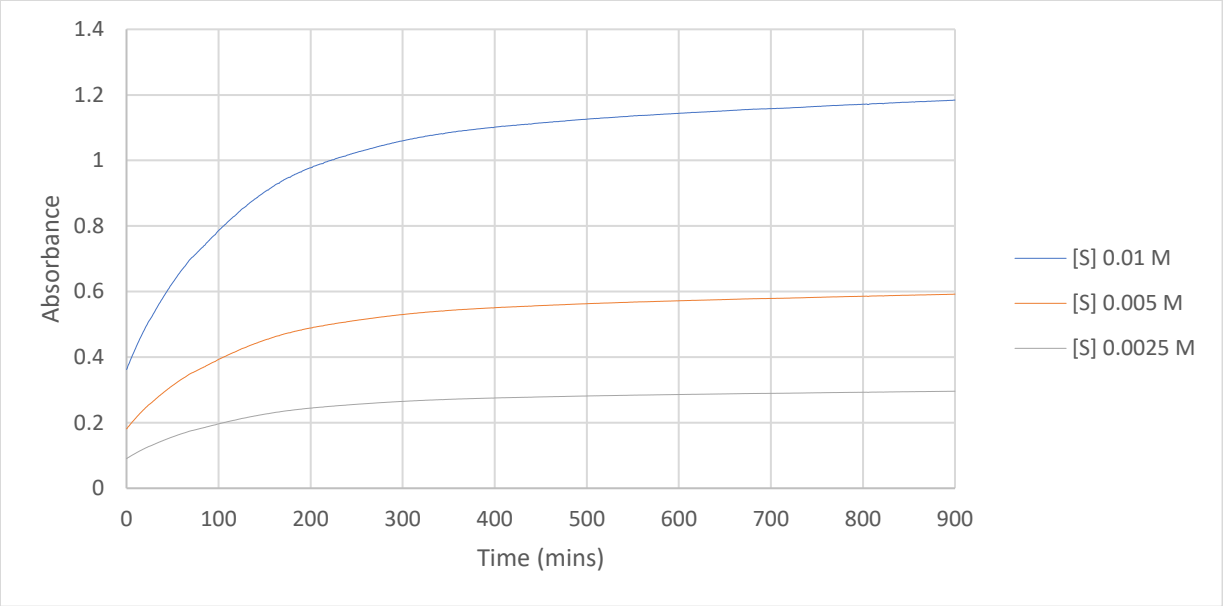

Figure 34 Enzyme activity on magnetic-dextran nanoparticles at different substrate concentrations and constant enzyme concentration

These graphs, as seen in Figure 35 and Figure 36 , showed a strong linear relationship and were used effectively to calculate Km and Vmax.

The estimated value of Km for the immobilized enzyme was 0.011664 10^{-6}M, which was lower than that of free trypsin, according to the Lineweaver-Burk equation (0.032877 10^{-6}M). Similarly, the free and immobilized enzymes had Vmax values of 0.681234 and 0.059203 mM/min, respectively, implying that immobilization of the enzyme resulted in lower activity than free trypsin. These values are expected as is the case for most immobilized enzymes, Since orientation of enzymes on the surfaces produces a steric effect in addition to the fact that the enzyme could be immobilize blocking partially or totally their active sites. However, the relevance of this work is that enzymes retain biological activity upon immobilization and in principle strong stability once immobilized.

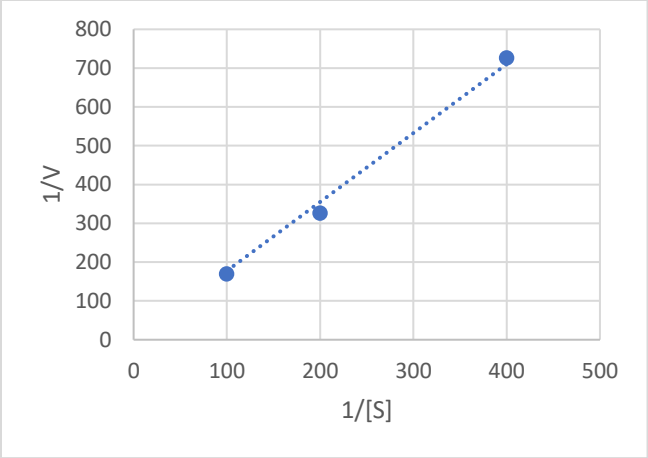

Figure 35 Lineweaver-Burk plots for the hydrolysis the substrate in the presence of the immobilized trypsin

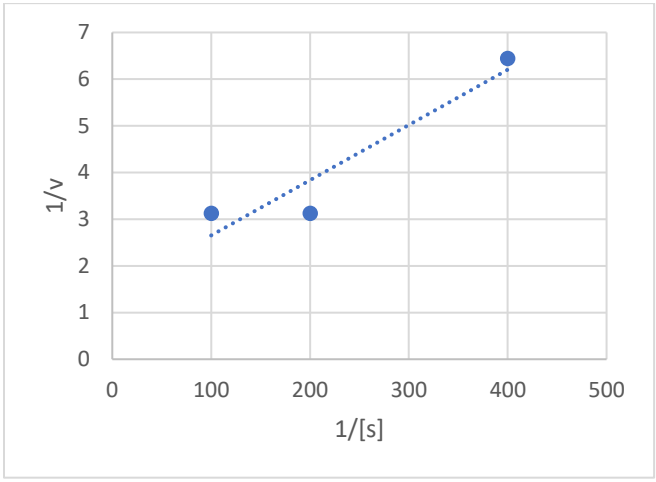

Figure 36 Lineweaver-Burk plots for the hydrolysis the substrate in the presence of the free trypsin

Conclusions

Magnetic-dextran nanocomposites was synthesized successfully following the reaction mixture of ferric and ferrous ions with dextran under alkaline condition. These nanocomposites were functionalized using sodium periodate in order to have an aldehyde groups on the surface. The magnetic-dextran derivatives are practically water soluble and biocompatible. The successful binding of trypsin on the surface of the nanocomposites was evaluated using UV-vis spectrophotometer, and the enzyme activity were evaluated using Michalis-Menten and the Lineweaver-Burk plot. It has been found that the trypsin that effectively immobilized on

Fe_3O_4@Dextran derivatives with excellent remaining enzyme stable activity towards the DL-BAPNA substrate. The immobilization of trypsin on dextran-coated Fe_3O_4 NPs was investigated and studied successfully, and the enzyme kinetics were determined. The magnetic-dextran-enzyme preparations did not aggregate at any point during the experimental work.

CHAPTER 7 - CONCLUSIONS

This work has particularly focused in the synthesis of hybrid magnetic engineered composite contrast agents (MECCA) nanoparticles with applications at the interface between materials science, biotechnology and medicine. The primary objective of this dissertation was to develop and prepare hybrid multifunctional engineered composite contrast agent nanoparticles for applications in energy conversion, light harvesting in optical and biomedical systems. Superparamagnetic iron oxide nanoparticles were the most common components in the preparation of synthesized nanocomposites. These nanoparticles were used as a core to add reactive moieties such as alkoxysilanes derivatives and polymers to introduce functional ligands including amino, epoxy and aldehyde groups. The most relevant working hypothesis in this dissertation is based on the concept that modified magnetic nanoparticles with semiconductor materials, specifically in this work, with titania thin films shells, provide a suitable surface for protein immobilization. Core-shell hybrid magnetic composites of an iron oxide core and a titania oxide shell were prepared by introducing a new method of synthesis that involves low temperature treatments, inexpensive precursors and with no special reaction conditions required. Magnetic derivatives modified with the linker, 3-Aminopropyltriethoxysilane (APTES) were used successfully to coat the nanoparticles with fluorescent dyes. The amino groups of the APTES moieties were further reacted with glutaraldehyde as a linker to attach amino group derivatives that included proteins (e.g., (enzymes, antibodies) and fluorescent dyes. Other nanostructures prepared in this work included hybrid materials with a core of iron oxide coated with intermediate layers of gold followed by an outer shell of titania oxide that can be used for further modifications. These systems provide properties of photo-corrosion resistance and protection from aggregation. Magnetic nanoparticles derivatives with specific applications in

magnetic resonance imaging (MRI) were prepared with coatings of dextran that after further activation with reducing agents the surface was modified via amino moieties. The successful synthesis was demonstrated with the attachment of the enzyme trypsin on different magnetic nanoparticle derivatives and the effective evaluation of the enzyme kinetic parameters. Based on these results it seems feasible to obtain similar effective attachment of any other protein, enzymes or antibodies. The nanoparticle magnetic derivatives coated with dextran provide a stable, water compatible without aggregation and thus suitable for diverse medical applications. Other nanoparticle derivatives produced in this work include quantum dots of different compositions, particularly simple methods to produce carbon dots for light harvesting applications. Silver and gold nanoparticles were produced as materials to promote synthesis of magnetic core and titania shell hybrids. Additionally, silver nanoparticles were used as seeds to deposit gold shells on the silver surface that after a galvanization process created hollow gold nanoparticles derivatives that are being used as photothermal agents to study their thermal ablation properties, technique with promising future in cancer therapy. The characterization of the nanoparticles was performed with SEM/TEM imaging for nanoparticle morphology and size. For optical properties, UV-vis spectroscopy has been used. EDS and XRD have been used to verify element composition. For functional groups analysis, we used FTIR. We used mathematical modeling, particularly, Mie theory to predict the behavior of light behavior and energy conversion of certain nanocomposites.

This work described a simple method implemented here to prepare magnetic nanoparticles with a thin layer of titanium oxides. In this approach heat treatments were not needed, neither the incorporation of surfactants and other mid layers adhesive components. This simple approach with simple titania precursors and control hydrolysis allowed the preparation of derivatives with

different thickness of titania oxides. The resulting nanoalloys showed excellent hydrophilic behavior, ideal for further functionalization.

The work also describes the preparation of three component nanoalloys that includes a magnetic core and a gold, and a titania shell layers. The size and the morphology of these derivatives were determined using scanning electron microscopy, transmitted electron microscopy. Energy dispersive spectroscopy (EDS) was performed to confirm the core-shell nanostructure. The experimental parameters obtained from these derivatives were applied to Mie theory and the comparison of the experimental plots and the ones produced with Mie theory was very good.

The incorporation of fluorescent probes and immobilized proteins (particularly the enzyme trypsin) on the surface of the magnetic synthesized derivatives was incorporated in, superparamagnetic nanoparticles, magnetic-titania and magnetic-gold-titania nanocomposites. The synthesis was carried using in general by incorporating first amino alkane silane, APTES, followed by reactivation with glutaraldehyde and finally attachment of enzymes. The enzyme kinetic activity for each of the preparations was evaluated using Michaelis-Menten kinetics and different linearization schemes. There results and kinetic parameters in all cases were determined successfully. The incorporation of the fluorescent dyes, fluorescein and rhodamine was performed by reacting directly to the nanoparticle-APTES derivatives.

In the last contribution of this work, the modification of magnetic nanoparticles were modified successfully with the polysaccharide dextran, a branched glucan made of many glucose molecules, and thus a biocompatible material that can be used in biological systems and in biomedical applications. To test the effectiveness of the systematic modification and coating of the magnetic nanoparticles, trypsin was incorporated and immobilized covalently via periodate oxidation and similarly to the previous enzyme analysis describe in this work. Michaelis Menten

kinetic parameters were experimentally evaluated consistently and accurately and compared well with values reported in the literature for similar trypsin immobilization.

Thus, this work has particularly focused in the synthesis of hybrid magnetic engineered composite contrast agents (MECCA) nanoparticles with biomolecules, particularly with an enzyme as a system for applications at the interface between materials science, biotechnology, and medicine. Overall, the findings of this study can contribute to the production of hybrid magnetic multifunctional nanocomposites for biomedical applications, energy conversion, and light harvesting and they may open up exciting new possibilities, especially in imaging and diagnostic applications such as contrast agents. Nanoparticle derivative of silver, gold and carbon dots were prepared that could be used to develop novel biomedical and technological systems, particularly as new materials for solar conversion, light harvesting, imaging and diagnostic biomedical applications.

REFERENCES

[1] N. Sanvicens and M. P. Marco, “Multifunctional nanoparticles - properties and prospects for their use in human medicine,” *Trends Biotechnol.*, vol. 26, no. 8, pp. 425–433, 2008, doi: 10.1016/j.tibtech.2008.04.005.

[2] K. T. Yong, I. Roy, M. T. Swihart, and P. N. Prasad, “Multifunctional nanoparticles as biocompatible targeted probes for human cancer diagnosis and therapy,” *J. Mater. Chem.*, vol. 19, no. 27, pp. 4655–4672, 2009, doi: 10.1039/b817667c.

[3] Yadong Yin1& A. Paul Alivisatos, “Colloidal nanocrystal synthesis and the organic–inorganic interfac,” *Nature*, vol. 437, pp. 664–670, 2005.

[4] P. N. Prasad, “Polymer science and technology for new generation photonics and biophotonics,” *Curr. Opin. Solid State Mater. Sci.*, vol. 8, no. 1, pp. 11–19, 2004, doi: 10.1016/j.cossms.2004.01.011.

[5] W. C. Law *et al.*, “Optically and magnetically doped organically modified silica nanoparticles as efficient magnetically guided biomarkers for two-photon imaging of live cancer cells,” *J. Phys. Chem. C*, vol. 112, no. 21, pp. 7972–7977, 2008, doi: 10.1021/jp712090y.

[6] C. Loo, A. Lowery, N. Halas, J. West, and R. Drezek, “Immunotargeted nanoshells for integrated cancer imaging and therapy,” *Nano Lett.*, vol. 5, no. 4, pp. 709–711, 2005, doi: 10.1021/nl050127s.

[7] I. C. Scott and D. Y. R. Stainier, “Fishing out a new heart.,” *Science*, vol. 298, no. 5601, pp. 2141–2, 2002, [Online]. Available: http://www.ncbi.nlm.nih.gov/pubmed/12481123.

[8] D. Gerion *et al.*, “Synthesis and properties of biocompatible water-soluble silica-coated CdSe/ZnS semiconductor quantum dots,” *J. Phys. Chem. B*, vol. 105, no. 37, pp. 8861–

8871, 2001, doi: 10.1021/jp0105488.

[9] W. W. Yu, E. Chang, R. Drezek, and V. L. Colvin, “Water-soluble quantum dots for biomedical applications,” *Biochem. Biophys. Res. Commun.*, vol. 348, no. 3, pp. 781–786, 2006, doi: 10.1016/j.bbrc.2006.07.160.

[10] D. Li, G. Li, W. Guo, P. Li, E. Wang, and J. Wang, “Glutathione-mediated release of functional plasmid DNA from positively charged quantum dots,” *Biomaterials*, vol. 29, no. 18, pp. 2776–2782, 2008, doi: 10.1016/j.biomaterials.2008.03.007.

[11] Y. Xing, M. kyung So, A. L. Koh, R. Sinclair, and J. Rao, “Improved QD-BRET conjugates for detection and imaging,” *Biochem. Biophys. Res. Commun.*, vol. 372, no. 3, pp. 388–394, 2008, doi: 10.1016/j.bbrc.2008.04.159.

[12] C. S. S. R. Kumar, *Nanomaterials for Cancer Diagnosis*. New York: Wley-VCH Verlaq GmbH, 2007.

[13] G. Yu, J. Liang, Z. He, and M. Sun, “Quantum Dot-Mediated Detection of γ-Aminobutyric Acid Binding Sites on the Surface of Living Pollen Protoplasts in Tobacco,” *Chem. Biol.*, vol. 13, no. 7, pp. 723–731, 2006, doi: 10.1016/j.chembiol.2006.05.007.

[14] M. Bruchez, M. Moronne, P. Gin, S. Weiss, and A. P. Alivisatos, “Semiconductor nanocrystals as fluorescent biological labels,” *Science (80-.).*, vol. 281, no. 5385, pp. 2013–2016, 1998, doi: 10.1126/science.281.5385.2013.

[15] C. B. Murray, C. R. Kagan, and M. G. Bawendi, “Self-organization of CdSe nanocrystallites into three-dimensional quantum dot superlattices,” *Science (80-.).*, vol. 270, no. 5240, pp. 1335–1338, 1995, doi: 10.1126/science.270.5240.1335.

[16] W. T. Liu, “Nanoparticles and their biological and environmental applications,” *J. Biosci.*

Bioeng., vol. 102, no. 1, pp. 1–7, 2006, doi: 10.1263/jbb.102.1.

[17] C. Shi *et al.*, "Quantum Dots: Emerging applications in urologic oncology," *Urol. Oncol. Semin. Orig. Investig.*, vol. 26, no. 1, pp. 86–92, 2008, doi: 10.1016/j.urolonc.2007.03.018.

[18] B. Kang, S. Q. Chang, Y. D. Dai, and D. Chen, "Synthesis of green CdSe/chitosan quantum dots using a polymer-assisted γ-radiation route," *Radiat. Phys. Chem.*, vol. 77, no. 7, pp. 859–863, 2008, doi: 10.1016/j.radphyschem.2007.11.008.

[19] P. Mayer-Kuckuk and D. Banerjee, "Strategies for imaging biology in cancer and other diseases," *Cancer Imaging*, pp. 3–14, 2008, doi: 10.1016/B978-012374212-4.50005-5.

[20] H. Yang, S. Santra, G. A. Walter, and P. H. Holloway, "GdIII-functionalized fluorescent quantum dots as multimodal imaging probes," *Adv. Mater.*, vol. 18, no. 21, pp. 2890–2894, 2006, doi: 10.1002/adma.200502665.

[21] F. Pinaud *et al.*, "Advances in fluorescence imaging with quantum dot bio-probes," *Biomaterials*, vol. 27, no. 9, pp. 1679–1687, 2006, doi: 10.1016/j.biomaterials.2005.11.018.

[22] X. Wang, L. Yang, Z. Chen, and D. M. Shin, "Application of Nanotechnology in Cancer Therapy and Imaging," *CA. Cancer J. Clin.*, vol. 58, no. 2, pp. 97–110, 2008, doi: 10.3322/ca.2007.0003.

[23] K. Park, S. Lee, E. Kang, K. Kim, K. Choi, and I. C. Kwon, "New generation of multifunctional nanoparticles for cancer imaging and therapy," *Adv. Funct. Mater.*, vol. 19, no. 10, pp. 1553–1566, 2009, doi: 10.1002/adfm.200801655.

[24] W. C. W. Chan and S. Nie, "Quantum dot bioconjugates for ultrasensitive nonisotopic detection," *Science (80-.).*, vol. 281, no. 5385, pp. 2016–2018, 1998, doi:

10.1126/science.281.5385.2016.

[25] J. S. Hrkach, M. T. Peracchia, A. Domb, N. Lotan, and R. Langer, “Nanotechnology for biomaterials engineering: Structural characterization of amphiphilic polymeric nanoparticles by 1H NMR spectroscopy,” *Biomaterials*, vol. 18, no. 1, pp. 27–30, 1997, doi: 10.1016/S0142-9612(96)00077-4.

[26] L. R. Hirsch *et al.*, “Metal nanoshells,” *Ann. Biomed. Eng.*, vol. 34, no. 1, pp. 15–22, 2006, doi: 10.1007/s10439-005-9001-8.

[27] D. L. J. Thorek, A. K. Chen, J. Czupryna, and A. Tsourkas, “Superparamagnetic iron oxide nanoparticle probes for molecular imaging,” *Ann. Biomed. Eng.*, vol. 34, no. 1, pp. 23–38, 2006, doi: 10.1007/s10439-005-9002-7.

[28] M. C. Daniel and D. Astruc, “Gold Nanoparticles: Assembly, Supramolecular Chemistry, Quantum-Size-Related Properties, and Applications Toward Biology, Catalysis, and Nanotechnology,” *Chem. Rev.*, vol. 104, no. 1, pp. 293–346, 2004, doi: 10.1021/cr030698+.

[29] R. Elghanian, J. J. Storhoff, R. C. Mucic, R. L. Letsinger, and C. A. Mirkin, “Selective colorimetric detection of polynucleotides based on the distance-dependent optical properties of gold nanoparticles,” *Science (80-.).*, vol. 277, no. 5329, pp. 1078–1081, 1997, doi: 10.1126/science.277.5329.1078.

[30] J. Nam, C. S. Thaxton, and C. A. Mirkin, “Nanoparticle-Based Bio – Bar Codes for the Ultrasensitive,” *Science (80-.).*, vol. 301, no. September, pp. 1884–1887, 2003.

[31] X. Zhao *et al.*, “A rapid bioassay for single bacterial cell quantitation using bioconjugated nanoparticles,” *Proc. Natl. Acad. Sci. U. S. A.*, vol. 101, no. 42, pp. 15027–15032, 2004, doi: 10.1073/pnas.0404806101.

[32] D. P. O'Neal, L. R. Hirsch, N. J. Halas, J. D. Payne, and J. L. West, "Photo-thermal tumor ablation in mice using near infrared-absorbing nanoparticles," *Cancer Lett.*, vol. 209, no. 2, pp. 171–176, 2004, doi: 10.1016/j.canlet.2004.02.004.

[33] C. H. Luo, V. Shanmugam, and C. S. Yeh, "Nanoparticle biosynthesis using unicellular and subcellular supports," *NPG Asia Mater.*, vol. 7, no. 8, 2015, doi: 10.1038/am.2015.90.

[34] M. Annadhasan, T. Muthukumarasamyvel, V. R. Sankar Babu, and N. Rajendiran, "Green synthesized silver and gold nanoparticles for colorimetric detection of Hg2+, Pb2+, and Mn2+ in aqueous medium," *ACS Sustain. Chem. Eng.*, vol. 2, no. 4, pp. 887–896, 2014, doi: 10.1021/sc400500z.

[35] J. Chen *et al.*, "Gold nanocages: Bioconjugation and their potential use as optical imaging contrast agents," *Nano Lett.*, vol. 5, no. 3, pp. 473–477, 2005, doi: 10.1021/nl047950t.

[36] R. Ferrando, J. Jellinek, and R. L. Johnston, "Nanoalloys: From theory to applications of alloy clusters and nanoparticles," *Chem. Rev.*, vol. 108, no. 3, pp. 845–910, 2008, doi: 10.1021/cr040090g.

[37] B. Bartosewicz, M. Michalska-Domanska, M. Liszewska, D. Zasada, and B. J. Jankiewicz, "Synthesis and characterization of noble metal-titania core-shell nanostructures with tunable shell thickness," *Beilstein J. Nanotechnol.*, vol. 8, no. 1, pp. 2083–2093, 2017, doi: 10.3762/bjnano.8.208.

[38] C. K. Lo, D. Xiao, and M. M. F. Choi, "Homocysteine-protected gold-coated magnetic nanoparticles: synthesis and characterisation{," *J. Mater. Chem.*, pp. 2418–2427, 2007, doi: 10.1039/b617500g.

[39] M. N. Sanz-Ortiz, K. Sentosun, S. Bals, and L. M. Liz-Marzán, "Templated Growth of Surface Enhanced Raman Scattering-Active Branched Gold Nanoparticles within Radial

Mesoporous Silica Shells," *ACS Nano*, vol. 9, no. 10, pp. 10489–10497, Sep. 2015, doi: 10.1021/acsnano.5b04744.

[40] B. J. Jankiewicz, D. Jamiola, J. Choma, and M. Jaroniec, "Silica-metal core-shell nanostructures," *Advances in Colloid and Interface Science*, vol. 170, no. 1–2. pp. 28–47, Jan. 15, 2012, doi: 10.1016/j.cis.2011.11.002.

[41] R. Jiang, B. Li, C. Fang, and J. Wang, "Metal/semiconductor hybrid nanostructures for plasmon-enhanced applications," *Advanced Materials*, vol. 26, no. 31. Wiley-VCH Verlag, pp. 5274–5309, Aug. 20, 2014, doi: 10.1002/adma.201400203.

[42] M. A. Fox and M. T. Dulay, "Heterogeneous Photocatalysis," 1993. [Online]. Available: https://pubs.acs.org/sharingguidelines.

[43] J.-L. Blin *et al.*, "Hierarchically Mesoporous/Macroporous Metal Oxides Templated from Polyethylene Oxide Surfactant Assemblies," *Angew. Chemie*, vol. 115, no. 25, pp. 2978–2981, 2003, doi: 10.1002/ange.200250816.

[44] A. Nakajima, H. Obata, Y. Kameshima, and K. Okada, "Photocatalytic destruction of gaseous toluene by sulfated TiO2 powder," *Catal. Commun.*, vol. 6, no. 11, pp. 716–720, Nov. 2005, doi: 10.1016/j.catcom.2005.07.006.

[45] Y. Bai, I. Mora-Seró, F. De Angelis, J. Bisquert, and P. Wang, "Titanium dioxide nanomaterials for photovoltaic applications," *Chemical Reviews*, vol. 114, no. 19. American Chemical Society, pp. 10095–10130, Oct. 08, 2014, doi: 10.1021/cr400606n.

[46] J. Bai and B. Zhou, "Titanium dioxide nanomaterials for sensor applications," *Chemical Reviews*, vol. 114, no. 19. American Chemical Society, pp. 10131–10176, Oct. 08, 2014, doi: 10.1021/cr400625j.

[47] S.-D. Mo and W. Y. Ching, "Electronic and optical properties of three phases of titanium

dioxide: Rutile, anatase, and brookite," 1994.

[48] G. D. Gesesse *et al.*, "Plasmonic core-shell nanostructure as an optical photoactive nanolens for enhanced light harvesting and hydrogen production," *Nanoscale*, vol. 10, no. 43, pp. 20140–20146, 2018, doi: 10.1039/c8nr07475e.

[49] Y. Bessekhouad, N. Chaoui, M. Trzpit, N. Ghazzal, D. Robert, and J. V. Weber, "UV-vis versus visible degradation of Acid Orange II in a coupled CdS/TiO2 semiconductors suspension," *J. Photochem. Photobiol. A Chem.*, vol. 183, no. 1–2, pp. 218–224, 2006, doi: 10.1016/j.jphotochem.2006.03.025.

[50] T. Butburee *et al.*, "Step-wise controlled growth of metal@TiO2 core-shells with plasmonic hot spots and their photocatalytic properties," *J. Mater. Chem. A*, vol. 2, no. 32, pp. 12776–12784, 2014, doi: 10.1039/c4ta01120a.

[51] A. F. Demirörs, A. Van Blaaderen, and A. Imhof, "A general method to coat colloidal particles with titania," *Langmuir*, vol. 26, no. 12, pp. 9297–9303, Jun. 2010, doi: 10.1021/la100188w.

[52] M. Abdulla-Al-Mamun, Y. Kusumoto, T. Zannat, and M. S. Islam, "Synergistic cell-killing by photocatalytic and plasmonic photothermal effects of Ag@TiO2 core-shell composite nanoclusters against human epithelial carcinoma (HeLa) cells," *Appl. Catal. A Gen.*, vol. 398, no. 1–2, pp. 134–142, May 2011, doi: 10.1016/j.apcata.2011.03.027.

[53] I. Pastoriza-Santos, D. S. Koktysh, A. A. Mamedov, M. Giersig, N. A. Kotov, and L. M. Liz-Marzân, "One-pot synthesis of Ag@TiO 2 core-shell nanoparticles and their layer-by-layer assembly," *Langmuir*, vol. 16, no. 6, pp. 2731–2735, 2000, doi: 10.1021/la991212g.

[54] H. W. Kwon, Y. M. Lim, S. K. Tripathy, B. G. Kim, M. S. Lee, and Y. T. Yu, "Synthesis of AU/TiO2 core-shell nanoparticles from titanium isopropoxide and thermal resistance

effect of TiO2 shell," *Japanese J. Appl. Physics, Part 1 Regul. Pap. Short Notes Rev. Pap.*, vol. 46, no. 4 B, pp. 2567–2570, Apr. 2007, doi: 10.1143/JJAP.46.2567.

[55] C. Fang *et al.*, "(Gold core)/(titania shell) nanostructures for plasmon-enhanced photon harvesting and generation of reactive oxygen species," *Energy Environ. Sci.*, vol. 7, no. 10, pp. 3431–3438, Oct. 2014, doi: 10.1039/c4ee01787k.

[56] P. Chanhom, N. Charoenlap, B. Tomapatanaget, and N. Insin, "Colloidal titania-silica-iron oxide nanocomposites and the effect from silica thickness on the photocatalytic and bactericidal activities," *J. Magn. Magn. Mater.*, vol. 427, no. October 2016, pp. 54–59, 2017, doi: 10.1016/j.jmmm.2016.10.123.

[57] A. A. Kumar, A. Rajini, and N. Venkatathri, "Synthesis and Characterization of Magnetically Separable Porous Titanium Silicate Nanocomposite Catalyst for Environmental Applications," *Mater. Today Proc.*, vol. 4, no. 1, pp. 19–24, 2017, doi: 10.1016/j.matpr.2017.01.188.

[58] S. Salamat, H. Younesi, and N. Bahramifar, "Synthesis of magnetic core-shell Fe3O4@TiO2 nanoparticles from electric arc furnace dust for photocatalytic degradation of steel mill wastewater," *RSC Adv.*, vol. 7, no. 31, pp. 19391–19405, 2017, doi: 10.1039/c7ra01238a.

[59] C. K. Lo, D. Xiao, and M. M. F. Choi, "Homocysteine-protected gold-coated magnetic nanoparticles: Synthesis and characterisation," *J. Mater. Chem.*, vol. 17, no. 23, pp. 2418–2427, 2007, doi: 10.1039/b617500g.

[60] M. Dahl, Y. Liu, and Y. Yin, "Composite titanium dioxide nanomaterials," *Chemical Reviews*, vol. 114, no. 19. American Chemical Society, pp. 9853–9889, Oct. 08, 2014, doi: 10.1021/cr400634p.

[61] U. Tamer, Y. Gündoğdu, I. H. Boyaci, and K. Pekmez, “Synthesis of magnetic core-shell Fe3O4-Au nanoparticle for biomolecule immobilization and detection,” *J. Nanoparticle Res.*, vol. 12, no. 4, pp. 1187–1196, May 2010, doi: 10.1007/s11051-009-9749-0.

[62] M. Kumagai *et al.*, “Enhanced in vivo magnetic resonance imaging of tumors by PEGylated iron-oxide-gold core-shell nanoparticles with prolonged blood circulation properties,” *Macromol. Rapid Commun.*, vol. 31, no. 17, pp. 1521–1528, 2010, doi: 10.1002/marc.201000341.

[63] S. Ahmad, Tanveer; Bae, Hongsub; Rhee, Ilsu; Chang, Yongmin; Jin, Seong-Uk; Hong, “Gold-Coated Iron Oxide Nanoparticles as a T 2 Contrast Agent in Magnetic Resonance Imaging,” *J. Nanosci. Nanotechnol.*, vol. 12, no. 7, pp. 5132–5137, 2012.

[64] R. V. Kayal, Sibnath; Ramanujan, “Anti-Cancer Drug Loaded Iron–Gold Core–Shell Nanoparticles (Fe@Au) for Magnetic Drug Targeting,” *J. Nanosci. Nanotechnol.*, vol. 10, no. 9, pp. 5527–5539, 2010.

[65] G. A. Sotiriou *et al.*, “Photothermal killing of cancer cells by the controlled plasmonic coupling of silica-coated Au/Fe2O3 nanoaggregates,” *Adv. Funct. Mater.*, vol. 24, no. 19, pp. 2818–2827, 2014, doi: 10.1002/adfm.201303416.

[66] C. S. Levin *et al.*, “Magnetic-plasmonic core-shell nanoparticles,” *ACS Nano*, vol. 3, no. 6, pp. 1379–1388, 2009, doi: 10.1021/nn900118a.

[67] J. Kim *et al.*, “Designed Fabrication of Multifunctional Magnetic Gold Nanoshells and Their Application to Magnetic Resonance Imaging and Photothermal Therapy,” *Angew. Chemie*, vol. 118, no. 46, pp. 7918–7922, 2006, doi: 10.1002/ange.200602471.

[68] S. G. Penn, L. He, and M. J. Natan, “Nanoparticles for bioanalysis,” *Curr. Opin. Chem. Biol.*, vol. 7, no. 5, pp. 609–615, 2003, doi: 10.1016/j.cbpa.2003.08.013.

[69] S. Mornet, S. Vasseur, F. Grasset, and E. Duguet, “Magnetic nanoparticle design for medical diagnosis and therapy,” *Journal of Materials Chemistry*, vol. 14, no. 14. pp. 2161–2175, Jul. 21, 2004, doi: 10.1039/b402025a.

[70] X. Shi *et al.*, “Dendrimer-functionalized shell-crosslinked iron oxide nanoparticles for in-vivo magnetic resonance imaging of tumors,” *Adv. Mater.*, vol. 20, no. 9, pp. 1671–1678, May 2008, doi: 10.1002/adma.200702770.

[71] S. Gao *et al.*, “Biopolymer-assisted green synthesis of iron oxide nanoparticles and their magnetic properties,” *J. Phys. Chem. C*, vol. 112, no. 28, pp. 10398–10401, Jul. 2008, doi: 10.1021/jp802500a.

[72] Y. Cui, Y. Wang, W. Hui, Z. Zhang, X. Xin, and C. Chen, “The Synthesis of GoldMag Nano-Particles and their Application for Antibody Immobilization,” Springer Science + Business Media, Inc. Manufactured in The Netherlands, 2005.

[73] W. Jiang *et al.*, “Preparation and properties of superparamagnetic nanoparticles with narrow size distribution and biocompatible,” *J. Magn. Magn. Mater.*, vol. 283, no. 2–3, pp. 210–214, 2004, doi: 10.1016/j.jmmm.2004.05.022.

[74] H. Deng, X. Li, Q. Peng, X. Wang, J. Chen, and Y. Li, “Monodisperse Magnetic Single-Crystal Ferrite Microspheres,” *Angew. Chemie*, vol. 117, no. 18, pp. 2842–2845, 2005, doi: 10.1002/ange.200462551.

[75] C. Li, Y. Wei, A. Liivat, Y. Zhu, and J. Zhu, “Microwave-solvothermal synthesis of Fe3O4 magnetic nanoparticles,” *Mater. Lett.*, vol. 107, pp. 23–26, 2013, doi: 10.1016/j.matlet.2013.05.117.

[76] J. Hu, H. Wang, F. Dong, and Z. Wu, “A new strategy for utilization of NIR from solar energy—Promotion effect generated from photothermal effect of Fe3O4@SiO2 for

photocatalytic oxidation of NO," *Appl. Catal. B Environ.*, vol. 204, pp. 584–592, 2017, doi: 10.1016/j.apcatb.2016.12.009.

[77] A. K. Gupta and M. Gupta, "Synthesis and surface engineering of iron oxide nanoparticles for biomedical applications," *Biomaterials*, vol. 26, no. 18, pp. 3995–4021, 2005, doi: 10.1016/j.biomaterials.2004.10.012.

[78] K. C. De Souza, G. F. Andrade, I. Vasconcelos, I. M. De Oliveira Viana, C. Fernandes, and E. M. B. De Sousa, "Magnetic solid-phase extraction based on mesoporous silica-coated magnetic nanoparticles for analysis of oral antidiabetic drugs in human plasma," *Mater. Sci. Eng. C*, vol. 40, pp. 275–280, 2014, doi: 10.1016/j.msec.2014.04.004.

[79] J. J. Gooding and S. Ciampi, "The molecular level modification of surfaces: From self-assembled monolayers to complex molecular assemblies," *Chem. Soc. Rev.*, vol. 40, no. 5, pp. 2704–2718, 2011, doi: 10.1039/c0cs00139b.

[80] S. A. Ansari and Q. Husain, "Potential applications of enzymes immobilized on/in nano materials: A review," *Biotechnol. Adv.*, vol. 30, no. 3, pp. 512–523, 2012, doi: 10.1016/j.biotechadv.2011.09.005.

[81] H. Vaghari *et al.*, "Application of magnetic nanoparticles in smart enzyme immobilization," *Biotechnol. Lett.*, vol. 38, no. 2, pp. 223–233, 2016, doi: 10.1007/s10529-015-1977-z.

[82] C. Binns *et al.*, "The behaviour of nanostructured magnetic materials produced by depositing gas-phase nanoparticles," *J. Phys. D. Appl. Phys.*, vol. 38, no. 22, 2005, doi: 10.1088/0022-3727/38/22/R01.

[83] C. S. Lee, H. Lee, and R. M. Westervelt, "Microelectromagnets for the control of magnetic nanoparticles," *Appl. Phys. Lett.*, vol. 79, no. 20, pp. 3308–3310, 2001, doi:

10.1063/1.1419049.

[84] L. Sun, L. Zhan, Y. Shi, L. Chu, G. Ge, and Z. He, “Microemulsion synthesis and electromagnetic wave absorption properties of monodispersed Fe3O4/polyaniline core-shell nanocomposites,” *Synth. Met.*, vol. 187, no. 1, pp. 102–107, 2014, doi: 10.1016/j.synthmet.2013.11.007.

[85] D. V. Wagle, A. J. Rondinone, J. D. Woodward, and G. A. Baker, “Polyol Synthesis of Magnetite Nanocrystals in a Thermostable Ionic Liquid,” *Cryst. Growth Des.*, vol. 17, no. 4, pp. 1558–1567, 2017, doi: 10.1021/acs.cgd.6b01511.

[86] S. Challagulla, R. Nagarjuna, R. Ganesan, and S. Roy, “Acrylate-based Polymerizable Sol-Gel Synthesis of Magnetically Recoverable TiO2 Supported Fe3O4 for Cr(VI) Photoreduction in Aerobic Atmosphere,” *ACS Sustain. Chem. Eng.*, vol. 4, no. 3, pp. 974–982, 2016, doi: 10.1021/acssuschemeng.5b01055.

[87] S. Periyasamy, V. Gopalakannan, and N. Viswanathan, “Enhanced Chromium Sorption and Quick Separation of Magnetic Hydrotalcite Anchored Biopolymeric Composites Using the Hydrothermal Method,” *J. Chem. Eng. Data*, vol. 63, no. 5, pp. 1286–1299, 2018, doi: 10.1021/acs.jced.7b00906.

[88] B. Guo *et al.*, “Fe3O4-CoPx Nanoflowers Vertically Grown on TiN Nanoarrays as Efficient and Stable Electrocatalysts for Overall Water Splitting,” *ACS Appl. Nano Mater.*, vol. 2, no. 1, pp. 40–47, 2019, doi: 10.1021/acsanm.8b01579.

[89] M. Anbarasu, M. Anandan, E. Chinnasamy, V. Gopinath, and K. Balamurugan, “Synthesis and characterization of polyethylene glycol (PEG) coated Fe 3O4 nanoparticles by chemical co-precipitation method for biomedical applications,” *Spectrochim. Acta - Part A Mol. Biomol. Spectrosc.*, vol. 135, pp. 536–539, 2015, doi:

10.1016/j.saa.2014.07.059.

[90] A. K. Gupta and A. S. G. Curtis, “Lactoferrin and ceruloplasmin derivatized superparamagnetic iron oxide nanoparticles for targeting cell surface receptors,” *Biomaterials*, vol. 25, no. 15, pp. 3029–3040, 2004, doi: 10.1016/j.biomaterials.2003.09.095.

[91] M. Chen, S. Yamamuro, D. Farrell, and S. A. Majetich, “Gold-coated iron nanoparticles for biomedical applications,” *J. Appl. Phys.*, vol. 93, no. 10 2, pp. 7551–7553, 2003, doi: 10.1063/1.1555312.

[92] J. L. Zhang, R. S. Srivastava, and R. D. K. Misra, “Core-shell magnetite nanoparticles surface encapsulated with smart stimuli-responsive polymer: Synthesis, characterization, and LCST of viable drug-targeting delivery system,” *Langmuir*, vol. 23, no. 11, pp. 6342–6351, 2007, doi: 10.1021/la0636199.

[93] C. Warren, “VCU Scholars Compass Synthesis , Characterization , and Functionalization of Magnetic Iron Nanoparticles for Enhanced Biological Applications,” 2013.

[94] R. L. Penn and J. F. Banfield, “Imperfect oriented attachment: Dislocation generation in defect-free nanocrystals,” *Science (80-.).*, vol. 281, no. 5379, pp. 969–971, 1998, doi: 10.1126/science.281.5379.969.

[95] J. F. Banfield, S. A. Welch, H. Zhang, T. T. Ebert, and R. L. Penn, “Aggregation-based crystal growth and microstructure development in natural iron oxyhydroxide biomineralization products,” *Science (80-.).*, vol. 289, no. 5480, pp. 751–754, 2000, doi: 10.1126/science.289.5480.751.

[96] A. Steingoetter *et al.*, “Magnetic Resonance Imaging for the in Vivo Evaluation of Gastric-Retentive Tablets,” *Pharm. Res.*, vol. 20, no. 12, pp. 2001–2007, 2003, doi:

10.1023/B:PHAM.0000008049.40370.5a.

[97] R. F. Egerton, *Physical Principles of Electron Microscopy: an introduction to TEM, SEM, and AEM*. New york, NY: Springer, 2005.

[98] M. Filella, J. Zhang, M. E. Newman, and J. Buffle, "Analytical applications of photon correlation spectroscopy for size distribution measurements of natural colloidal suspensions: Capabilities and limitations," *Colloids Surfaces A Physicochem. Eng. Asp.*, vol. 120, no. 1–3, pp. 27–46, 1997, doi: 10.1016/S0927-7757(96)03677-1.

[99] A. Heidari, N. Mir, and A. R. Nikkaran, "Phenylalanine Removal from Water by Fe3O4 Nanoparticles Functionalized with Two Different Surfactants," *J. Nanostructures*, vol. 6, no. 3, pp. 199–206, 2016, doi: 10.7508/JNS.2016.03.004.

[100] S. Laurent *et al.*, "Erratum: Magnetic iron oxide nanoparticles: Synthesis, stabilization, vectorization, physicochemical characterizations, and biological applications (Chemical Reviews (2008) 108 (2064))," *Chem. Rev.*, vol. 110, no. 4, p. 2574, 2010, doi: 10.1021/cr900197g.

[101] W. Wu, Q. He, and C. Jiang, "Magnetic iron oxide nanoparticles: Synthesis and surface functionalization strategies," *Nanoscale Res. Lett.*, vol. 3, no. 11, pp. 397–415, 2008, doi: 10.1007/s11671-008-9174-9.

[102] S. Liu, B. Yu, S. Wang, Y. Shen, and H. Cong, "Preparation, surface functionalization and application of Fe3O4 magnetic nanoparticles," *Adv. Colloid Interface Sci.*, vol. 281, p. 102165, 2020, doi: 10.1016/j.cis.2020.102165.

[103] J. S. Han, G. S. An, B. G. Park, and S. C. Choi, "The influence of functionalization of the Fe3O4 nanoparticle on its dispersion property," *J. Korean Ceram. Soc.*, vol. 55, no. 1, pp. 80–84, 2018, doi: 10.4191/kcers.2018.55.1.01.

[104] S. Mornet *et al.*, “Magnetic nanoparticle design for medical applications,” *Prog. Solid State Chem.*, vol. 34, no. 2–4, pp. 237–247, 2006, doi: 10.1016/j.progsolidstchem.2005.11.010.

[105] W. Gao, J. Cao, and J. Li, “Ch Ive,” vol. 19, no. 4, pp. 255–264, 2010.

[106] B. Feng *et al.*, “Synthesis of Fe3O4/APTES/PEG diacid functionalized magnetic nanoparticles for MR imaging,” *Colloids Surfaces A Physicochem. Eng. Asp.*, vol. 328, no. 1–3, pp. 52–59, 2008, doi: 10.1016/j.colsurfa.2008.06.024.

[107] J. Y. Park, P. Daksha, G. H. Lee, S. Woo, and Y. Chang, “Highly water-dispersible PEG surface modified ultra small superparamagnetic iron oxide nanoparticles useful for target-specific biomedical applications,” *Nanotechnology*, vol. 19, no. 36, 2008, doi: 10.1088/0957-4484/19/36/365603.

[108] M. Liong *et al.*, “Multifunctional inorganic nanoparticles for imaging, targeting, and drug delivery,” *ACS Nano*, vol. 2, no. 5, pp. 889–896, 2008, doi: 10.1021/nn800072t.

[109] D. H. Kim, D. E. Nikles, D. T. Johnson, and C. S. Brazel, “Heat generation of aqueously dispersed CoFe2O4 nanoparticles as heating agents for magnetically activated drug delivery and hyperthermia,” *J. Magn. Magn. Mater.*, vol. 320, no. 19, pp. 2390–2396, 2008, doi: 10.1016/j.jmmm.2008.05.023.

[110] A. Jordan *et al.*, “Endocytosis of dextran and silan-coated magnetite nanoparticles and the effect of intracellular hyperthermia on human mammary carcinoma cells in vitro,” *J. Magn. Magn. Mater.*, vol. 194, no. 1, pp. 185–196, 1999, doi: 10.1016/S0304-8853(98)00558-7.

[111] J. A. Frank *et al.*, “Clinically applicable labeling of mammalian and stem cells by combining superparamagnetic iron oxides and transfection agents,” *Radiology*, vol. 228,

no. 2, pp. 480–487, 2003, doi: 10.1148/radiol.2281020638.

[112] A. M. Schmidt, “Induction heating of novel thermoresponsive ferrofluids,” *J. Magn. Magn. Mater.*, vol. 289, pp. 5–8, 2005, doi: 10.1016/j.jmmm.2004.11.003.

[113] C. De las Heras Alarcón, S. Pennadam, and C. Alexander, “Stimuli responsive polymers for biomedical applications,” *Chem. Soc. Rev.*, vol. 34, no. 3, pp. 276–285, 2005, doi: 10.1039/b406727d.

[114] G. H. Du, Z. L. Liu, X. Xia, Q. Chu, and S. M. Zhang, “Characterization and application of Fe3O4/SiO 2 nanocomposites,” *J. Sol-Gel Sci. Technol.*, vol. 39, no. 3, pp. 285–291, 2006, doi: 10.1007/s10971-006-7780-5.

[115] T. K. H. Ta *et al.*, “Synthesis and surface functionalization of Fe3O4-SiO2 core-shell nanoparticles with 3-glycidoxypropyltrimethoxysilane and 1,1′-carbonyldiimidazole for bio-applications,” *Colloids Surfaces A Physicochem. Eng. Asp.*, vol. 504, pp. 376–383, 2016, doi: 10.1016/j.colsurfa.2016.05.008.

[116] C. H. Lu, G. H. Chen, B. Yu, H. L. Cong, L. M. Kong, and L. Guo, “Design and synthesis of Fe3O4@SiO2 core-shell nanomaterials,” *Integr. Ferroelectr.*, vol. 182, no. 1, pp. 46–52, 2017, doi: 10.1080/10584587.2017.1352383.

[117] L. F. O. Maia *et al.*, “Removal of mercury(II) from contaminated water by gold-functionalised Fe3O4 magnetic nanoparticles,” *Environ. Technol. (United Kingdom)*, vol. 41, no. 8, pp. 959–970, 2020, doi: 10.1080/09593330.2018.1515989.

[118] J. Isasi, P. Arévalo, E. Martin, and F. Martín-Hernández, “Preparation and study of silica and APTES–silica-modified NiFe2O4 nanocomposites for removal of Cu2+ and Zn2+ ions from aqueous solutions,” *J. Sol-Gel Sci. Technol.*, vol. 91, no. 3, pp. 596–610, 2019, doi: 10.1007/s10971-019-05067-3.

[119] F. Cheng, S. M. Sajedin, S. M. Kelly, A. F. Lee, and A. Kornherr, “UV-stable paper coated with APTES-modified P25 TiO2 nanoparticles,” *Carbohydr. Polym.*, vol. 114, pp. 246–252, 2014, doi: 10.1016/j.carbpol.2014.07.076.

[120] V. C. Karade *et al.*, “APTES monolayer coverage on self-assembled magnetic nanospheres for controlled release of anticancer drug Nintedanib,” *Sci. Rep.*, vol. 11, no. 1, pp. 1–12, 2021, doi: 10.1038/s41598-021-84770-0.

[121] G. Hermanson, *Bioconjugate Techniques*, Second edi. Rockford, Illinois, USA: Thermo Fisher Scientific, 2005.

[122] S. Avrameas, “Coupling of enzymes to proteins with glutaraldehyde. Use of the conjugates for the detection of antigens and antibodies,” *Immunochemistry*, vol. 6, no. 1, pp. 43–52, 1969, doi: 10.1016/0019-2791(69)90177-3.

[123] S. Avrameas and T. Ternynck, “Peroxidase labelled antibody and Fab conjugates with enhanced intracellular penetration,” *Immunochemistry*, vol. 8, no. June, pp. 1175–1179, 1971.

[124] X. Xie, D. Ma, and L.-M. Zhang, “Fabrication and properties of a supramolecular hybrid hydrogel doped with CdTe quantum dots,” *RSC Adv.*, vol. 5, no. 72, pp. 58746–58754, 2015, doi: 10.1039/c5ra09386d.

[125] I. L. Medintz, H. T. Uyeda, E. R. Goldman, and H. Mattoussi, “Quantum dot bioconjugates for imaging, labelling and sensing,” *Nat. Mater.*, vol. 4, no. 6, pp. 435–446, 2005, doi: 10.1038/nmat1390.

[126] I. U. Arachchige and S. L. Brock, “Highly luminescent quantum-dot monoliths,” *J. Am. Chem. Soc.*, vol. 129, no. 7, pp. 1840–1841, 2007, doi: 10.1021/ja066749c.

[127] S. Chaudhary, M. Ozkan, and W. C. W. Chan, “Trilayer hybrid polymer-quantum dot

light-emitting diodes," *Appl. Phys. Lett.*, vol. 84, no. 15, pp. 2925–2927, 2004, doi: 10.1063/1.1699476.

[128] T. Yoshle *et al.*, "Vacuum Rabi splitting with a single quantum dot in a photonic crystal nanocavity," *Nature*, vol. 432, no. 7014, pp. 200–203, 2004, doi: 10.1038/nature03119.

[129] C. X. Chen *et al.*, "Rapidly detecting antibiotics with magnetic nanoparticle coated CdTe quantum dots," *RSC Adv.*, vol. 10, no. 4, pp. 1966–1970, 2020, doi: 10.1039/c9ra09894a.

[130] D. Wang *et al.*, "Size control of CdS nanocrystals in block copolymer micelle," *Chem. Mater.*, vol. 11, no. 2, pp. 392–398, 1999, doi: 10.1021/cm980613z.

[131] H. Yusuf, W. G. Kim, D. H. Lee, Y. Guo, and M. G. Moffitt, "Size control of mesoscale aqueous assemblies of quantum dots and block copolymers," *Langmuir*, vol. 23, no. 2, pp. 868–878, 2007, doi: 10.1021/la0623634.

[132] M. Han, X. Gao, J. Z. Su, and S. Nie, "Quantum-dot-tagged microbeads for multiplexed optical coding of biomolecules," *Nat. Biotechnol.*, vol. 19, no. 7, pp. 631–635, 2001, doi: 10.1038/90228.

[133] R. E. Bailey, A. M. Smith, and S. Nie, "Quantum dots in biology and medicine," *Phys. E Low-Dimensional Syst. Nanostructures*, vol. 25, no. 1, pp. 1–12, 2004, doi: 10.1016/j.physe.2004.07.013.

[134] A. J. Sutherland, "Quantum dots as luminescent probes in biological systems," *Curr. Opin. Solid State Mater. Sci.*, vol. 6, no. 4, pp. 365–370, 2002, doi: 10.1016/S1359-0286(02)00081-5.

[135] Y. Zhang and T. H. Wang, "Quantum dot enabled molecular sensing and diagnostics," *Theranostics*, vol. 2, no. 7, pp. 631–654, 2012, doi: 10.7150/thno.4308.

[136] P. Chanhom, N. Charoenlap, B. Tomapatanaget, and N. Insin, "Colloidal titania-silica-iron

oxide nanocomposites and the effect from silica thickness on the photocatalytic and bactericidal activities," *J. Magn. Magn. Mater.*, vol. 427, no. June 2016, pp. 54–59, 2017, doi: 10.1016/j.jmmm.2016.10.123.

[137] S. Ge *et al.*, "Facile hydrothermal synthesis of iron oxide nanoparticles with tunable magnetic properties," *J. Phys. Chem. C*, vol. 113, no. 31, pp. 13593–13599, Aug. 2009, doi: 10.1021/jp902953t.

[138] B. Bartosewicz, M. Liszewska, B. Budner, M. Michalska-Domańska, K. Kopczyński, and B. J. Jankiewicz, "Fabrication of Ag-modified hollow titania spheres via controlled silver diffusion in Ag-TiO2 core-shell nanostructures," *Beilstein J. Nanotechnol.*, vol. 11, pp. 141–146, 2020, doi: 10.3762/bjnano.11.12.

[139] R. Rosman, B. Saifullah, S. Maniam, D. Dorniani, M. Z. Hussein, and S. Fakurazi, "Improved anticancer effect of magnetite nanocomposite formulation of gallic acid (Fe3 o4 -peg-ga) against lung, breast and colon cancer cells," *Nanomaterials*, vol. 8, no. 2, pp. 1–14, 2018, doi: 10.3390/nano8020083.

[140] R. A. Sperling and W. J. Parak, "Surface modification, functionalization and bioconjugation of colloidal Inorganic nanoparticles," *Philos. Trans. R. Soc. A Math. Phys. Eng. Sci.*, vol. 368, no. 1915, pp. 1333–1383, 2010, doi: 10.1098/rsta.2009.0273.

[141] M. Chastellain, A. Petri, A. Gupta, K. V. Rao, and H. Hofmann, "Superparamagnetic silica-iron oxide nanocomposites for application in hyperthermia," *Adv. Eng. Mater.*, vol. 6, no. 4, pp. 235–241, 2004, doi: 10.1002/adem.200300574.

[142] J. Liu, S. Z. Qiao, Q. H. Hu, and G. Q. Lu, "Magnetic nanocomposites with mesoporous structures: Synthesis and applications," *Small*, vol. 7, no. 4, pp. 425–443, 2011, doi: 10.1002/smll.201001402.

[143] H. Zhang, R. G. Mcdowell, L. R. Martin, and Y. Qiang, “Selective Extraction of Heavy and Light Lanthanides from Aqueous Solution by Advanced Magnetic Nanosorbents,” *ACS Appl. Mater. Interfaces*, vol. 8, no. 14, pp. 9523–9531, 2016, doi: 10.1021/acsami.6b01550.

[144] M. Kaur, H. Zhang, L. Martin, T. Todd, and Y. Qiang, “Conjugates of magnetic nanoparticle - Actinide specific chelator for radioactive waste separation,” *Environ. Sci. Technol.*, vol. 47, no. 21, pp. 11942–11959, 2013, doi: 10.1021/es402205q.

[145] S. Dagher *et al.*, “Photocatalytic removal of methylene blue using titania- and silica-coated magnetic nanoparticles,” *Mater. Res. Express*, vol. 5, no. 6, 2018, doi: 10.1088/2053-1591/aacad4.

[146] J. ming Wu, S. Hayakawa, K. Tsuru, and A. Osaka, “In vitro bioactivity of anatase film obtained by direct deposition from aqueous titanium tetrafluoride solutions,” *Thin Solid Films*, vol. 414, no. 2, pp. 275–280, 2002, doi: 10.1016/s0040-6090(02)00498-4.

[147] Akira FujishimaTata N. RaoDonald A. Tryk, “Titanium dioxide photocatalysis,” *Rev. Infirm.*, vol. 1, no. 180, pp. 1–21, 2000.

[148] Q. He, Z. Zhang, J. Xiong, Y. Xiong, and H. Xiao, “A novel biomaterial - Fe3O4:TiO2 core-shell nano particle with magnetic performance and high visible light photocatalytic activity,” *Opt. Mater. (Amst).*, vol. 31, no. 2, pp. 380–384, 2008, doi: 10.1016/j.optmat.2008.05.011.

[149] M. Advincula, X. Fan, J. Lemons, and R. Advincula, “Surface modification of surface sol-gel derived titanium oxide films by self-assembled monolayers (SAMs) and non-specific protein adsorption studies,” *Colloids Surfaces B Biointerfaces*, vol. 42, no. 1, pp. 29–43, 2005, doi: 10.1016/j.colsurfb.2004.12.009.

[150] H. Honda, K. Suzaki, and Y. Sugahara, “Control of hydrolysis and condensation reactions of titanium tert-butoxide by chemical modification with catechol,” *J. Sol-Gel Sci. Technol.*, vol. 22, no. 1–2, pp. 133–138, 2001, doi: 10.1023/A:1011280723772.

[151] J. Lee, T. Isobe, and M. Senna, “Preparation of ultrafine Fe3O4 particles by precipitation in the presence of PVA at high pH,” *J. Colloid Interface Sci.*, vol. 177, no. 2, pp. 490–494, 1996, doi: 10.1006/jcis.1996.0062.

[152] R. Ghosh Chaudhuri and S. Paria, “Core/shell nanoparticles: Classes, properties, synthesis mechanisms, characterization, and applications,” *Chemical Reviews*, vol. 112, no. 4. pp. 2373–2433, Apr. 11, 2012, doi: 10.1021/cr100449n.

[153] M. B. Gawande *et al.*, “Core-shell nanoparticles: synthesis and applications in catalysis and electrocatalysis,” *Chemical Society Reviews*, vol. 44, no. 21. Royal Society of Chemistry, pp. 7540–7590, Nov. 07, 2015, doi: 10.1039/c5cs00343a.

[154] S. J. Oldenburg, R. D. Averitt, S. L. Westcott, and N. J. Halas, “Nanoengineering of optical resonances,” 1998.

[155] F. Caruso, “Nanoengineering of Particle Surfaces**,” 1995.

[156] Y. S. Kang, S. Risbud, J. F. Rabolt, and P. Stroeve, “Synthesis and Characterization of Nanometer-Size Fe 3 O 4 and γ-Fe 2 O 3 Particles,” 1996. [Online]. Available: https://pubs.acs.org/sharingguidelines.

[157] X. Shi, T. P. Thomas, L. A. Myc, A. Kotlyar, and J. R. Baker, “Synthesis, characterization, and intracellular uptake of carboxyl-terminated poly(amidoamine) dendrimer-stabilized iron oxide nanoparticles,” *Phys. Chem. Chem. Phys.*, vol. 9, no. 42, pp. 5712–5720, 2007, doi: 10.1039/b709147h.

[158] J. Tang, M. Myers, K. A. Bosnick, and L. E. Brus, “Magnetite Fe3O4 nanocrystals:

Spectroscopic observation of aqueous oxidation kinetics," *J. Phys. Chem. B*, vol. 107, no. 30, pp. 7501–7506, Jul. 2003, doi: 10.1021/jp027048e.

[159] G. Mie, "Beiträge zur Optik trüber Medien, speziell kolloidaler Metallösungen," *Ann. der Phys.*, vol. 330, pp. 337–445, 1908.

[160] E. P. Turevskaya, M. I. Yanovskaya, and N. Ya Turova, "Preparation of Oxide Materials from Metal Alkoxides," 2000.

[161] J. Livage, M. Henry, and C. Sanchez, "SOL-GEL CHEMISTRY OF TRANSITION METAL OXIDES," 1988.

[162] X. Jiang, T. Herricks, and Y. Xia, "Monodispersed spherical colloids of titania: Synthesis, characterization, and crystallization," *Adv. Mater.*, vol. 15, no. 14, pp. 1205–1209, 2003, doi: 10.1002/adma.200305105.

[163] W. Wang, J. Zhang, F. Chen, D. He, and M. Anpo, "Preparation and photocatalytic properties of Fe3+-doped Ag@TiO2 core-shell nanoparticles," *J. Colloid Interface Sci.*, vol. 323, no. 1, pp. 182–186, 2008, doi: 10.1016/j.jcis.2008.03.043.

[164] nanocomposix, "nanoComposix." https://nanocomposix.com/pages/mie-theory-calculator#target.

[165] H. F. Zarick *et al.*, "Improving Light Harvesting in Dye-Sensitized Solar Cells Using Hybrid Bimetallic Nanostructures," *ACS Photonics*, vol. 3, no. 3, pp. 385–394, 2016, doi: 10.1021/acsphotonics.5b00552.

[166] E. Amstad, M. Textor, and E. Reimhult, "Stabilization and functionalization of iron oxide nanoparticles for biomedical applications," *Nanoscale*, vol. 3, no. 7, pp. 2819–2843, 2011, doi: 10.1039/c1nr10173k.

[167] Y. M. Huh *et al.*, "In vivo magnetic resonance detection of cancer by using

multifunctional magnetic nanocrystals," *J. Am. Chem. Soc.*, vol. 127, no. 35, pp. 12387–12391, 2005, doi: 10.1021/ja052337c.

[168] M. Ferrari, "Cancer nanotechnology: Opportunities and challenges," *Nat. Rev. Cancer*, vol. 5, no. 3, pp. 161–171, 2005, doi: 10.1038/nrc1566.

[169] A. H. Latham and M. E. Williams, "Controlling transport and chemical functionality of magnetic nanoparticles," *Acc. Chem. Res.*, vol. 41, no. 3, pp. 411–420, 2008, doi: 10.1021/ar700183b.

[170] Z. Xu, Q. Liu, and J. A. Finch, "Silanation and stability of 3-aminopropyl triethoxy silane on nanosized superparamagnetic particles: I. Direct silanation," *Appl. Surf. Sci.*, vol. 120, no. 3–4, pp. 269–278, 1997, doi: 10.1016/S0169-4332(97)00234-1.

[171] S. Iron *et al.*, "Preclinical Safety and Pharmacokinetic Profile of," *Animals*, vol. 41, no. 3, pp. 313–324, 2006.

[172] T. K. Jain, M. K. Reddy, M. A. Morales, D. L. Leslie-Pelecky, and V. Labhasetwar, "Biodistribution, clearance, and biocompatibility of iron oxide magnetic nanoparticles in rats," *Mol. Pharm.*, vol. 5, no. 2, pp. 316–327, 2008, doi: 10.1021/mp7001285.

[173] J. M. Perez, F. J. Simeone, Y. Saeki, L. Josephson, and R. Weissleder, "Viral-induced self-assembly of magnetic nanoparticles allows the detection of viral particles in biological media," *J. Am. Chem. Soc.*, vol. 125, no. 34, pp. 10192–10193, 2003, doi: 10.1021/ja036409g.

[174] C. Boyer, M. R. Whittaker, V. Bulmus, J. Liu, and T. P. Davis, "The design and utility of polymer-stabilized iron-oxide nanoparticles for nanomedicine applications," *NPG Asia Mater.*, vol. 2, no. 1, pp. 23–30, 2010, doi: 10.1038/asiamat.2010.6.

[175] I. J. Bruce and T. Sen, "Surface modification of magnetic nanoparticles with alkoxysilanes

and their application in magnetic bioseparations," *Langmuir*, vol. 21, no. 15, pp. 7029–7035, 2005, doi: 10.1021/la050553t.

[176] N. Frickel, R. Messing, T. Gelbrich, and A. M. Schmidt, "Functional silanes as surface modifying primers for the preparation of highly stable and well-defined magnetic polymer hybrids," *Langmuir*, vol. 26, no. 4, pp. 2839–2846, 2010, doi: 10.1021/la902904f.

[177] S. Onclin, B. J. Ravoo, and D. N. Reinhoudt, "Engineering silicon oxide surfaces using self-assembled monolayers," *Angew. Chemie - Int. Ed.*, vol. 44, no. 39, pp. 6282–6304, 2005, doi: 10.1002/anie.200500633.

[178] W. Brullot *et al.*, "Versatile ferrofluids based on polyethylene glycol coated iron oxide nanoparticles," *J. Magn. Magn. Mater.*, vol. 324, no. 11, pp. 1919–1925, 2012, doi: 10.1016/j.jmmm.2012.01.032.

[179] L. Bouffier, H. H. P. Yiu, and M. J. Rosseinsky, "Chemical grafting of a DNA intercalator probe onto functional iron oxide nanoparticles: A physicochemical study," *Langmuir*, vol. 27, no. 10, pp. 6185–6192, 2011, doi: 10.1021/la104745x.

[180] C. Flesch, Y. Unterfinger, E. Bourgeat-Lami, E. Duguet, C. Delaite, and P. Dumas, "Poly(ethylene glycol) surface coated magnetic particles," *Macromol. Rapid Commun.*, vol. 26, no. 18, pp. 1494–1498, 2005, doi: 10.1002/marc.200500402.

[181] B. Arkles, "Tailoring Surfaces with Silanes," *Chemtech*, vol. 7, no. May, pp. 766–778, 2019, doi: 10.5281/zenodo.3555609.

[182] N. Kohler, C. Sun, A. Fichtenholtz, J. Gunn, C. Fang, and M. Zhang, "Methotrexate-immobilized poly(ethylene glycol) magnetic nanoparticles for MR imaging and drug delivery," *Small*, vol. 2, no. 6, pp. 785–792, 2006, doi: 10.1002/smll.200600009.

[183] N. Kohler, G. E. Fryxell, and M. Zhang, "A bifunctional poly(ethylene glycol) silane

immobilized on metallic oxide-based nanoparticles for conjugation with cell targeting agents," *J. Am. Chem. Soc.*, vol. 126, no. 23, pp. 7206–7211, 2004, doi: 10.1021/ja049195r.

[184] M. Mikhaylova *et al.*, "BSA immobilization on amine-functionalized superparamagnetic iron oxide nanoparticles," *Chem. Mater.*, vol. 16, no. 12, pp. 2344–2354, 2004, doi: 10.1021/cm0348904.

[185] H. Kobayashi and T. Matsunaga, "Amino-silane modified superparamagnetic particles with surface-immobilized enzyme," *J. Colloid Interface Sci.*, vol. 141, no. 2, pp. 505–511, 1991, doi: 10.1016/0021-9797(91)90347-B.

[186] W. Kühne, "Ueber das Trypsin (Enzym des Pankreas)," *FEBS Lett.*, vol. 62, no. February, pp. E8–E12, 1976, doi: 10.1016/0014-5793(76)80848-4.

[187] H.-K. S. Leiros, "Trypsin specificity as elucidated by LIE calculations, X-ray structures, and association constant measurements," *Protein Sci.*, vol. 13, no. 4, pp. 1056–1070, 2004, doi: 10.1110/ps.03498604.

[188] Y. Liu, Y. Li, X. M. Li, and T. He, "Kinetics of (3-aminopropyl)triethoxylsilane (aptes) silanization of superparamagnetic iron oxide nanoparticles," *Langmuir*, vol. 29, no. 49, pp. 15275–15282, 2013, doi: 10.1021/la403269u.

[189] T. AQUINAS, "Chapter 15," *Comment. Gospel John*, vol. 679, no. 1, pp. 96–129, 2017, doi: 10.2307/j.ctt31nk8p.6.

[190] L. S. Jeremy Mark Berg, John L. Tymoczko, *Biochemistry, Fifth Edition*. Michelle Julet, 2002.

[191] C. Zhou, X. Yu, X. Qin, H. Ma, A. E. G. A. Yagoub, and J. Hu, "Hydrolysis of rapeseed meal protein under simulated duodenum digestion: Kinetic modeling and antioxidant

activity," *LWT - Food Sci. Technol.*, vol. 68, pp. 523–531, 2016, doi: 10.1016/j.lwt.2015.11.057.

[192] C. F. Chi, B. Wang, Y. Y. Deng, Y. M. Wang, S. G. Deng, and J. Y. Ma, "Isolation and characterization of three antioxidant pentapeptides from protein hydrolysate of monkfish (Lophius litulon) muscle," *Food Res. Int.*, vol. 55, pp. 222–228, 2014, doi: 10.1016/j.foodres.2013.11.018.

[193] T. R. Silva *et al.*, "Immobilization of trypsin onto poly(ethylene terephthalate)/poly(lactic acid) nonwoven nanofiber mats," *Biochem. Eng. J.*, vol. 104, pp. 48–56, 2015, doi: 10.1016/j.bej.2015.04.026.

[194] M. L. Verma, R. Chaudhary, T. Tsuzuki, C. J. Barrow, and M. Puri, "Immobilization of β-glucosidase on a magnetic nanoparticle improves thermostability: Application in cellobiose hydrolysis," *Bioresour. Technol.*, vol. 135, pp. 2–6, 2013, doi: 10.1016/j.biortech.2013.01.047.

[195] J. N. Talbert and J. M. Goddard, "Characterization of lactase-conjugated magnetic nanoparticles," *Process Biochem.*, vol. 48, no. 4, pp. 656–662, 2013, doi: 10.1016/j.procbio.2013.03.001.

[196] C. Bernal, A. Illanes, and L. Wilson, "Heterofunctional hydrophilic-hydrophobic porous silica as support for multipoint covalent immobilization of lipases: Application to lactulose palmitate synthesis," *Langmuir*, vol. 30, no. 12, pp. 3557–3566, 2014, doi: 10.1021/la4047512.

[197] W. J. Goh *et al.*, "Iron oxide filled magnetic carbon nanotube-enzyme conjugates for recycling of amyloglucosidase: Toward useful applications in biofuel production process," *Langmuir*, vol. 28, no. 49, pp. 16864–16873, 2012, doi: 10.1021/la303046m.

[198] D. Goradia, J. Cooney, B. K. Hodnett, and E. Magner, “The adsorption characteristics, activity and stability of trypsin onto mesoporous silicates,” *J. Mol. Catal. B Enzym.*, vol. 32, no. 5–6, pp. 231–239, 2005, doi: 10.1016/j.molcatb.2004.12.007.

[199] C. G. Liu, K. G. H. Desai, X. G. Chen, and H. J. Park, “Preparation and characterization of nanoparticles containing trypsin based on hydrophobically modified chitosan,” *J. Agric. Food Chem.*, vol. 53, no. 5, pp. 1728–1733, 2005, doi: 10.1021/jf040304v.

[200] Y. Jiang, C. Guo, H. Xia, I. Mahmood, C. Liu, and H. Liu, “Magnetic nanoparticles supported ionic liquids for lipase immobilization: Enzyme activity in catalyzing esterification,” *J. Mol. Catal. B Enzym.*, vol. 58, no. 1–4, pp. 103–109, 2009, doi: 10.1016/j.molcatb.2008.12.001.

[201] D. H. Chen and M. H. Liao, “Preparation and characterization of YADH-bound magnetic nanoparticles,” *J. Mol. Catal. - B Enzym.*, vol. 16, no. 5–6, pp. 283–291, 2002, doi: 10.1016/S1381-1177(01)00074-1.

[202] H. Sun *et al.*, “Novel core-shell structure polyacrylamide-coated magnetic nanoparticles synthesized via photochemical polymerization,” *Surf. Coatings Technol.*, vol. 201, no. 1–2, pp. 250–254, 2006, doi: 10.1016/j.surfcoat.2005.11.112.

[203] U. T. Bornscheuer, “Immobilizing enzymes: How to create more suitable biocatalysts,” *Angew. Chemie - Int. Ed.*, vol. 42, no. 29, pp. 3336–3337, 2003, doi: 10.1002/anie.200301664.

[204] J. Kim, J. W. Grate, and P. Wang, “Nanostructures for enzyme stabilization,” *Chem. Eng. Sci.*, vol. 61, no. 3, pp. 1017–1026, 2006, doi: 10.1016/j.ces.2005.05.067.

[205] G. Bayramoğlu, S. Kiralp, M. Yilmaz, L. Toppare, and M. Y. Arica, “Covalent immobilization of chloroperoxidase onto magnetic beads: Catalytic properties and

stability," *Biochem. Eng. J.*, vol. 38, no. 2, pp. 180–188, 2008, doi: 10.1016/j.bej.2007.06.018.

[206] Y. Zhang, Y. Zhang, H. Wang, B. Yan, G. Shen, and R. Yu, "An enzyme immobilization platform for biosensor designs of direct electrochemistry using flower-like ZnO crystals and nano-sized gold particles," *J. Electroanal. Chem.*, vol. 627, no. 1–2, pp. 9–14, 2009, doi: 10.1016/j.jelechem.2008.12.010.

[207] J. Huang, R. Zhao, H. Wang, W. Zhao, and L. Ding, "Immobilization of glucose oxidase on Fe3O4/SiO2 magnetic nanoparticles," *Biotechnol. Lett.*, vol. 32, no. 6, pp. 817–821, 2010, doi: 10.1007/s10529-010-0217-9.

[208] B. Chertok *et al.*, "Iron oxide nanoparticles as a drug delivery vehicle for MRI monitored magnetic targeting of brain tumors," *Biomaterials*, vol. 29, no. 4, pp. 487–496, 2008, doi: 10.1016/j.biomaterials.2007.08.050.

[209] G. Bayramoglu, Y. Tunali, and M. Y. Arica, "Immobilization of β-galactosidase onto magnetic poly(GMA-MMA) beads for hydrolysis of lactose in bed reactor," *Catal. Commun.*, vol. 8, no. 7, pp. 1094–1101, 2007, doi: 10.1016/j.catcom.2006.10.029.

[210] P. Tartaj, M. P. Morales, T. González-Carreño, S. Veintemillas-Verdaguer, and C. J. Serna, "Advances in magnetic nanoparticles for biotechnology applications," *J. Magn. Magn. Mater.*, vol. 290-291 PART 1, pp. 28–34, 2005, doi: 10.1016/j.jmmm.2004.11.155.

[211] Z. Yang, S. Si, and C. Zhang, "Magnetic single-enzyme nanoparticles with high activity and stability," *Biochem. Biophys. Res. Commun.*, vol. 367, no. 1, pp. 169–175, 2008, doi: 10.1016/j.bbrc.2007.12.113.

[212] O. Bomatí-Miguel *et al.*, "Fe-based nanoparticulate metallic alloys as contrast agents for magnetic resonance imaging," *Biomaterials*, vol. 26, no. 28, pp. 5695–5703, 2005, doi:

10.1016/j.biomaterials.2005.02.020.

[213] L. M. Lacava *et al.*, “Magnetic resonance of a dextran-coated magnetic fluid intravenously administered in mice,” *Biophys. J.*, vol. 80, no. 5, pp. 2483–2486, 2001, doi: 10.1016/S0006-3495(01)76217-0.

[214] C. Wilhelm, C. Billotey, J. Roger, J. N. Pons, J. C. Bacri, and F. Gazeau, “Intracellular uptake of anionic superparamagnetic nanoparticles as a function of their surface coating,” *Biomaterials*, vol. 24, no. 6, pp. 1001–1011, 2003, doi: 10.1016/S0142-9612(02)00440-4.

[215] M. Arruebo, R. Fernández-Pacheco, M. R. Ibarra, and J. Santamaría, “Magnetic nanoparticles for drug delivery The potential of magnetic NPs stems from the intrinsic properties of their magnetic cores combined with their drug loading capability and the biochemical properties that can be bestowed on them by means of a suitab,” vol. 2, no. 3, pp. 22–32, 2007, [Online]. Available: https://pdfs.semanticscholar.org/1844/8eb43dc235f82cb591983bc8df5ed799984c.pdf.

[216] D. D. Stark *et al.*, “Superparamagnetic iron oxide: Clinical application as a contrast agent for MR imaging of the liver,” *Radiology*, vol. 168, no. 2, pp. 297–301, 1988, doi: 10.1148/radiology.168.2.3393649.

[217] J. T. Ferrucci and S. Siani, “Ferrite Particles as an MR Contrast Agent,” no. December, p. 1988, 1988.

[218] P. F. Hahn and D. Stark, “to MR in Vascular of Superparamagnetic Imaging of Tissue,” pp. 361–366, 1990.

[219] M. F. Bellin, C. Beigelman, and S. Precetti-Morel, “Iron oxide-enhanced MR lymphography: Initial experience,” *Eur. J. Radiol.*, vol. 34, no. 3, pp. 257–264, 2000, doi: 10.1016/S0720-048X(00)00204-7.

[220] H. L. Duan, Z. Q. Shen, X. W. Wang, F. H. Chao, and J. W. Li, “Preparation of immunomagnetic iron-dextran nanoparticles and application in rapid isolation of E.coli 0157:H7 from foods,” *World J. Gastroenterol.*, vol. 11, no. 24, pp. 3660–3664, 2005, doi: 10.3748/wjg.v11.i24.3660.

[221] H. Pardoe, W. Chua-Anusorn, T. G. St. Pierre, and J. Dobson, “Detection limits for ferrimagnetic particle concentrations using magnetic resonance imaging based proton transverse relaxation rate measurements,” *Phys. Med. Biol.*, vol. 48, no. 6, 2003, doi: 10.1088/0031-9155/48/6/401.

[222] M. Barbara Wilson and P. K. Nakane, “The covalent coupling of proteins to periodate-oxidized sephadex: A new approach to immunoadsorbent preparation,” *J. Immunol. Methods*, vol. 12, no. 1–2, pp. 171–181, 1976, doi: 10.1016/0022-1759(76)90107-1.